CHALMERS
UNIVERSITY OF TECHNOLOGY

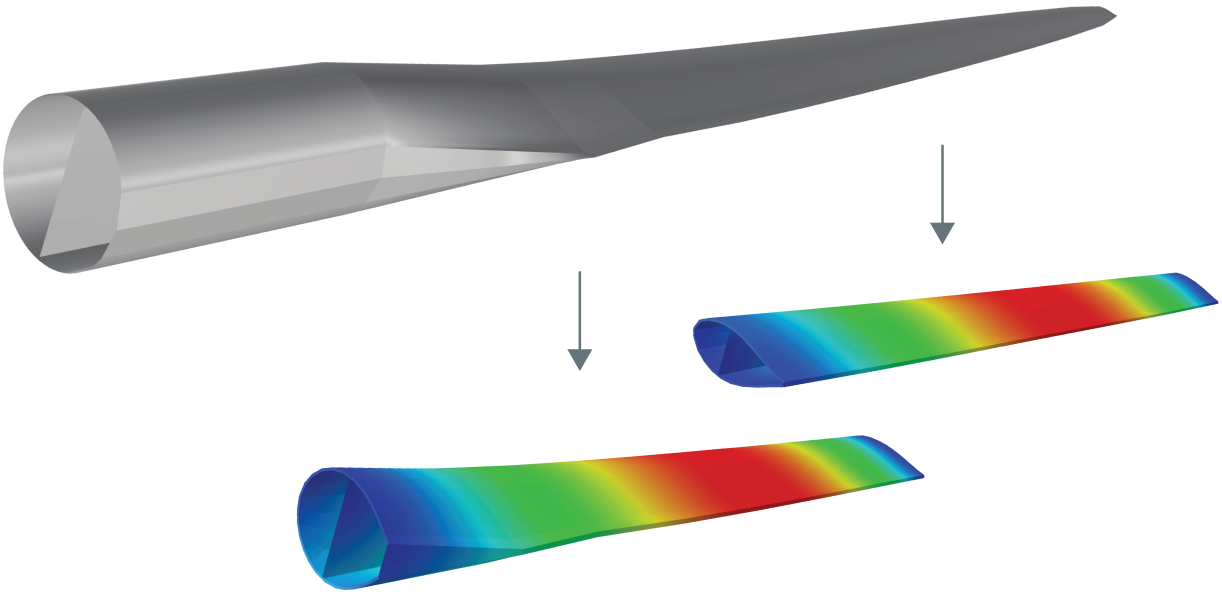

Reuse of Decommissioned Wind Turbine Blades in Pedestrian Bridges

Detailed investigation of deflection and dynamic response

Master's thesis in Structural Engineering and Building Technology

JOHAN DAHLÉN
CHRISTOFFER HÄRNBORG

DEPARTMENT OF ARCHITECTURE AND CIVIL ENGINEERING
CHALMERS UNIVERSITY OF TECHNOLOGY
Gothenburg, Sweden 2021
www.chalmers.se

Master's thesis 2021

Reuse of Decommissioned Wind Turbine Blades in Pedestrian Bridges

Detailed investigation of deflection and dynamic response

JOHAN DAHLÉN
CHRISTOFFER HÄRNBORG

CHALMERS
UNIVERSITY OF TECHNOLOGY

Department of Architecture and Civil Engineering
Division of Structural Engineering
Lightweight Structures
Chalmers University of Technology
Gothenburg, Sweden 2021

Reuse of Decommissioned Wind Turbine Blades in Pedestrian Bridges
Detailed investigation of deflection and dynamic response
JOHAN DAHLÉN, CHRISTOFFER HÄRNBORG

Supervisors: David Nygren & Georgi Nedev, Sweco Sverige AB. Alann André, RISE
Examiner and supervisor: Professor Reza Haghani Dogaheh, Department of Architecture and Civil Engineering, Chalmers University of Technology

Master's Thesis 2021
Department of Architecture and Civil Engineering
Division of Structural Engineering
Lightweight structures
Chalmers University of Technology
SE-412 96 Gothenburg
Telephone +46 31 772 1000

Cover: Illustrative example of parametric study for wind turbine blade sections using finite element analysis.

Typeset in LaTeX
Gothenburg, Sweden 2021

Reuse of decommissioned wind turbine blades in pedestrian bridges
Detailed investigation of deflection and dynamic response
JOHAN DAHLÉN
CHRISTOFFER HÄRNBORG
Department of Architecture and Civil Engineering
Chalmers University of Technology

Abstract

The increasing demand for sustainable energy has led to a rapid growth of wind turbine production. Since wind turbine blades are mainly composed of glass fibre reinforce polymers, which has no viable recycling methods, measures to reuse the blades is necessary to deem the energy production method as a sustainable long term solution. One possibility is to utilise the wind turbine blades as structural components for pedestrian bridges. Serviceability deflections and vibrations is studied to verify the viability of the concept. There are ongoing projects investigating how wind turbine blades can be used for bridge applications, however, little to no dynamic calculations have been performed.

Within the wind turbine blade manufacturing industry there is a corporate secrecy regarding blade design and material constituents due to competitive purposes. This aggravates the existing difficulties of performing accurate analyses of the decommissioned blades for pedestrian bridge applications. However, a data sheet of a 28.3-meter-long wind turbine blade was supplied by its manufacturer which allows for detailed verification validating the models in the present work. To investigate the response for several sections with different lengths extracted from different positions of the blade a parametric script was written. The script is compatible with the finite element software BRIGADE/Plus used for the analyses.

The analyses performed conclude that there might be possibilities of utilising the blades for structural members for pedestrian bridges. For the specific blade and bridge configuration studied, blade sections up to 14.0 meters show promising results and may be possible to proceed with construction. However, it is necessary to note that the longer sections require the stiffest and also largest parts of the blade to be used. Furthermore, when performing sensitivity analyses it was noticed that the results are largely dependent on assumed damping ratio and stiffness properties which are difficult to confidently assess. To validate each concept full-scale testing may be necessary both to validate the material properties and subsequently the dynamic behaviour of the constructed bridge.

Keywords: Wind turbine blades, Fibre reinforced polymer (FRP), Pedestrian bridge, Dynamic response, Finite element analysis, Parametric scripting

Acknowledgements

We would like to acknowledge our supervisors for their support throughout the progression of the master's thesis. David Nygren at Sweco Sverige, studied the reuse of decommissioned wind turbine blades during his master's project the previous year. David has been cooperative regarding his findings and difficulties working with the subject. Georgi Nedev at Sweco Sverige has been keen to share his expertise regarding dynamic behaviour of bridges which has been very much appreciated. Dr. Alann André at RISE has shared his extended knowledge of FRP in infrastructure applications. Alann also arranged a trip where we examined a pair of decommissioned blades which was very much appreciated. Examiner and Supervisor, Prof. Reza Haghani Dogaheh at Chalmers University of Technology has provided much appreciated guidance during the progression of the thesis.

The work was carried out at Sweco Sverige's office in Gothenburg. We are thankful for the opportunity and to everyone at the department for their reception.

Johan Dahlén and Christoffer Härnborg, Gothenburg, May 2021

Contents

1
Introduction

Over the past decades, there has been a rapid increase of the construction of wind turbines due to an increasing demand for renewable energy. In Sweden, over 3000 wind turbines have been installed (Andersen et al., 2016). A primary concern due to this increase is the subsequent increase in decommissioned wind turbines, as the lifetime of wind turbines is 20 to 25 years. By 2034 the annual waste of blade material is estimated to be 28,000 tonnes in Sweden alone. A major problem is that wind turbine blades mainly are made of thermosetting glass fibre reinforced polymers (GFRP), which has no viable recycling method. Environmentally friendly management of the blades plays a vital role in maintaining the concept of wind power as a sustainable energy source.

This project acts as continuation of the master's thesis *Reuse of decommissioned wind turbine blades in pedestrian bridges* by Johanna Kullberg and David Nygren (Nygren & Kullberg, 2020). The main goal of their study was to perform a conceptual study producing a viable bridge configuration using wind turbine blades which is illustrated in Figure 1.1.

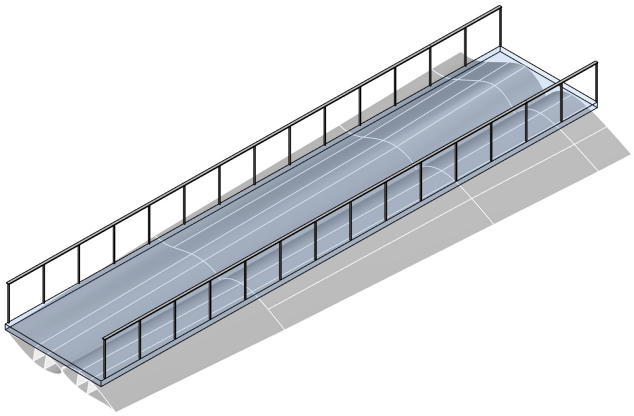

Figure 1.1 Illustration of the most promising blade bridge concept (Nygren & Kullberg, 2020, p. 42)

In addition to the conceptual study, preliminary dynamic calculations resulted in low eigenfrequencies which may cause vibrational discomfort for pedestrians. Due to trade secrets from manufacturers, calculations were based on a downscaled theoretical model with known properties to simulate the most common wind turbine blade used in Sweden, Vestas V90.

For this project, a specification sheet of a 28.3-meter wind turbine blade has been supplied by its manufacturer, ATV composites. The first four eigenfrequencies for the blade are given which can be utilised for verification purposes. Also, sectional properties at different sections such as bending stiffness, mass, and height are given in a table.

Fibre reinforced polymer (FRP) is a relatively new construction material to use in civil engineering applications, and few guidelines and no standards exist in Sweden for the design of FRP structures, such as bridges. Compared to bridges built with traditional construction material, FRP bridges has low mass, low damping and low stiffness which makes it particularly sensitive to dynamic excitation (Živanović et al., 2014). Currently, there is a lack of data on vibrations and dynamic behaviour of FRP structures and current design codes and guidelines is primarily applicable to traditional construction materials only. On the other hand, previous studies suggest that FRP bridges is significantly more responsive to resonant excitation compared to traditional pedestrian bridges, as a result of their low mass (Wei et al., 2019). To be able to use the material in the optimal manner, a better understanding of the dynamic behaviour is needed.

In the year 2000, during the opening day of the Millennium Bridge in London the walking crowd could be seen to cause large lateral movement of the 350-meter steel suspension bridge. The phenomena causing the bridge to sway were caused by the crowd walking in synchronisation with the bridge movement (BBC, 2002). The bridge was closed three days after its inauguration as reparations were considered necessary by the engineers. To prevent the large movement, it was deemed that the viscous and mass dampers had to be added to the structure (Fairs, 2002). The bridge was closed during a 20-month period with an additional cost of £5 million to the original construction cost of £18.2 million. This incident demonstrates that dynamic calculations and verification are crucial when designing pedestrian bridges.

In Denmark a blade bridge is planned to be constructed during 2021 using a set of two 49-meter-long blades with a span length of 23 meters. An interview was conducted with David Stien Pedersen who is involved in the project and has 13 years of experience as a project manager at blade manufacturer Siemens Gamesa. Pedersen indicates that the eigenfrequency for the bridge is low and that there are some concerns regarding the dynamic behaviour of the bridge. For a full summary of the interview together with an illustration of the bridge, see Appendix A.

The Re-wind multidisciplinary research project investigates sustainable re-purposing and recycling of wind turbine blades (Re-Wind, 2021). In the Re-wind project (Suhail et al., 2019), an 8.5 meter long concept pedestrian bridge is designed and planned to be constructed in 2021 using two modified versions of Vestas V27 14.3 meter long wind turbine blades as main girders. The paper concludes that the blades fulfil the criteria with regard to strength in ultimate limit state and deflection criteria in serviceability limit state (SLS) according to Eurocode. Furthermore, the

paper states that the calculated eigenfrequency for the first bending mode of the blade is equal to 5 Hz, and thereby equal to the limit below which verification of accelerations is required. However, the paper makes no attempt to further verify this even though eigenfrequency is to a large extent dependent on several parameters with uncertainties in an early design stage. Furthermore, no conclusions whether vibration performance could be an issue for bridges with longer spans are given.

1.1 Aim and Objectives

The aim is to analyse the response of wind turbine blades when used as the main structural element of pedestrian bridges. To achieve this the following objectives have to be accomplished.

- Perform a literature study to understand the regulations when designing pedestrian bridges. Moreover, a study of the main material used for wind turbine blades manufacturing, fibre reinforced polymers, is necessary.

- Verify the usage of a beam model for the parametric studies by creating a shell model based on equivalent elastic properties and comparing the given four frequencies with the two models. Moreover, a verification using hand calculations should be conducted.

- Create a robust parametric Python script compatible with finite element software BRIGADE/Plus which automatically studies eigenfrequencies, acceleration, and deflection for several blade sections along the blade using equivalent beam sections.

1.2 Methodology

The first objective to perform accurate calculations and consequently achieve reliable results is to implement a literature study. At the present time there are no European standard accounting for the design of fibre reinforced civil engineering structures nor human-induced vibrations. As a result, the reports, *Design of Lightweight Footbridges for Human Induced Vibrations* (EUR 23984 EN) and *Prospect for new guidance in the design of FRP* published by the European Commission – Joint Research Centre which acts as a guidance for development of forthcoming Eurocodes, will be studied. To verify the adoption, other recommendations or codes such as the Dutch *CROW-CUR Recommendation for fibre-reinforced polymers in buildings and civil engineering structures (96:2019)*, *Basis of structural design* (SS-EN 1990) and *Footbridges, assessment of vibrational behaviour of footbridges under pedestrian loading* by Sétra must be reviewed.

A clarification of the design of wind turbine blades including geometry and material constituents will be made. Since a 3D-model of the studied blade has been supplied

by the manufacturer it is possible to create a shell model based on equivalent elastic properties. The model can be optimised to match the known parameters of mass and first four eigenfrequencies for the blade. Utilising and interpolating the supplied sectional mass and stiffness an equivalent beam model can be created using rectangular beam sections. The shell and beam model can be compared with regards to eigenfrequencies and mode shapes to justify the implementation of a beam model for the parametric calculations.

To perform the many analyses required for different span lengths and sections a parametric script must be created, compatible with the finite element software BRIGADE/Plus. The script can be designed to create an equivalent beam for each iteration for which a frequency, acceleration, and deflection analysis can be performed automatically. The analyses should be verified to comply with the recommendations and regulations for designing a footbridge. Moreover, the script and its implementation within the software must be controlled so the calculations is performed as intended. Since the analyses will result in a lot of data a procedure of presenting the results as understandable as possible has to be implemented.

1.3 Limitations

Due to the secrecy within the industry, it is generally difficult to obtain information about the structural composition of wind turbine blades, especially from larger manufacturers producing the most common blades. Therefore, the study is limited to only analysing one type of blade for which data have been supplied.

The load models for dynamic analyses used in this study considers a harmonic load model for pedestrians walking, according to JRC and Sétra. Other guidelines suggest models as harmonic concentrated forces, moving or non-moving, or considering the pedestrian load as a Fourier sum. The aforementioned load models are not considered in this study. In addition, load models for joggers or runners exist. However, the proposed load model for joggers in JRC require specialised programs since it is very difficult to apply with currently used commercial finite element software. Therefore, the load case for joggers is not implemented in this study. Sétra also states that the time joggers spend on the bridge is short and therefore both the time for excessive resonant vibrations to develop, as well as the time joggers may feel discomfort is limited. Therefore, the effect of joggers is not considered.

Furthermore, the study is limited to only study human induced vibrations. Other sources such as wind is not taken into account. Typically, for short span pedestrian bridges dynamic excitation due to wind is not an issue, but due to the abnormal shape of wind turbine blades in combination with its low weight this might be needed to be further investigated.

1.4 Thesis Outline

The thesis contains nine chapters, a bibliography list and 11 appendices

Chapter 1 - Is the introductory chapter presenting the background to the project together with aim, objectives, and limitations.

Chapter 2 - Presents a literature review of fibre reinforced polymers (FRP)

Chapter 3 - Contains a literature review clarifying how to proceed when studying the dynamic response of pedestrian bridges, as well as a review of vibration performance of some FRP footbridges.

Chapter 4 - Visualises the wind turbine blade, NWP28.3 ATV used for the calculations for which sectional stiffness and mass properties together with the first four eigenfrequencies were given.

Chapter 5 - Explains the modelling process were a shell and beam model were created which eigenfrequencies were compared to the frequencies supplied by the manufacture. A verification was made to support the utilisation of the beam model for the parametric script.

Chapter 6 - Contains an explanation of the parametric study with a throughout clarification of the parametric script used for the calculations. Also, the analyses to be made are declared.

Chapter 7 - Illustrates the results from the parametric study for different blade sections together with a sensitivity analysis. The results are summarised in a table highlighting the best section for each span length.

Chapter 8 - Contains a discussion based on the results.

Chapter 9 - States the conclusion of the thesis together with a suggestion for further studies.

2
Fibre Reinforced Polymer

According to Mishnaevsky et al. (2017) modern wind turbine blades are typically made of fibre reinforced polymer (FRP) composite material. In a composite material several constituents with different mechanical properties are combined into one. The resulting new material often has high strength to weight ratio (Damberg, 2001). In FRP materials, fibres with high strength and high modulus of elasticity are combined with a polymer matrix. The fibres, the reinforcing phase, provides strength and stiffness while the continuous phase, the matrix, function as a way to maintain the fibre orientation and as protection of the fibres (Campbell, 2010).

2.1 Fibres

In general, two different types of fibres are used within wind turbine blades, glass and carbon fibre (Mishnaevsky et al., 2017). There are other fibres such as aramid, however, its mechanical properties and high price make it better suitable for other applications (Agarwal et al., 2006). Additional types of fibres are flax fibres and basalt fibres. Flax fibers are a type of plant-based bio-fibers (Yan et al., 2014). Flax fibers can be considered more sustainable in comparison with glass or carbon fibers. It is also cost effective, and it has good mechanical properties that are comparable to those of glass fibers. Basalt fibers, used in mineral-based FRP composites, have low cost, good fire resistance, and thermal properties (Wang et al., 2019). It also has relatively high tensile strength.

2.1.1 Glass Fibre

Due to its relatively low cost, high tensile strength, corrosion resistance, electrical isolating and thermal properties glass fibre has become the conventional fibre for polymer materials. The most common glass fibre is E-glass which indicates its electrical grade as it was first developed for electrical applications. There are other fibres such as S-glass with higher strength, C-glass with better chemical resistance and D-glass with a lower dialectic grade, all compared to E-glass (Damberg, 2001). E-glass is the glass fibre used in wind turbine blades (Beauson & Brøndsted, 2016).

2.1.2 Carbon Fibre

Compared to glass fibre, carbon fibre has better mechanical properties such as higher modulus of elasticity, higher strength, lower weight and superior fatigue life. The disadvantage is the relatively higher cost of the material (Damberg, 2001). However, it is possible to optimise glass fibre polymer structures using the higher stiffness carbon fibre at critical sections.

2.2 Matrices

Fibres need to be embedded into a matrix to be able to transfer loads between them. Apart from protecting the fibres, the matrix material function as a binder and distribute the load between fibres and layers of fibres (Damberg, 2001). The matrix material mainly influences the shear- and compressive strength of the composite material (Agarwal et al., 2006). Polymers are the most commonly used matrix material and mainly two different types of polymers are used, thermosets and thermoplastics.

2.2.1 Thermosets

Thermosets are the most used type of matrix material for manufacturing of wind turbine blades (Mishnaevsky et al., 2017). Advantages of thermosets are that they can be cured in low temperatures and its low viscosity which makes the manufacturing easier. On the other hand, thermosets can not be melted and reshaped and therefore makes them difficult to recycle. In blade manufacturing, polyester is typically used as matrix material in the composite blades, but for larger wind turbine blades epoxy resin is now the most common matrix material.

2.2.2 Thermoplastics

Characteristics for thermoplastic are that it melts when exposed to high temperature, in a range from 80 °C to 200 °C depending on the type of thermoplastic, and is possible to reshape. An advantage of this is that it makes it easier to recycle. Disadvantages are that it is more expensive and the mechanical properties are not as good as for thermosets. In addition, it requires high processing temperature.

2.3 Laminates

Different types of laminates can be utilised depending on their application. The fibres can be unidirectionally oriented for purposes that require high strength in one direction or interlaced together in a weave to achieve high strength in several directions. There are different types of weaves and depending on the weaving pattern different characteristics regarding density, workability, and strength can be achieved. Plain weave is most common although the fibres can be interlaced in other ways such as twill or satin weave (Damberg, 2001).

2.4 Sandwich Panels

Laminates themselves are relatively strong but can have low stiffness in structural applications due to their low thickness. In order to achieve higher stiffness, a core dividing the laminate layers can be used. It adds thickness without increasing the weight much, compared to usage of laminates solely (European Commission - Joint Research Centre [JRC], 2016). Sandwich panels can be compared to a traditional I-beam where the core acts as a shear web while the laminates carry the compressive and tensile forces from bending. This concept implies that the members stiffness can be increased with core thickness.

There are mainly three different types of cores to use for Sandwich panels: foam, honeycomb and solid cores. Foam cores are made of cellular plastics such as polyvinyl chloride (PVC), polyurethane and polyacrylamide. Honeycomb cores which are constructed as a hexagonal grid, most often by aluminium or fibre reinforced polymers. Solid cores are made of wood, usually balsa wood due to its low density (Damberg, 2001).

2.5 Material Properties

CROW (2019) presents indicative values for material properties for FRP. An indicative value means a value that can be used as a reference or to assess the feasibility. Table 2.1 shows indicative values for fibre properties for E-glass fibres and high-strength carbon fibres.

Table 2.1 Indicative values for fibre properties (CROW, 2019)

Material properties	E-glass	HS Carbon
Density [kg/m^3]	2750	1790
Tensile strength $\parallel$ [MPa]	2750	3600
Tensile strength $\perp$ [MPa]	1750	135
Young's modulus $\parallel$ [MPa]	73100	238000
Young's modulus $\perp$ [MPa]	73100	15000
Shear modulus [MPa]	30000	50000

Indicative values for two common thermoset resins, Polyester and Epoxy, are given in Table 2.2.

Table 2.2 Indicative values for thermoset resins (CROW, 2019)

Material properties	Polyester	Epoxy
Density [kg/m^3]	1.2	1.25
Poisson's ratio [-]	0.38	0.39
T_g [°C]	60-100	80-150
Stiffness in tension [MPa]	3550	3100
Shear modulus [MPa]	1350	1500

Indicative values for rigid foam core materials, PVC and PUR, are given in Table 2.3. Due to large variations in density, natural core materials such as balsa wood have a greater variety in material properties. Therefore, no indicative values for balsa wood are given in CROW (2019).

Table 2.3 Indicative values for structural foam core properties (CROW, 2019)

Material properties	PVC	PUR
Density [kg/m^3]	40	50
Elasticity modulus [MPa]	20-30	6-10
Shear modulus [MPa]	10	4-5

2.5.1 Conversion Factors

In order to account for temperature, humidity, creep and fatigue effects for the material properties for FRP, JRC (2016) use conversion factors reducing the material properties. The total conversion factor is calculated as the product of the conversion factors for the separate effects, see Equation (2.1)

$$\eta_c = \eta_{ct} \cdot \eta_{cm} \cdot \eta_{cv} \cdot \eta_{cf} \tag{2.1}$$

where

η_{ct} - Conversion factor due to high temperature effects
= 0.9 or 1.0 depending on the maximum service temperature

η_{cm} - Conversion factor due to humidity and moisture effects
= 0.9 for outdoor conditions with temperatures below 30°C.

η_{cv} - Conversion factor due to creep
= 0.25 to 1.0 depending on load duration class
This factor is disregarded in frequency analyses.

η_{cf} - Conversion factor due to fatigue
= 0.9 in Serviceability limit state (SLS)

2.6 Classical Lamination Theory

FRP laminates are constructed by stacking of layers, laminae, with varying thickness and fibre orientation. The laminae are bonded together and act as a homogeneous structural element (Zoghi, 2013). In classical lamination theory (CLT) the laminate is seen as one homogeneous material with equivalent elastic properties. This is a simplification that assumes that the out-of-plane shear strains are zero. In other words, plane sections perpendicular to the mid plane remains plane after deformation. According to CROW (2019), CLT can be used in design situations to obtain characteristic values for laminate properties using characteristic ply properties.

2.6.1 Equivalent Elastic Properties

From the determined elastic properties of each lamina, the equivalent elastic properties for the laminate can be calculated following the procedure described in Clarke (1996). For an anisotropic material in a two-dimensional status, assuming a thin laminate, Hooke's law is represented by Equation (2.2). The indices 1 and 2 correspond to the directions parallel and perpendicular to the fibre direction.

$$\begin{Bmatrix} \sigma_1 \\ \sigma_2 \\ \tau_{12} \end{Bmatrix} = \underbrace{\begin{bmatrix} Q_{11} & Q_{12} & 0 \\ Q_{12} & Q_{22} & 0 \\ 0 & 0 & Q_{66} \end{bmatrix}}_{Q} \begin{Bmatrix} \epsilon_1 \\ \epsilon_2 \\ \gamma_{12} \end{Bmatrix} \tag{2.2}$$

where

Q - Reduced stiffness matrix

The inverse of Hooke's law for an anisotropic material is represented by Equation (2.3).

$$\begin{Bmatrix} \epsilon_1 \\ \epsilon_2 \\ \gamma_{12} \end{Bmatrix} = \begin{bmatrix} S_{11} & S_{12} & 0 \\ S_{12} & S_{22} & 0 \\ 0 & 0 & S_{66} \end{bmatrix} \begin{Bmatrix} \sigma_1 \\ \sigma_2 \\ \tau_{12} \end{Bmatrix} \tag{2.3}$$

where

S_{ij} - Compliance components

The compliance components can be calculated from the material properties of the lamina, see Equation (2.4) to (2.7).

$$S_{11} = \frac{1}{E_1} \tag{2.4}$$

$$S_{22} = \frac{1}{E_2} \tag{2.5}$$

$$S_{12} = \frac{-\nu_{12}}{E_1} \tag{2.6}$$

$$S_{66} = \frac{1}{G_{12}} \tag{2.7}$$

Since the fibres may be oriented in different directions the transformation matrix (T) from local coordinate system of a lamina to global coordinates is used to obtain the transformed reduced stiffness matrix for a given orientation angle θ, see Equation (2.8).

$$T = \begin{bmatrix} c^2 & s^2 & 2sc \\ s^2 & c^2 & -2sc \\ -sc & sc & c^2 - s^2 \end{bmatrix} \tag{2.8}$$

where

s - $\sin(\theta)$

c - $\cos(\theta)$

The transformed lamina reduced stiffness matrix is calculated using the transformation matrix, see Equation (2.9)

$$\bar{Q} = TQ \tag{2.9}$$

The membrane stiffness matrix terms A_{ij}, the coupling stiffness matrix terms B_{ij} and the bending stiffness matrix terms D_{ij} are shown in Equations (2.10) to (2.12),

where n is the number of laminae in the laminate and h_k is as defined in Figure 2.1.

$$A_{ij} = \sum_{k=1}^{n} (\bar{Q}_{ij})_k (h_k - h_{k-1}) \tag{2.10}$$

$$B_{ij} = \frac{1}{2} \sum_{k=1}^{n} (\bar{Q}_{ij})_k (h_k^2 - h_{k-1}^2) \tag{2.11}$$

$$D_{ij} = \frac{1}{3} \sum_{k=1}^{n} (\bar{Q}_{ij})_k (h_k^3 - h_{k-1}^3) \tag{2.12}$$

Figure 2.1 shows a laminate with n number of plies where h_{k-1} is the distance from mid-plane to the lower surface of the k:th layer and h_k is the distance to the upper surface.

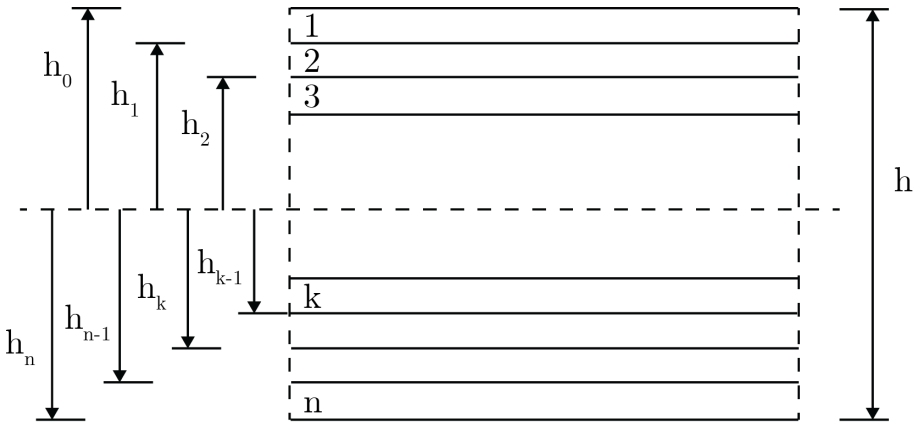

Figure 2.1 Laminate with n number of plies (CROW, 2019)

The compliance terms d_{ij} can then be calculated by inverting the bending stiffness matrix. The equivalent bending elastic constants can then finally be calculated from the compliance terms and total height of the laminate, see Equations (2.13) to (2.16).

$$E_x = \frac{12}{h^3 d_{11}} \tag{2.13}$$

$$E_y = \frac{12}{h^3 d_{22}} \tag{2.14}$$

$$G_{xy} = \frac{12}{h^3 d_{66}} \tag{2.15}$$

$$\nu_{xy} = \frac{-d_{12}}{d_{11}} \tag{2.16}$$

3
Dynamic Response

Fibre reinforced polymer (FRP) bridge structures have relatively low mass and stiffness properties compared to traditional materials such as concrete and steel. These characteristics have shown to increase risk of excessive vibrations due to dynamic loading which in many cases have been governing for the overall design (Russell et al., 2020).

Most often structural bridge members have low eigenfrequencies which result in large risk for resonance from pedestrian induced loading. Resonance develops when an eigenfrequency of the system coincides with the frequency of excitation. For footbridges this can be described as the step frequency from pedestrians. Dynamic actions from other sources such as cyclists can be neglected. The vibrations can generate serviceability problems, however, collapse or even structural damage caused by pedestrian induced vibration is rare according to European Commission - Joint Research Centre, EUR 23984 EN (JRC, 2009) which acts as a basis for the upcoming Eurocode.

Eurocode: Basis of structural design SS-EN 1990/A1:2005, Swedish Standards Institute (SIS, 2005) states that vertical and lateral accelerations must be evaluated for the structure if the eigenfrequency is within certain limits. These limits vary for different standards and codes which must be evaluated since there is not yet a standardised Eurocode published for fibre reinforced polymer bridges. According to JRC (2009) there are different limits for maximum allowable acceleration in vertical and lateral direction depending on the chosen comfort class.

3.1 Design Situation

When designing a footbridge, it is necessary to assess different design situations which may occur during the bridge service life. A design situation consists of a traffic class, an acceptable comfort class and how often it takes place, for example weekly or daily.

3.1.1 Traffic Classes

The load situation of a pedestrian bridge differs between permanent, temporary, and exceptional situations. In order to be able to make reasonable assumptions of load situations, JRC (2009) defines five traffic classes (TC), TC1 to TC5, ranging

from very weak traffic to exceptionally dense traffic. The technical department for transport, roads and bridges engineering and road safety of France (Sétra, 2006) has a similar definition of traffic classes. See Table 3.1 for traffic classes and pedestrian densities.

Table 3.1 Traffic classes and densities in accordance with JRC (2009, p. 14)

Traffic Class	Density (P = pedestrians)	Description
TC1	15 P/A_{Deck}	Very weak traffic
TC2	0.2 P/m^2	Weak traffic
TC3	0.5 P/m^2	Dense traffic
TC4	1.0 P/m^2	Very dense traffic
TC5	1.5 P/m^2	Exceptionally dense traffic

3.1.2 Comfort Classes

To ensure the comfort for pedestrians crossing the bridge there is a set limit for acceleration. JRC (2009) defines limiting accelerations for four comfort classes, CL 1 – CL 4, each corresponding to a degree of comfort as visualised in Table 3.2. In Sweden, CL2, is the recommended minimum comfort criteria (The Swedish Transport Administration [Trafikverket], 2019)

Table 3.2 Comfort classes and its degree of comfort (JRC, 2009, p. 15)

Comfort class	Degree of comfort
CL 1	Maximum
CL 2	Medium
CL 3	Minimum
CL 4	Unacceptable

The perception of motion and vibrations are subjective and depend on several aspects such as number of people on the bridge, height above ground, exposure time, and expectancy of vibration due to the appearance of the bridge. Therefore, the values for limiting accelerations vary between different standards, codes and other literature. For example, Sétra (2006) defines three comfort levels dependent on how perceptible the accelerations are to the user.

3.2 Load Model

In order to calculate the maximum acceleration for the different design situations JRC (2009) implies that two different methods can be used, single degree of freedom

(SDOF) method and the finite element method for which harmonic load models could be utilised.

3.2.1 Load Application

There are two different harmonic models provided by JRC (2009) where the number of equivalent pedestrians (n') on the loaded area differs depending on the traffic class, see Equations 3.2 and 3.3. The equivalent number of pedestrians is included in the general expression for uniformly distributed harmonic load as:

$$p(t) = P \cdot \cos(2\pi f_s t) \cdot n' \cdot \psi \tag{3.1}$$

where

P	-	Force component for a single pedestrian
f_s	-	Step frequency equal to the bridge eigenfrequency
n'	-	Equivalent pedestrians
ψ	-	Reduction coefficient considering if footfall frequency approaches critical eigenfrequency

The dynamic force acting on the bridge, induced by a pedestrian, have components in vertical, lateral, and longitudinal direction. The step frequency of pedestrians when walking, with a high probability of occurrence, varies between 1.25 Hz to 2.3 Hz according to JRC (2009). The magnitude of the force component for a single pedestrian in vertical and longitudinal direction is dependent on the step frequency and the body weight. The lateral component is generated by the shift in centre of gravity when shifting from one foot to the other and has a frequency of half the aforementioned step frequency. The relatively large vertical force component is due to the heel impact and subsequent push-of. The force components in lateral and longitudinal direction are much smaller in comparison with the vertical and are to a larger extent dependent on the way of walking such as posture and arm-swinging and for example type of shoes.

The equivalent stream where each footfall is applied at the rate of the eigenfrequency is derived to cause the same structural vibration as the more realistic case with a stream of random people. The expressions for a number of equivalent pedestrians are derived based on simulations and are described by the total number of pedestrians on the bridge. For TC1 - TC3, also the structural damping affects the number of equivalent pedestrians. (JRC, 2009).

$$\text{For TC1 - TC3:} \qquad n' = \frac{10.8\sqrt{\xi\, n}}{S} \quad \left[\frac{1}{m^2}\right] \tag{3.2}$$

$$\text{For TC4 \& TC5:} \qquad n' = \frac{1.85\sqrt{n}}{S} \quad \left[\frac{1}{m^2}\right] \tag{3.3}$$

where

ξ	-	Structural damping ratio
n	-	Number of pedestrians on loaded area
S	-	Loaded area

The reduction factor ψ (JRC, 2009) is illustrated in Figure 3.1a and 3.1b.

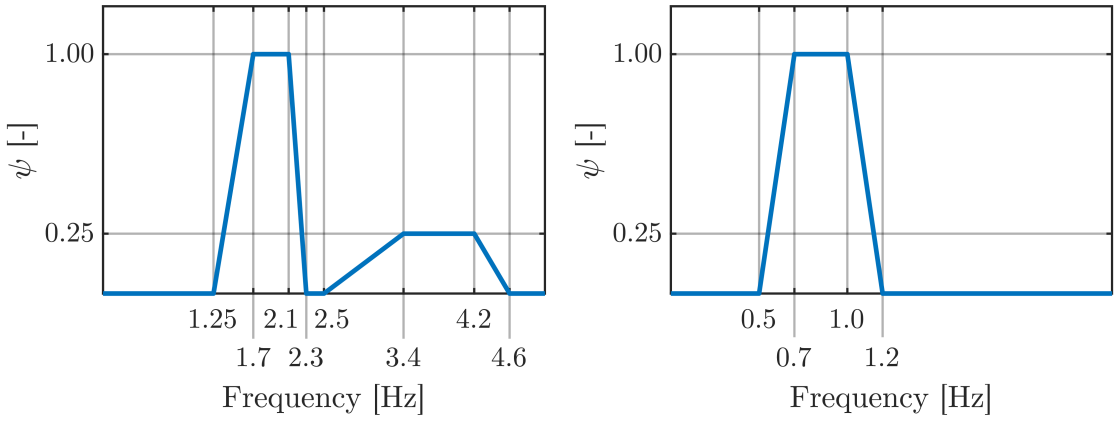

(a) Vertical and longitudinal reduction coefficient

(b) Horizontal reduction coefficient

Figure 3.1 Acceleration load reduction coefficient ψ for different directions (JRC, 2009)

Due to uncertainties when predicting the eigenfrequencies of FRP structures, with regard to structural mass, other non-structural mass such as handrails or effects of connections and supports, CROW (2019) recommends that the reduction for vertical and longitudinal vibrations should be limited to a minimum of 0.25 for frequencies between 2.2 Hz and 3.4 Hz. Otherwise, the uncertainty should be included by a detailed sensitivity analysis of the influencing parameters.

3.2.2 SDOF Method

In general, it is possible to evaluate the acceleration response by modal analysis. The structure oscillation can be described by a linear combination of single degree of freedom (SDOF) systems where each equivalent SDOF has a modal mass and eigenfrequency. Figure 3.2 illustrates the concept of using an equivalent SDOF system for one eigenfrequency, corresponding to one eigenmode, of the bridge.

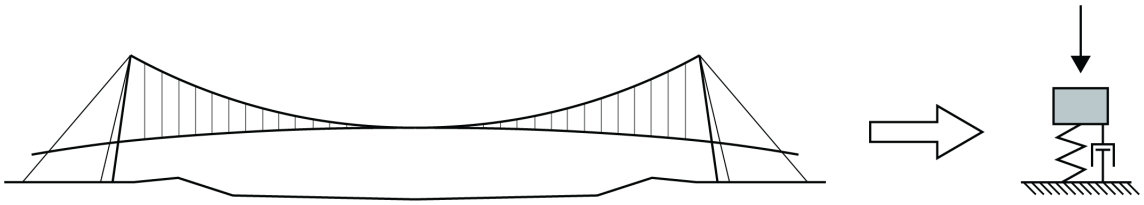

Figure 3.2 Equivalent SDOF oscillator for one natural frequency corresponding to one vibration mode of the structure (JRC, 2009)

The eigenfrequency of a SDOF system can be calculated as in Equation 3.4.

$$f = \frac{1}{2\pi}\sqrt{\frac{K}{M}} \tag{3.4}$$

where

K - Stiffness

M - Mass

For every eigenfrequency of the pedestrian bridge within the critical range of frequencies, an equivalent SDOF system should be used when determining the maximum acceleration, which can be described as in Equation 3.5 (JRC, 2009).

$$a_{max} = \frac{p^*}{m^*}\frac{\pi}{\delta} = \frac{p^*}{m^*}\frac{1}{2\xi} \tag{3.5}$$

where

p^* - Generalised load

m^* - Generalised modal mass

ξ - Structural damping ratio

δ - Logarithmic deduction of damping

For the case of a simply supported beam with constant mass- and stiffness distribution, the generalised mass m^* is described by Equation (3.6) and the generalised load p^* is described by Equation (3.7) for the first mode shape.

$$m^* = \frac{1}{2}\mu L \tag{3.6}$$

$$p^* = \frac{2}{\pi}p(x)L \tag{3.7}$$

where

μ - Mass distribution per length

$p(x)$ - Distributed load

L - Length

3.3 Requirements

In order to satisfy the requirements of pedestrian comfort the bridge should be designed in a way to avoid large accelerations in vertical and lateral directions for certain critical eigenfrequencies.

3.3.1 Eigenfrequency

JRC (2009) states that the acceleration verification should be assessed if the eigenfrequency is in the interval between 1.25 Hz and 2.3 Hz for vertical and longitudinal vibrations and since footbridges may also be excited by the 2^{nd} harmonic load it implies that the interval should be extended to 1.25 Hz and 4.6 Hz. For lateral vibration the critical range is within 0.5 Hz to 1.2 Hz.

Eurocode SS-EN 1990/A1:2005 (SIS, 2005):
Vertical vibrations: $f \leq 5.00$ Hz
Lateral and torsional vibrations: $f \leq 2.50$ Hz

JRC (2009):
Vertical and longitudinal vibrations: $1.25 \text{ Hz} \leq f \leq 4.60$ Hz
Lateral vibrations: $0.50 \text{ Hz} \leq f \leq 1.20$ Hz

3.3.2 Acceleration

Determined by the comfort classes described in Section 3.1.2 JRC (2009) provides criteria for maximum acceleration listed in Table 3.3. These limiting values coincide with the acceleration criteria stated by Sétra (2006).

Table 3.3 Limiting acceleration for different comfort classes in accordance with JRC (2009, p. 15)

Comfort class	Vertical a_{limit} [m/s^2]	Lateral a_{limit} [m/s^2]
CL 1	< 0.50	< 0.10
CL 2	0.50 - 1.00	0.10 - 0.30
CL 3	1.00 - 2.50	0.30 - 0.80
CL 4	> 2.50	> 0.80

3.3.3 Lateral lock-in

Lateral lock-in is a phenomenon that can cause an amplified response and large vibrations in low-damped bridges. When walking, pedestrians repeatedly shift their centre of gravity in lateral direction. The frequency in which the lateral ground reaction forces are applied is, according to JRC (2009) half the walking frequency.

Pedestrians are sensible to lateral vibrations of the bridge and therefore try to compensate the movement, resulting in excitation of the bridge with resonance frequency. The lock-in effect leads to an automatic synchronisation of the pedestrians' walking patterns, which in turn leads to an amplification of the lateral movement (Ingólfsson et al., 2012). Figure 3.3 shows a schematic description of synchronous walking, adapted from JRC (2009).

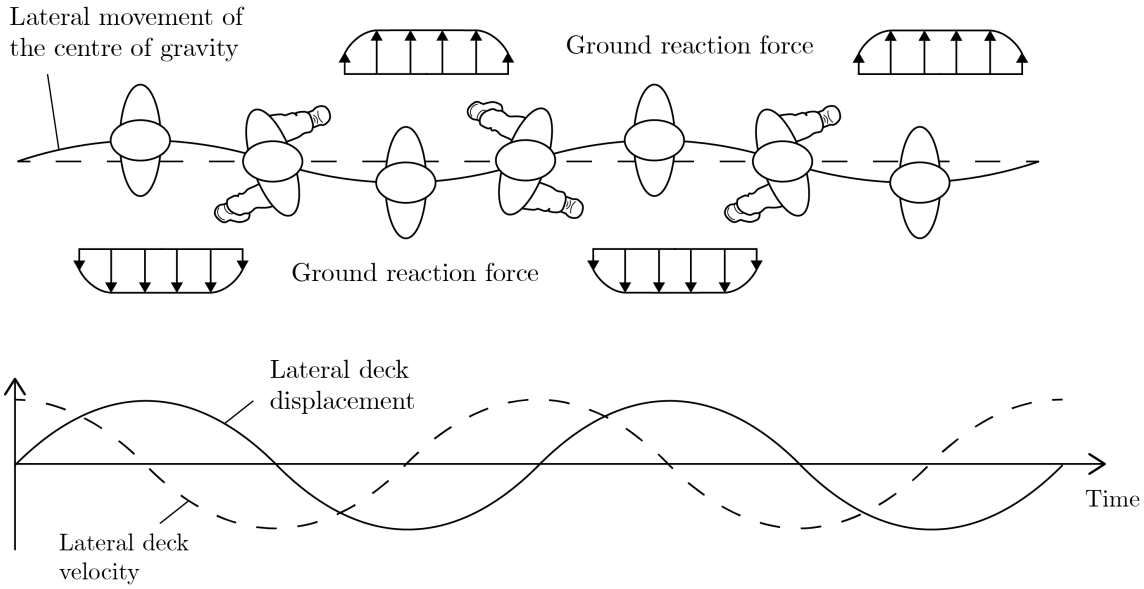

Figure 3.3 Schematic description of synchronous walking (JRC, 2009)

Consequently, the magnitude of the force generated by the pedestrians is proportional to the magnitude of the lateral displacements. This cause and effect cycle may result in movement so large that normal walking no longer is possible. According to JRC (2009), the amplitude of acceleration when the lock-in phenomenon begins is $a_{\text{lock-in}}$ equal to 0.1 to 0.15 m/s^2. Sétra (2006) recommends that for all load situations the horizontal acceleration is limited to 0.1 m/s^2.

3.4 Damping

Theoretically an undamped system can vibrate freely, and the magnitude of the oscillations is constant. However, practically some of the systems' energy is dissipated by the motion of the structure itself or by additional dampers. Therefore the magnitude of the vibrations decreases until it eventually stops. The amount of damping depends on the level of excitation and it has a significant influence on the dynamic response (JRC, 2009).

Damping is a complex phenomenon and it is therefore only possible to accurately assess the damping parameters by performing measurements when the bridge has been constructed. If the results of the dynamic analyses show that the comfort criteria may not be fulfilled with regard to vibrations, the possibility of post-installing dampers should however be considered in the structural design of the pedestrian

bridge (Baus & Schlaich, 2008). Various types of damping systems exist, the most common are viscous dampers and tuned mass dampers (TMD). The viscous damper function by the principle of having a piston dissipate the energy of the excitation force by a viscous fluid. The TMD works as an external mass-spring system tuned to reduce the vibrations for a specific mode when excited by a force close to the eigenfrequency of that mode (Sétra, 2006). One disadvantage for viscous dampers is that in order for them to be effective they require large deflections. Tuned mass dampers, on the other hand, are effective only for a specific frequency range, and they need to have a relatively large mass in relation to the mass of the structure (Baus & Schlaich, 2008).

3.4.1 Rayleigh Damping

Rayleigh damping assumes that the damping is a combination of the system mass and stiffness (JRC, 2009). It is a good assumption for lightly damped systems and when linear behaviour can be expected. The system damping matrix C proportional to the mass matrix M and stiffness matrix K, see Equation 3.8. The relation between the modal damping and the Rayleigh damping factors is described by Equation 3.9.

$$C = \alpha \cdot M + \beta \cdot K \tag{3.8}$$

$$\xi_n = \frac{1}{2}\left(\frac{\alpha}{\omega_n} + \beta\omega_n\right) \tag{3.9}$$

where

ξ_n	-	Modal damping for mode n
ω_n	-	Eigenfrequency for mode n
α, β	-	Rayleigh damping factors

3.4.2 Damping of FRP Structures

JRC (2009) and Sétra (2006) recommend minimum and average damping ratios for some different construction materials, but have no recommendations of damping ratios for FRP. The damping of an FRP material is dependent on multiple factors such as fibre orientation and fibre volume content. According to CROW-CUR Recommendation 96:2019 (CROW, 2019) it is also affected by connections and other construction details.

Table 3.4 shows a summary of recommended damping ratios from JRC report: Prospect for new guidance in design of FRP (JRC, 2016), CROW-CUR Recommendation 96:2019 (CROW, 2019) and the Danish standard for loads and safety of wind turbine construction (Danish Standards Foundation [DS], 2007).

Table 3.4 Recommended damping ratios for glass fibre reinforced polymers

Standard	Minimum [%]	Mean [%]
JRC	1.0	1.5
CROW-CUR	0.5	1.0
DS 472	-	0.8

According to Uyttersprot et al. (2021), these recommended values are too conservative and do not reflect the true dynamic behaviour of FRP pedestrian bridges. This is partly because of the presence of connections within the structure, for example between primary and secondary elements, and due to support conditions. Uyttersprot et al. (2021) state that by applying an increased damping ratio of 4.5% in design it is possible to fulfil serviceability requirements with regard to comfort for slimmer bridges with a lower depth to span ratio. Furthermore, the damping may be even higher due to the fact that lightweight FRP bridges benefit from human induced damping, also referred to as human-structure interaction. Human-structure interaction is a phenomenon where the human body acts as an additional dynamic system interacting with the dynamic system of the structure. Therefore, the human body can be seen as an external damper to the bridge. Current guidelines for design of FRP structures and human induced vibrations, such as (CROW, 2019) and (JRC, 2009) do not take this phenomenon into account which may lead to overconservative assumptions for the damping ratio (Uyttersprot & De Corte, 2021).

In their paper, Uyttersprot and De Corte (2021) present results from measurements of dynamic behaviour of ten web-core sandwich panel FRP footbridges in Belgium. The study concludes that the damping ratio is to a large extent dependent on the number of people interacting with the bridge. Averages of measurements of the different bridges show that for a ratio between pedestrian mass and structural mass of the bridge of about 0.5% the mean value of the damping ratio is 1.7%. When increasing the ratio to 1% the damping ratio increases to an average value of approximately 2.0% and for a ratio between pedestrian mass and structural mass slightly above 2.5% the damping ratio is above 3%.

3.5 Vibration Performance of FRP Footbridges

In their extensive study of dynamic properties for FRP footbridges, Wei et al. (2019) measured the mass, eigenfrequencies, damping ratio and acceleration peaks for six different FRP footbridges and compared the results with the dynamic behaviour of 124 non-FRP footbridges built during the last two decades. The study concludes that for bridges with similar span lengths, deck widths and mode shapes the fundamental frequencies are also similar. On the other hand, comparing the acceleration peaks of FRP bridges to conventional footbridges a large difference is present and the FRP bridges are approximately 3.5 times more responsive to dynamic excitation. This difference is due to the relatively lower mass of FRP structures. However, the

measured damping ratios for the FRP bridges are significantly higher in comparison with conventional footbridges, with a mean value of 2.5%. The results of the measurements also show that the damping ratio increases for higher modes.

An example from Wei et al. (2019) is the single span Parson's pedestrian bridge. The bridge is an all-FRP footbridge in Aberystwyth in Wales. The bridge consists of a box cross-section and it spans 16.9 meters. The total mass of the bridge is approximately 1800 kg. The bridge was excited by a force representing the second harmonic matching the eigenfrequency of the bridge at 4.88 Hz. The resulting acceleration is illustrated in Figure 3.4 with a peak of around 5 m/s^2

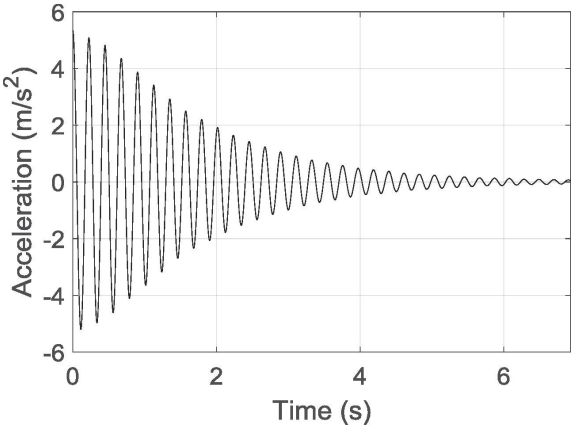

Figure 3.4 Filtered frequency decay at the mid-span of the Parson's bridge, by Wei et al. (2019). Measured dynamic properties for FRP footbridges and their critical comparison against structuresmade of conventional construction materials. Composite Structures. https://doi.org/10.1016/j.compstruct.2019.110956Z, CC BY 4.0

Another bridge studied by Živanović et al. (2020) is a 16.8 meter long, simply supported FRP footbridge. The measured eigenfrequency of the first vertical bending mode is 2.35 Hz with a damping ratio of 1.7%, based on a stochastic model of the dynamic force. The peak acceleration is 10 m/s^2 for a pacing frequency matching the eigenfrequency of the bridge. The results were compared with the results of an equivalent simply supported composite steel-concrete bridge, having the same span length and the same eigenfrequency. The peak acceleration for the steel-concrete bridge is around 1.6 m/s^2, hence the peak acceleration is considerably higher for the FRP bridge. Both bridges have been designed in a way that they are particularly sensitive to dynamic excitation, in order to obtain a better comparison. Therefore, the magnitude of the acceleration peaks may not be representative to actual FRP footbridges.

In a study performed by Živanović et al. (2014) the dynamic response of five FRP footbridges was compared to pedestrian bridges built with conventional construction materials. The result indicates that the response of the FRP bridges is livelier in comparison with the other bridges. All bridges in the study have similar span lengths and natural frequencies. The study claims that the ranges for critical fre-

quencies given in traditional codes, for example avoiding eigenfrequencies below 5Hz for vertical bending modes might not be applicable. This is because they imply that bridges with similar mode shapes and eigenfrequencies have similar dynamic response, but this may not be the case when comparing FRP pedestrian bridges with conventional pedestrian bridges.

4

Nordic Windpower NWP28.3 ATV Blade

Two wind turbine blades of model Nordic Wind Power NWP28.3 ATV has been disassembled and stored on the site by the owner. The owner of the wind turbine has supplied a data sheet of the blades from the manufacturer which includes technical information such as sectional properties for mass and stiffness together with measurements of the four first eigenfrequencies. A trip was arranged to visit the site of the blades to get a perception of geometries and the response when subjecting the member to pedestrian forces such as walking and jumping. A picture of the blade from the visit is illustrated in Figure 4.1

Figure 4.1 Decommissioned NWP28.3 ATV blade near Halmstad, Sweden

Cross-sectional data for the blade at different radii including mass as well as vertical and horizontal stiffness has been supplied by the manufacturer together with a computer model of the blade geometry. Therefore, both a finite element shell and beam model of the blade can be created The beam model can be verified by comparing the behaviour with the shell model and the given first four eigenfrequencies for the blade.

4.1 Blade Geometry

The studied blade, NWP28.3 ATV, is 28.3 meters long including the 3.8 meter blade tip not included in the analysis implying that the length of the blade to be studied is

24.5 meters. The geometry of the blade is based on NACA 6-series airfoils which were developed by the National Advisory Committee for Aeronautics at the beginning of 1940 for aircraft applications (Ladson & Brooks Jr, 1974). The specific NACA 6-series airfoil for the blade is NACA 63-4XX where the second index indicates the tenth of chord position with minimum pressure area and third the lift coefficient in tenths. The thickness in percentage relative to the chord length is indicated by XX which varies for different sections. The airfoils of the blade are illustrated in Figure 4.2.

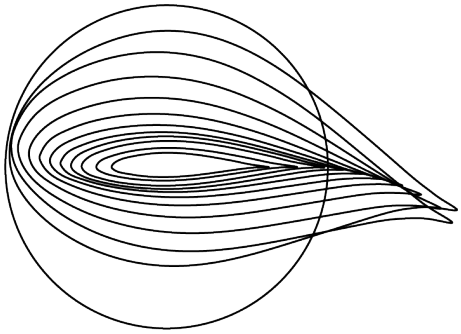

Figure 4.2 Illustration of the NACA 63-4XX Airfoils used for the NWP28.3 ATV blade

4.2 Blade Design and Material Constituents

The blade is made of four main elements: root, shell (leading and trailing edge), spar caps and shear web illustrated in Figure 4.3

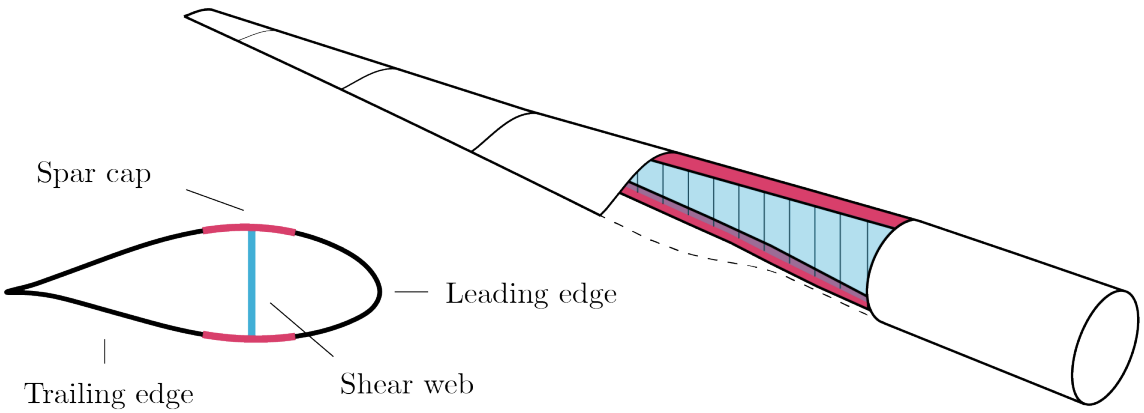

Figure 4.3 Wind turbine blade composition

The cylindrical root of the blade is designed to carry the bending moments to the inserts. The root must be thicker than the other parts to avoid damage of the laminate at the bolt attachments. The root consists of most layers at a direction of +/- 45° together with some unidirectional lamina.

The shell composed of the trailing and leading shell is designed to generate as much lifting force as possible. Cores are used between the thin lamination layers since It is important that the shell is light and stiff enough to avoid buckling (Bladena, 2019).

The spar caps are designed to carry the aerodynamic loads acting on the shell and are mainly subjected to compression or tension. The spar caps are primarily constructed using unidirectional fibres, however, to resist torsion and twisting some fibres with varying orientation should be used. The webs are designed to transfer the shear loads and are relative to the other parts easy to manufacture. It is done by using piles of +/- 45° separated by a core (Bladena, 2019). The combination of the spar caps and shear webs can be compared to a regular beam fixed at one end.

4.3 Material Properties Estimation

The exact material composition and thicknesses are unknown, although some information about material types used for the blade has been supplied by ATV composites. Furthermore, the material composition can be thoroughly approximated using the known mass and stiffness cross-sectional data, using a reverse-engineering procedure. Classical lamination theory described in Section 2.6 is used in order to estimate the material properties for the various elements of the blade, i.e. root, shell, spar cap, and shear web. Elastic lamina properties are based on data from Sandia national laboratories report for an 100 meter baseline wind turbine blade (Griffith & Ashwill, 2011) and the OPTIDAT research program database of reference materials obtained from Alshannaq et al. (2019). These values resemble those used in wind turbine blade production in Europe. Characteristic material properties of unidirectional carbon are taken from Meng (2020). A summary of the used material properties is provided in Table 4.1.

Table 4.1 Representative material properties from OPTIDAT database (Alshannaq et al., 2019)[1], SANDIA SNL 100-00 report (Griffith & Ashwill, 2011)[2] and (Meng, 2020)[3]

	E_1 [MPa]	E_2 [MPa]	G_{12} [MPa]	ν_{12} [-]
Bi-axial[2]	13600	13300	11800	0.49
Tri-axial[1]	24800	11500	4861	0.42
Carbon (UD)[3]	114500	8390	5990	0.27
Foam[2]	256	256	22	0.3

4.4 Sectional Properties

The sectional properties of each section illustrated in Figure 4.4 are listed in Table 4.2.

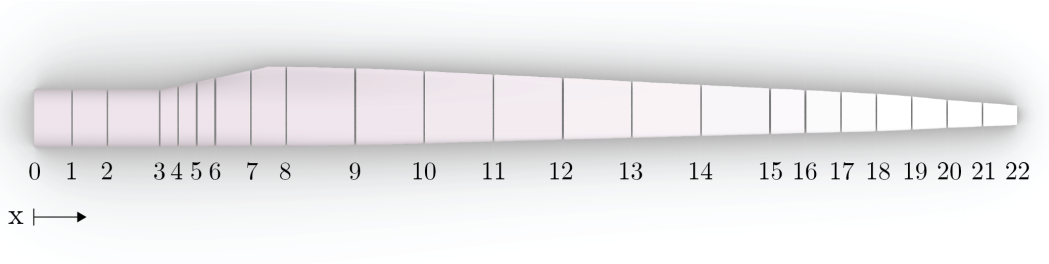

Figure 4.4 Blade sections NWP28.3 ATV

Table 4.2 Sectional blade data NWP28.3 ATV

Section	x-coordinate [m]	Mass [kg/m]	$EI_{vertical}$ [MNm^2]	$EI_{horizontal}$ [MNm^2]
0	0.0	753.6	1310.0	1360.0
1	1.1	286.4	1230.0	1360.0
2	2.1	240.0	863.0	1050.0
3	3.6	240.0	863.0	1050.0
4	4.1	240.0	863.0	1050.0
5	4.6	240.0	863.0	1050.0
6	5.1	216.8	741.0	1050.0
7	6.1	204.8	687.0	1060.0
8	7.1	175.2	406.0	886.0
9	9.1	136.8	219.0	508.0
10	11.1	126.4	127.0	427.0
11	13.1	102.4	68.9	295.0
12	15.1	103.2	39.0	208.0
13	17.1	88.0	22.5	134.0
14	19.1	79.2	16.2	102.0
15	21.1	89.6	9.3	64.4
16	22.1	80.8	6.65	47.3
17	23.1	73.6	4.24	38.2
18	24.1	61.6	2.73	32.0
19	25.1	35.2	1.27	17.1
20	26.1	31.2	0.479	10.2
21	27.1	28.0	0.163	4.85
22	28.1	15.2	0.030	0.97

5
Modelling

The aim of the modelling and analyses was to perform a parametric study for which it could be concluded which blade sections that are suitable to use as bridge members. One shell and one beam model of the blade were implemented. The beam model is more computationally efficient and deemed accurate enough to capture the global response to be studied. However, the beam model should be verified using the more accurate shell model to implement within the parametric studies. The parametric study is performed using scripting in Python 3.0 together with finite element software BRIGADE/Plus with integrated Abaqus FEA solver. Figure 5.1 shows the workflow for the modelling.

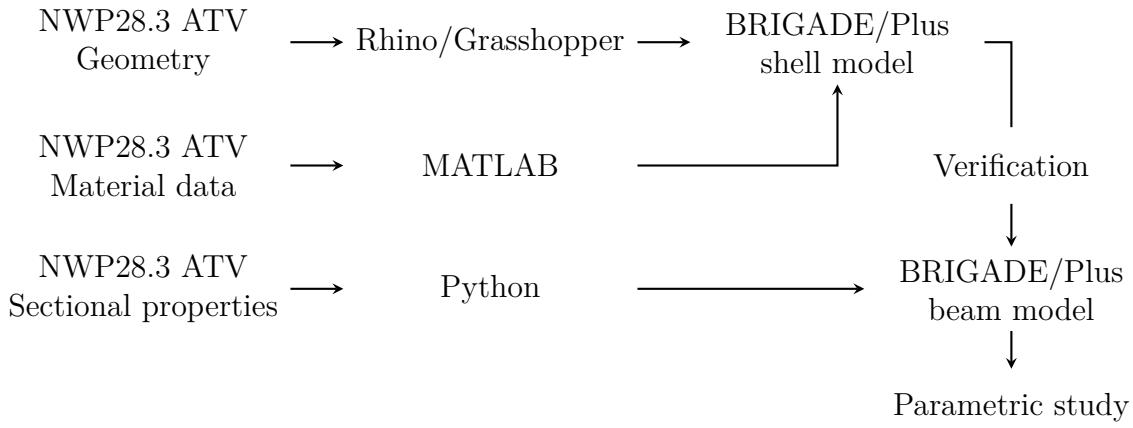

Figure 5.1 Modelling and verification process

5.1 Finite Element Modelling of FRP Structures

CROW (2019) gives guidelines for finite element modelling for analysis of FRP structures. The model should show the expected structural behaviour to a high degree of accuracy. Furthermore, it should be suitable for modelling of FRP structures taking into account properties of laminates and fibre directions and their associated orthotropic properties. Classical lamination theory shall be used for determination of equivalent elastic properties. Time dependent effects such as creep, humidity effects and fatigue should be included when relevant for the performed analysis, by application of conversion factors. When modelling FRP structures it is also important to take shear deformation into account since its contribution can be significant.

This is important when choosing element type for the analysis. In general, element types shall be chosen based on the nature of the situation.

5.1.1 Beam Elements

A beam element is a geometrically simple one-dimensional line element in two- or three-dimensional space, and it utilises beam theory to obtain a one dimensional approximation of a three-dimensional continuum (SIMULIA, 2014, Ch. 29.3.1). It assumes that the behaviour of the beam element can be estimated from defined material properties and beam section profiles. Beam elements in three-dimensional space have six degrees of freedom at each node, three translational degrees of freedom and three rotational degrees of freedom. In a case when the beam element is supposed to represent a non-solid cross section, phenomenon such as local buckling or sectional collapse is not accounted for in beam theory resulting in a possible large difference between the behaviour of the model and the real structure.

In the beam model, two-noded linear, shear deformable elements are used. These elements are suitable for both slender and non-slender beams and are the most effective beam elements in Abaqus (BRIGADE/Plus) according to the Abaqus documentation (SIMULIA, 2014, Ch. 27.1.1).

5.1.2 Shell Elements

A shell element is a two-dimensional element where the thickness is defined as a section property. Shell elements can be used when the thickness is significantly small in comparison to global dimensions such as the distance between supports or the length between nodes in the highest eigenmode of interest (SIMULIA, 2014, Ch. 29.6.1). Shell elements have displacement and rotational degrees of freedom and it assumes, similar to beam theory, that plane sections perpendicular to the mid-surface remain plane.

In the shell model linear four-node shell elements are used. This element is suitable for modelling FRP structures since it takes the influence of shear deformation into account (SIMULIA, 2014, Ch. 29.6.2). Local material directions can be defined for each shell element, representing the orthotropic FRP material (SIMULIA, 2014, Ch. 29.6.1).

5.2 Models

To perform meticulous analyses without exact knowledge of material composition, it was deemed that an optimised model with matching stiffness and mass properties was sufficient for studying the global behaviour. First, the blade was modelled and analysed using shell elements based on geometry supplied by ATV composites. A

model of the blade using equivalent beam elements was then created which structural behaviour was compared to the shell model.

5.2.1 Shell Model

Based on the supplied geometry, the components of the blade were modelled using Rhino 7 and Grasshopper. The components were then exported to BRIGADE/-Plus and to optimise the model Python scripting was utilised to change sectional properties more easily for each component. Stiffness properties were calculated using equivalent elastic properties as described in Section 2.6.1. To achieve a model equivalent to the real blade, the material stiffness and density properties had to be optimised. The blade model in Rhino 7 is illustrated in Figure 5.2

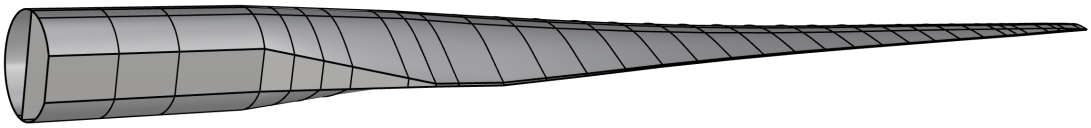

Figure 5.2 Rhino shell model geometry exported to BRIGADE/Plus

Linearly varying properties for stiffness , density and material thickness used for the shell model are shown in Table 5.1.

Table 5.1 Start (at the root) and end (blade tip) values assumed linearly varying for material properties for shell model

	E_1 [GPa]	E_2 [GPa]	G [GPa]	ρ [kg/m^3]	t [mm]
Trailing edge	12.1 - 12.2	12.6 - 12.7	6.6 - 6.7	200 - 1350	40 - 10
Leading edge	12.8 - 12.9	12.6 - 12.7	6.6 - 6.7	200 - 1350	40 - 10
Spar cap	24.5	8.4	3.0	1400 - 1100	20
Web	3.6 - 9.7	3.5 - 9.4	3.0 - 8.3	300 - 800	220 - 30

5.2.2 Beam Model

To achieve a more precise model the given sectional properties of the blade was linearly interpolated using steps of 0.1 meter, see Figure 5.3. This was useful during the parametric study where the blade should be divisible in specific spans.

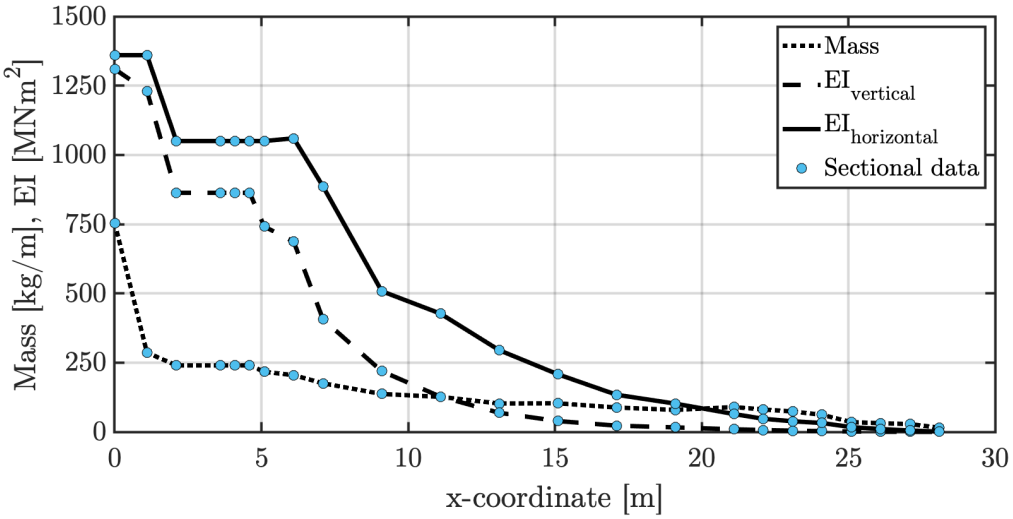

Figure 5.3 Interpolation of given sectional properties

A Python script was written which iterates the sectional geometry for a hollow, rectangular section based on constant stiffness and density to match the given sectional properties. The script was designed such that if the specific sectional property is not within a certain tolerance of the given data it alters the geometry of the section until its vertical and horizontal stiffness together with mass properties is within the tolerance. For the stiffness the script alters the total width or height of the section whereas for the mass the thickness is changed. See Section 5.3 for a flowchart describing the beam model iteration.

5.3 Flowchart Beam Model Iteration

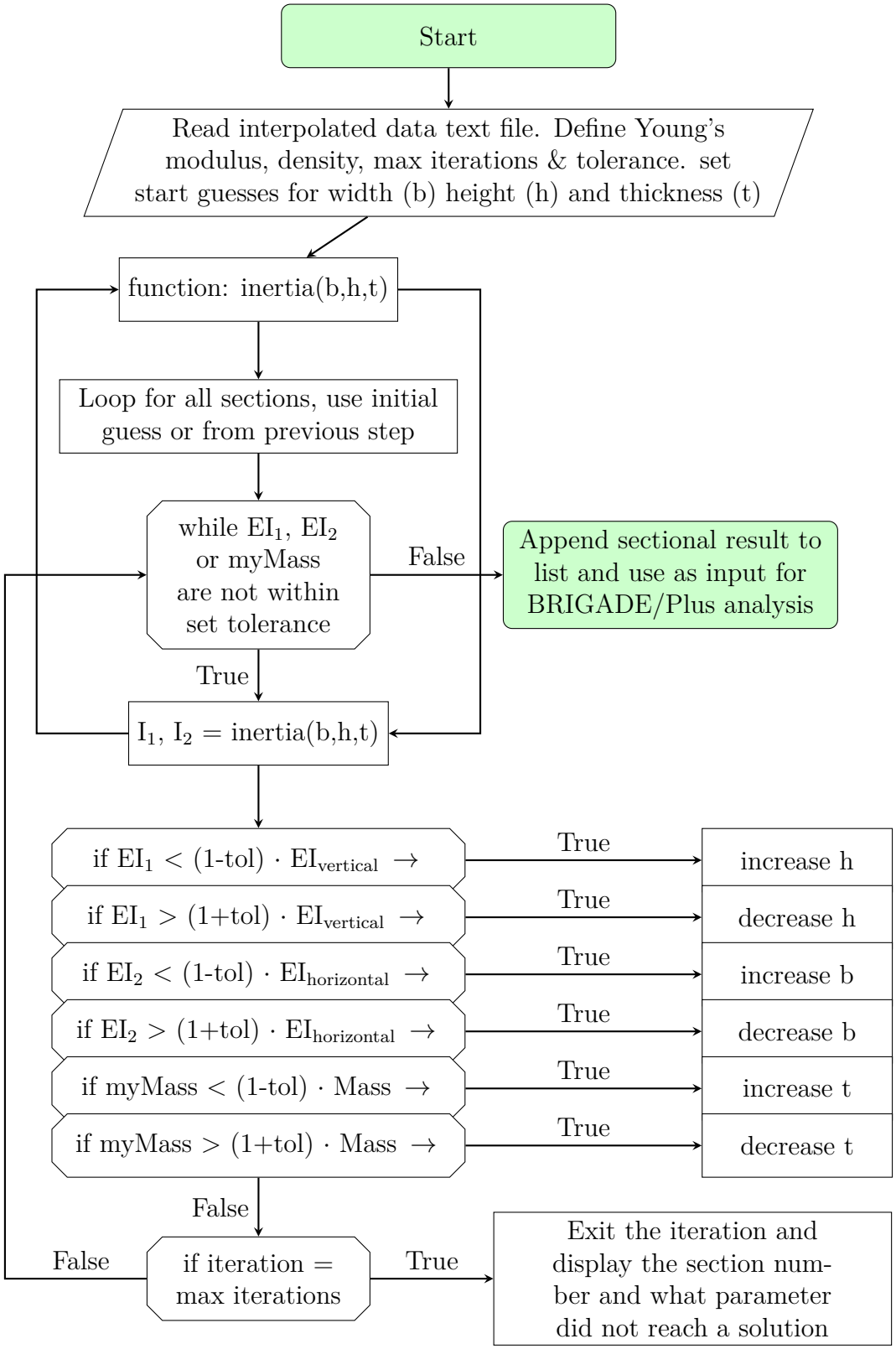

5.4 Verification

To verify the accuracy of the shell and beam model, first a convergence analysis was performed in order to determine sufficient element sizes. Secondly the mass was compared for the blade and the two models. Then a frequency analysis was conducted with fixed root in order to compare the four lowest eigenfrequencies which were supplied by the manufacturer. Finally, a comparison of the modes shapes for the beam and shell model using the modal assurance criterion was conducted. A summary of all verifications is listed in Table 5.4

For an illustration of shell and beam model mode shapes see Appendix B and C respectively. A comparison of all mode shapes for the two models is visualised in Appendix D.

5.4.1 Convergence Analysis

A convergence analysis was conducted to verify that the number of elements in the FE model is sufficient to yield accurate numerical results, see Figure 5.4a. For the beam model it was noted that a converged solution was reached even for fewer elements and that approximately 300 elements will be sufficient to achieve accurate results. A convergence study was also performed with the shell model, see Figure 5.4b. It was noted that it requires a fine mesh (approx. 40,000 elements) in order to reach a converged solution which requires longer computational time.

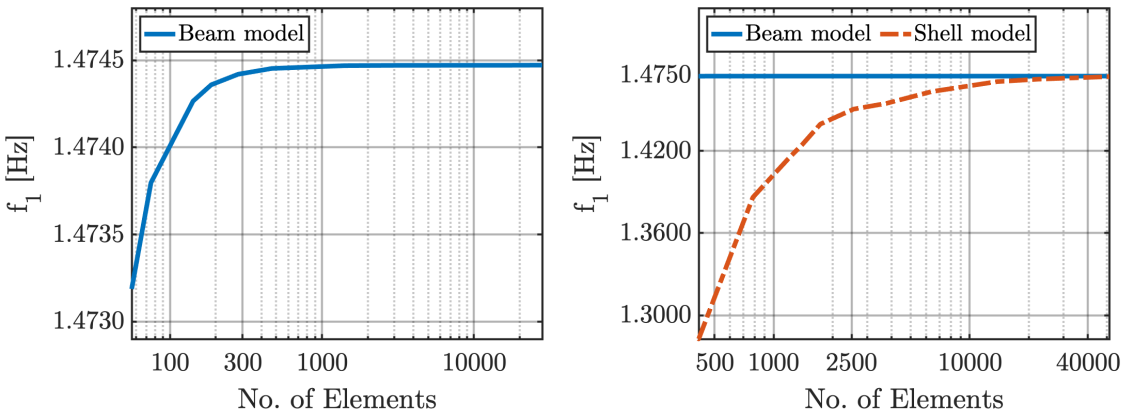

(a) Beam model **(b)** Beam and shell model

Figure 5.4 Convergence analysis for first eigenfrequency (f_1), note the different scaled y-axes

5.4.2 Mass

The mass centre from the root and total mass was compared for the NWP28.3 ATV blade together with the shell and beam model as illustrated in Table 5.2. For the shell model its thickness and density properties for each component (web, leading

edge, trailing edge and spar caps) were designed to match the given mass properties of total mass and mass centre from the root.

Table 5.2 Mass properties for NWP28.3 ATV blade and the shell and beam model

	ATV	Shell Model	Beam Model
Mass centre	9.00 m	9.00 m	9.00 m
Total mass	3852 kg	3849 kg	3849 kg

It was concluded that the two models mass properties match well with the real blade which is significant for obtaining accurate results when analysing the frequency and dynamic response.

5.4.3 Eigenfrequency

The first four eigenfrequencies were given with the blade's sectional properties. A frequency analysis was performed for the two blade models with fixed root to evaluate and verify the model. The results are illustrated in Table 5.3.

Table 5.3 Comparison of the first two eigenfrequencies for NWP28.3 ATV blade, shell and beam model

Mode shape	ATV [Hz]	Shell Model [Hz]	Beam Model [Hz]
1^{st} vertical	1.47	1.47	1.48
1^{st} horizontal	2.47	2.47	2.45
2^{nd} vertical	4.50	4.50	4.45
2^{nd} horizontal	8.74	8.71	8.47

The eigenfrequencies for the two models match well with the given frequencies. Stiffness properties for the shell model were calculated using equivalent elastic properties as described in Section 2.6.1. It was concluded that the equivalent elastic properties result in too high eigenfrequencies compared to the given values which imply that the stiffness is overestimated. To resolve this, the stiffness was adjusted until the eigenfrequencies matched. If the shell model were to be used in the parametric study a more throughout investigation would be necessary, however, as mentioned the exact material composition is difficult to acquire due to secrecy.

5.4.4 Modal Assurance Criterion (MAC)

Modal assurance criterion (MAC) is a way to quantitatively compare mode shapes. It is calculated as shown in Equation 5.1, and can be seen as an approximation of

an orthogonality check of two eigenvectors (Pastor et al., 2012). If the mode shapes are fully correlated the MAC value is equal to one and if they are orthogonal to each other, and thus fully uncorrelated the MAC value is equal to zero. MAC values greater than 0.95 indicates a high degree of consistency and values below 0.8 poor correlation. Figure 5.5 shows the MAC matrix comparing the mode shapes of the shell and beam model.

$$MAC(i,j) = \frac{(\phi_S{}^T \phi_B)^2}{(\phi_S{}^T \phi_S)(\phi_B{}^T \phi_B)} \tag{5.1}$$

where

ϕ_S - mode shape vector of the shell model

ϕ_B - mode shape vector of the beam model

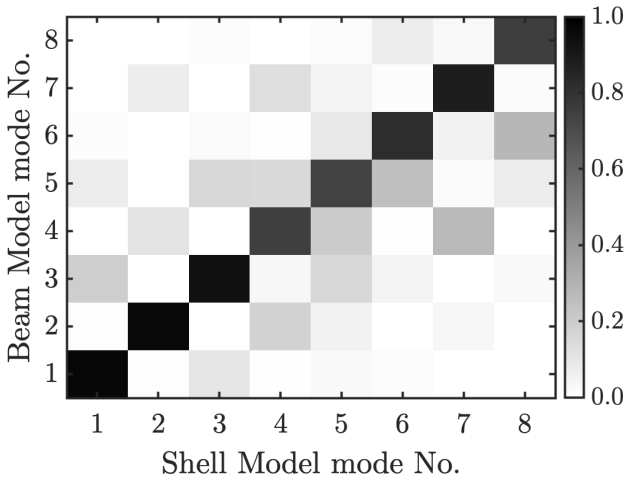

Figure 5.5 Modal assurance criterion matrix

As seen in Figure 5.5, a high correlation between the mode shapes for the first vertical and first horizontal mode with MAC values above 0.95. For higher modes the correlation is slightly lower resulting in an average value of 0.85 of the diagonal entries in the MAC matrix. Consequently, this shows that the beam model is able to resemble the shell model regarding mode shapes accurately for lower modes but less accurate for higher modes. On the other hand, MAC does not take into account differences in frequencies between the two different models. Therefore, a significant shift in frequencies may be present and a comparison of eigenfrequencies is also needed, see a summary in Table 5.4.

5.4.5 Summary

A summary of the verification process is illustrated in Table 5.4. It was concluded that the beam model would yield accurate results for the lower eigenfrequencies

which is critical for human induced vibrations. The beam model is preferable to use during the parametric study since it requires considerably less computational time compared to the shell model. Another advantage utilising the beam model was the simplicity of studying different configurations where for the shell model different geometries would be necessary to model for each case.

Table 5.4 Comparison of the given eigenfrequencies for NWP28.3 ATV blade, shell and beam model together with modal assurance criterion (MAC) for beam and shell model

Mode shape	ATV [Hz]	Shell Model [Hz]	Beam Model [Hz]	MAC [-]
1st vertical	1.47	1.47	1.48	0.97
1st horizontal	2.47	2.47	2.45	0.96
2nd vertical	4.50	4.50	4.45	0.93
2nd horizontal	8.74	8.71	8.47	0.75
3rd vertical	-	9.34	8.48	0.74
4th vertical	-	15.96	14.59	0.82
3rd horizontal	-	20.14	18.18	0.88
5th vertical	-	23.65	22.07	0.76

5.5 Bridge Configuration

The bridge is based on the most promising concept from the conceptual design in Nygren and Kullberg (2020). Two blades are positioned parallel to each other spanning the whole length of the bridge, resulting in a single-symmetric bridge configuration as illustrated in Figure 5.6. The blades are not directly connected to each other and is assumed to act separately.

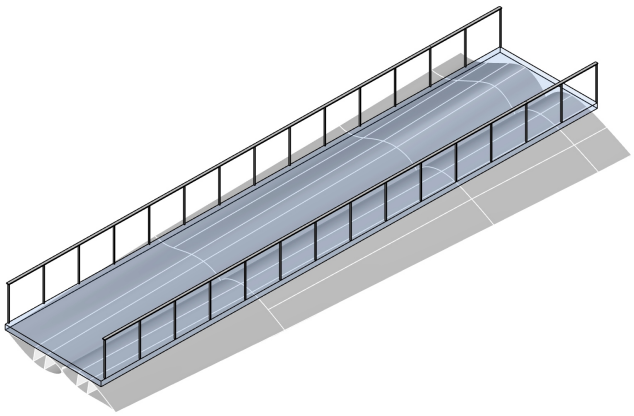

Figure 5.6 Blade bridge concept (Nygren & Kullberg, 2020, p. 42)

The analyses are done for two different support configurations. In the main configuration the bridge is simply supported with one span, but in the case of exceeding limits for deflection or acceleration for large spans an additional intermediate support can be added in the analysis to evaluate the feasibility. Furthermore, since the bending stiffness in horizontal direction is larger it is possible to perform the analyses with the blades rotated 90 degrees, as illustrated in Figure 5.7.

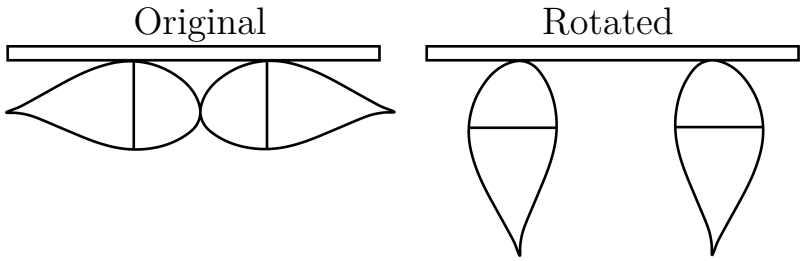

Figure 5.7 Illustration of the original and rotated blade composition

5.6 Implementation

To verify the usage of the blade as structural member the accelerations and deflections in SLS has to be calculated. The two blades were assumed to act independently of each other implying that symmetry of the concept can be utilised for the analyses.

The different design situations which are expected to occur during the bridge service life are to be decided by the designer. For this case two different dimensioning situations were decided for the bridge, service state and exceptional situation which is listed in Table 5.5.

Table 5.5 Chosen design situations of traffic class and comfort class

	Traffic class	Pedestrian density	Comfort class
Service state	TC3	0.5 P/m^2	CL2
Exceptional situation	TC4	1.0 P/m^2	CL3

The mass from the overlaying deck has to be included in the analysis since the mass affects the eigenfrequencies of the bridge. The additional mass for the concept includes the deck, surfacing and railing and was calculated by Nygren and Kullberg (2020) to be 1.54 kN/m utilising symmetry implying half a deck width of 1.9 meters. This mass was included in the analysis using non structural mass in BRIGADE/Plus.

5.6.1 Boundary Conditions

The bridge was analysed as simply supported implying that the translation is fixed at both ends in vertical and horizontal direction and fixed in longitudinal direction

at one end. The model is free to rotate in all directions at both supports.

5.6.2 Acceleration

The harmonic load based on the number of equivalent pedestrians described in Section 2.3.1 is applied as a distributed force over the entire span of the bridge. In order to obtain the maximum acceleration, the sign of the amplitude of the load is in phase with the mode shape. In the case of a mode with multiple nodes, the mode shape changes direction, implying full synchronisation between all pedestrians interacting with the bridge and the direction of the mode shape, see Figure 5.8 (Sétra, 2006).

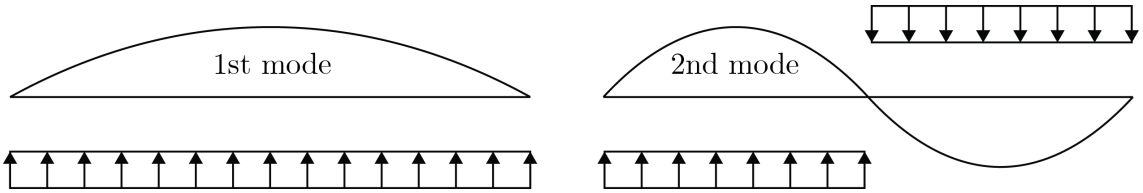

Figure 5.8 Acceleration load application (Sétra, 2006)

According to JRC (2009, p. 28) the force component for a single pedestrian is 280 N in vertical direction, 140 N in longitudinal direction and 35 N in horizontal direction. Furthermore, each pedestrian has a 700 N contribution to the non-structural mass. In addition to the force component (P in equation 5.2 introduced in Section 3.2.1) the equivalent stream has to be calculated according to Equation 3.2 or 3.3 depending on the traffic class.

$$p(t) = P \cdot \cos(2\pi f_s t) \cdot n' \cdot \psi \tag{5.2}$$

The selected maximum vertical accelerations within the intervals for the comfort classes is listed in Table 5.6.

Table 5.6 Design situations acceleration, limiting values utilised for the analyses

	Comfort class	$a_{v,max}$ [m/s^2]	$a_{h,max}$ (lock-in) [m/s^2]
Service state	CL2	< 0.70	< 0.10
Exceptional situation	CL3	< 1.50	< 0.10

5.6.3 Deflection

In order to verify the structural capabilities of each different bridge section, it is necessary to also verify the maximum serviceability deflection which according to Trafikverket (2019) is 1/400 of the theoretical span. Load model 4 for crowd loading, in SS-EN 1990 (SIS, 2002) consists of a uniformly distributed characteristic design load equal to 5 kPa. This load is reduced by a factor ψ equal to 0.4 according to SS-EN 1990/A1:2005 (SIS, 2005). The design load for deflection and the serviceability

requirement is illustrated in Table 5.7.

Table 5.7 Design criteria for deflection in accordance to Trafikverket (2019)

	Deflection load	Max deflection
All situations	2.0 kPa	L/400

In the case of a continuous bridge in two spans the uniformly distributed load is applied in the span with lower stiffness to obtain the maximum serviceability deflection.

5.6.4 Conversion Factors

Two conversion factors was calculated that accounted for the reduced material properties. In accordance with Section 2.5.1, Equation 2.1 and JRC (2016) values for η_{ct} ,η_{cm}, η_{cv} and η_{cf} were taken as:

η_{ct}	=	0.90	(JRC, 2016, Sec. 2.3.6.1)	Verification of strength
η_{cm}	=	0.90	(JRC, 2016, Tab. 2.5)	Outdoor climate $<$ 30 °C
η_{cv}	=	0.80	(JRC, 2016, Fig. 2.1)	Short term loading
η_{cf}	=	0.90	(JRC, 2016, Sec. 2.3.6.4)	Serviceability verification

Resulting in total conversion factors for frequency and deflection analysis:

$$\eta_{c,frequency} = \eta_{ct} \cdot \eta_{cm} \cdot \eta_{cf} = 0.73$$

$$\eta_{c,deflection} = \eta_{ct} \cdot \eta_{cm} \cdot \eta_{cv} \cdot \eta_{cf} = 0.58$$

5.6.5 Analysis

The dynamic analysis was performed as a modal analysis in BRIGADE/Plus. Modal analysis is based on modal superposition, where the response of the system is expressed as a linear combination of the eigenmodes. The response is determined from the physical properties of the system, mass distribution, stiffness distribution and damping parameters. The mass, stiffness and damping matrices together form a set of differential equations. The modal superposition principle enables a transformation of these equations into a standard eigenvalue problem, which solution gives eigenfrequencies and the mode shapes as eigenvectors (Fu & He, 2001). The following steps were performed for each analysis.

Step 1: Eigenvalue extraction
Linear perturbation procedure to obtain eigenfrequencies and the corresponding mode shapes. Calculates the response about the base state, in this case the initial

conditions.

Step 2: Steady-state modal analysis step
Based on the extracted modal data from Step 1 a steady-state modal analysis is performed to calculate the steady-state dynamic response of the system to harmonic excitation. The analysis is done as a frequency sweep, applying the load at a series of different frequencies in a user set interval.

Step 3: SLS deflection
A linear elastic static analysis is performed to calculate the deflection in SLS. The load is applied as a line load, taking into account the width of the bridge deck.

5.6.6 Comparison with Analytical Calculations

To validate the implementation of the analysis steps a basic model representing a problem with a well-established analytical solution was set up. See Appendix E for the analytical calculations. Analytical solutions were compared to the results of the finite element analysis of a further simplified beam model, with constant cross section, constant stiffness and uniform mass distribution. The mass and stiffness properties were chosen arbitrarily but in a way to avoid frequencies in the slanted parts of the graphs for vertical and horizontal reduction coefficients. This was done in order to ensure the same reduction factors for both the analytical calculations and the FE-analysis. The eigenfrequencies and maximum acceleration for TC3 were computed using the SDOF method. A comparison between the computed maximum deflection in SLS, the first two vertical eigenfrequencies, and maximum accelerations is shown in Table 5.8.

Table 5.8 Comparison between the results of FE-analysis and analytical calculation

	FE-analysis	Analytical	Difference
Deflection in SLS	30.4 mm	29.9 mm	1.7 %
1^{st} vertical	3.4 Hz	3.5 Hz	2.9 %
1^{st} horizontal	4.8 Hz	4.9 Hz	2.1 %
2^{nd} vertical	13.3 Hz	13.9 Hz	4.4 %
2^{nd} horizontal	18.1 Hz	19.7 Hz	8.5 %
Maximum acceleration	2.6 m/s^2	2.6 m/s^2	0.0 %

6
Parametric Study

A parametric study was conducted to study numerous blade sections for which the human-induced accelerations and deflections could be evaluated. The parametric study aimed to conclude which sections were suitable for footbridge applications. Also, sensitivity studies were performed with varying stiffness and damping properties. Visualised in Figure 6.1 is a simple example of how the parametric studies for varying blade sections were conducted.

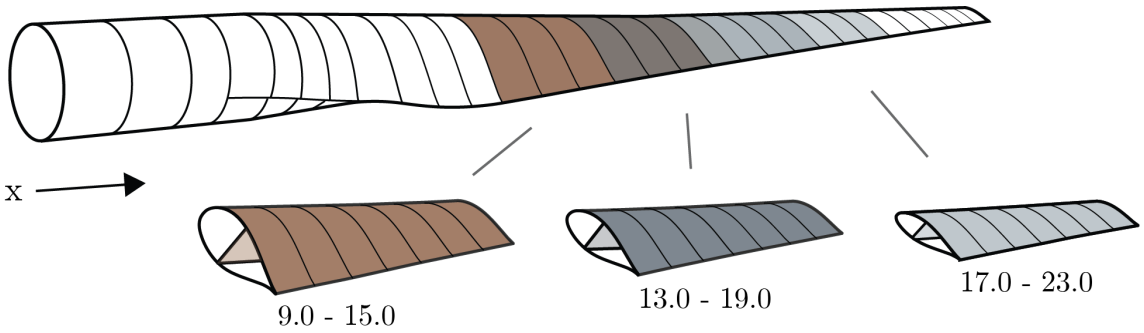

Figure 6.1 Simple illustrative example of parametric study. For this case the section of the blade between 9.0 to 23.0 meters is studied with step length of 4.0 meters and bridge span equal to 6.0 meters

To conduct the several hundreds of analyses required for the parametric study the process was automated utilising Python scripting which is compatible with BRIGADE/Plus. The Python script is explained in detail in Section 6.1. The full script is included in Appendix F. Furthermore, a verification of the script was made and is outlined in Appendix G.

6.1 Python Scripting

The parametric script was written in Python 3.0 which is compatible with BRIGADE/-Plus. The script was structured to complete all analyses automatically. The computational time was dependent on the number of critical eigenfrequencies for which the accelerations needed to be verified. When one acceleration verification was necessary, one iteration required approximately 20-25 seconds of computational time. See Section 6.1.1 to Section 6.1.9 for a detailed explanation of all steps for the parametric script.

6.1.1 Input Data

First, the range, segment length, and step length were specified together with step length for each iteration. The script was modified to investigate the influence of varying damping ratio and elastic modulus for one specific blade section.

A number of parameters that are constant throughout the analysis were defined. Young's modulus and density had to be specified for the equivalent beam iteration along with the conversion factors influencing the assumed stiffness. Thereafter the mass per pedestrian for the acceleration analysis and variable load for the deflection analysis were defined. Other parameters such as deck width and non-structural mass from the bridge deck were required to obtain accurate results. The maximum critical frequency value for longitudinal, vertical, and horizontal modes was set. If resulting eigenfrequencies were below the critical frequency, acceleration calculations were performed.

6.1.2 Sectional Data

A text file containing the interpolated data, described in Section 5.2.2 was imported. Radial position, vertical and horizontal stiffness properties, blade height and mass per meter for each section were extracted. If the sectional data were out of the specified range the script will exit and display the error. For each iteration only the sectional data within the set interval were extracted.

6.1.3 Loads, Traffic Class, and Comfort Class

Based on the traffic and comfort class specified the mass from pedestrians and the acceleration loads were assigned for each analysis. For verification purposes when performing the analyses all masses and loads were calculated and displayed for each iteration together with start and end coordinate for the span.

6.1.4 Equivalent Beam Iteration

The next step was to calculate the equivalent beam sections. For a detailed description of the beam iteration process see Section 5.3.

6.1.5 BRIGADE/Plus Scripting

A material was created based on user input of density and Young's modulus, reduced with frequency conversion factor, and was constant for all sections. A line was then drawn between starting and endpoint for which all beam sections were applied. Then beam profiles were generated based on the data from the beam iteration

and were assigned to the correct section.

The loads and non-structural mass were to be divided and assigned to each node. First, the length and influence length of each segment were iterated for which the load and mass could be applied. The load and mass, defined per meter, was multiplied with the influence length for each node.

After the loads and mass had been applied, all instances in the model were assembled. Start and end boundary conditions was assigned and then the mesh was created with appropriate mesh sizing as described in Section 5.4.1. After the mesh had been created the frequency step was defined and a job was created and submitted in BRIGADE/Plus.

6.1.6 Frequency and Mode Shape Analysis

When the job is completed, the script iterated through and appends the eigenfrequency for each mode in a list. Since the acceleration application and magnitude were dependent on the mode shape, the script was written to extract all mode shapes. As the acceleration load has to be applied according to Figure 5.8 each nodal position with a change of negative/positive deflection was saved for the acceleration application. The script checked if any of the eigenfrequencies were below the set limit for critical eigenfrequencies and displayed each critical frequency and mode shape.

6.1.7 Acceleration Analysis

First, the vertical and horizontal load reduction was defined according to Figures 3.1a and 3.1b. The acceleration analysis was only performed for the critical eigenfrequencies, if there was none this step was ignored, and the script continues with the deflection analysis. The acceleration load was applied in the same way as the non-structural mass which was done by defining a load on each node. For each critical frequency, the acceleration load and maximum allowed acceleration depending on mode shape was extracted.

Based on the specified traffic class and damping ratio the load reduction for equivalent pedestrians as described in Section 3.2.1 was calculated. If there were no load dividers (1^{st} mode shape) for the acceleration application, the load can be applied in one direction. If load dividers exist (2^{nd} and higher mode shapes) the script changes the direction of load application at the positions for the load dividers (see Figure 5.8). The script also checks if the mode was vertical, horizontal or longitudinal and applied the load in the corresponding x, y or z-direction. In BRIGADE/Plus a steady-state modal step which includes the damping ratio was specified. Then the job was created and submitted for analysis.

6.1.8 Extraction of Acceleration Results

The script extracted the accelerations for all nodes within the defined frequency range. The maximum accelerations were saved in a list for post-processing. The maximum acceleration for the analysis together with maximum allowable acceleration based on traffic class was shown in the BRIGADE/Plus display window for each iteration.

6.1.9 Serviceability Limit State

To verify a blade section, the deflection for SLS should be calculated. The creation of the model was used in the same way as for the frequency and acceleration analyses using the equivalent beam iteration technique. The BRIGADE/Plus scripting was similar to the frequency analyses. What differed was that Young's modulus was reduced with the conversion factor for SLS deflection and that a variable load of 2 kPa was applied for the whole span.

When the analysis was completed, the displacement for each node was extracted and the maximum value was saved and displayed together with the allowed deflection of L/400.

All results of interest were saved to a text file which is automatically named based on the user input and can be used for post-processing the results. See Appendix H for the displayed results for some example iterations in the BRIGADE/Plus message area.

6.2 Varying Span and Section Study

To find blade sections suitable for bridge applications the parametric script was utilised. Sections along the whole length were studied with steps varying between 0.2 meter for the longest to 0.5 meter for the shortest sections resulting in 20-30 iterations for each length. Sectional lengths of 6.0, 8.0, 10.0, 12.0, 14.0, 16.0 and 20.0 meter were studied.

6.3 Sensitivity Studies

Since it is difficult to determine stiffness and damping properties a sensitivity study was performed. The stiffness was altered between 75% and 125%, the analysis was performed for stiffness above 100% to account for the conversion factors which could be overestimated. For the damping ratio, a linear ratio between 0.5% and 2.0% was used.

Furthermore, an analysis with the different traffic classes (TC1 – TC5) was conducted to understand the influence of different pedestrian dynamic loading.

7
Results

The primary goal was to study possible span lengths recovered from different positions of the blade. Due to the large quantity of results, only a selection will be presented in this Chapter, for all results see Appendix J. Moreover, sensitivity analyses were performed to understand the influence of the uncertainty of the exact stiffness and damping properties. Lastly, other possible bridge configurations as utilising a mid-support and different blade orientations were studied.

7.1 Varying Length and Section

Deflection and acceleration with the two different design situations are presented in separate figures for the different span lengths. Since constructional height is of importance the minimum and maximum sectional blade height are visualised in each deflection figure. Each section is distinguished by its starting coordinate as illustrated in Figure 7.1. See Appendix I for a detailed clarification of the result presentation.

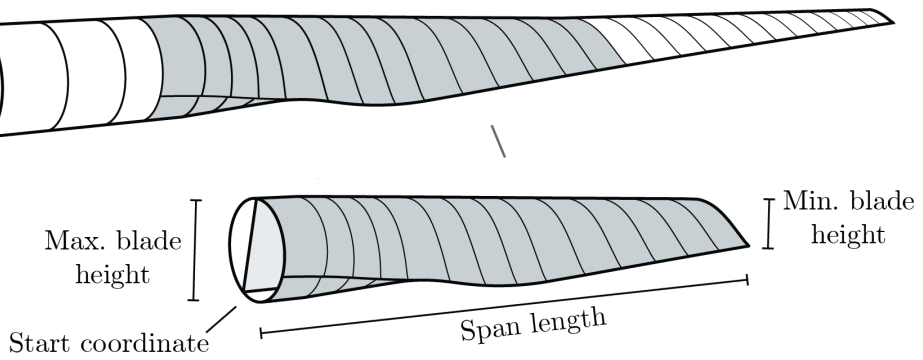

Figure 7.1 Clarification of the span length, max. and min. blade height and start coordinate for each analysis.

The following abbreviations are used when presenting the results in the graphs.

f	-	Frequency
$\mathbf{f_i}$	-	Eigenfrequency for mode nr. i
$\mathbf{A_v}$	-	Vertical acceleration
$\mathbf{A_h}$	-	Horizontal acceleration
$\mathbf{A_{lim}}$	-	Allowable acceleration for mode and traffic class (Table 5.6)
L	-	Section span length
L/400	-	Allowable deflection (Section 5.6.3)
TC	-	Traffic class (Section 3.1.1)
CL	-	Comfort class (Section 3.1.2)

For the span lengths up to 16.0 meters, there were only critical eigenfrequencies for the first vertical mode. For the longer 20.0 meter span there were also critical first horizontal and second vertical modes. The deflection criteria of L/400 are possible for some sections up to 16.0 meters. A summary of the best sections for each studied length is shown in Table 7.1 The best section is characterised by the thinnest member that fulfils the criteria.

7.1.1 Results for 12 Meter Span

Figure 7.2 shows the maximum deflection together with blade height for 12 meter span using different sections of the blade used as simply supported beams in the bridge. As seen, the deflection is below the limit for allowed maximum deflection according to Figure 7.2 for sections with start coordinates up to 7 meters. However, worth noticing is that the maximum blade height is significantly larger for these sections.

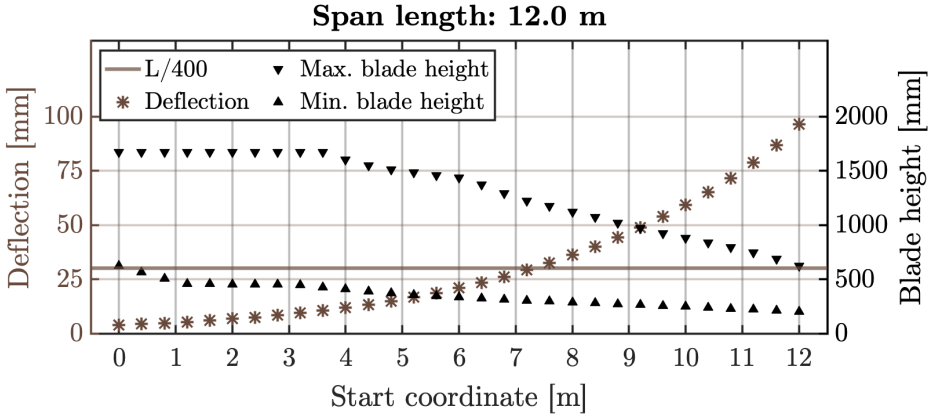

Figure 7.2 Resulting deflection together with minimum and maximum blade height for 12 meter span at different positions.

On the other hand, the sections that are feasible with regard to the deflection criteria as shown in Figure 7.2 are more susceptible to dynamic excitation. This is because the eigenfrequencies for the mode of interest lies within the interval of common walking forcing frequency, between 1.25 Hz and 4.6 Hz considering the first and second harmonic of the pedestrian load. The height of the blade is considerably smaller for these sections, therefore also the total mass resulting in lower eigenfrequency. Figure 7.3 illustrates the eigenfrequency for the first vertical mode for different 12 meter long sections of the blade. It also shows the corresponding peak accelerations for the section. Considering the service state, TC 3, and CL 2 the limiting value of peak acceleration is shown as a horizontal line in Figure 7.3.

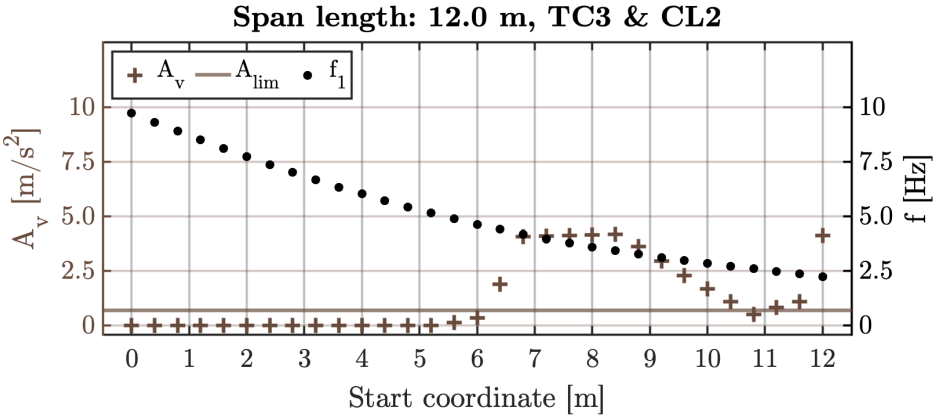

Figure 7.3 Resulting eigenfrequency and acceleration response for 12 meter span at different positions. Service state: TC3 & CL2

The dip in maximum acceleration at an eigenfrequency of 2.5 Hz is expected since this frequency is between the ranges for the first and second harmonic and therefore not prone to dynamic excitation by either one of them. However, due to modelling uncertainties these sections of the blades might not be recommended to use. This is further discussed in Chapter 8.

Figure 7.4 shows the same results as Figure 7.3 but for TC 4 and CL 3. There are several similarities between the two figures, but the higher load in TC4 results in a higher maximum acceleration of over 7.5 m/s^2. The small deviation in frequency is due to the increased mass of pedestrians.

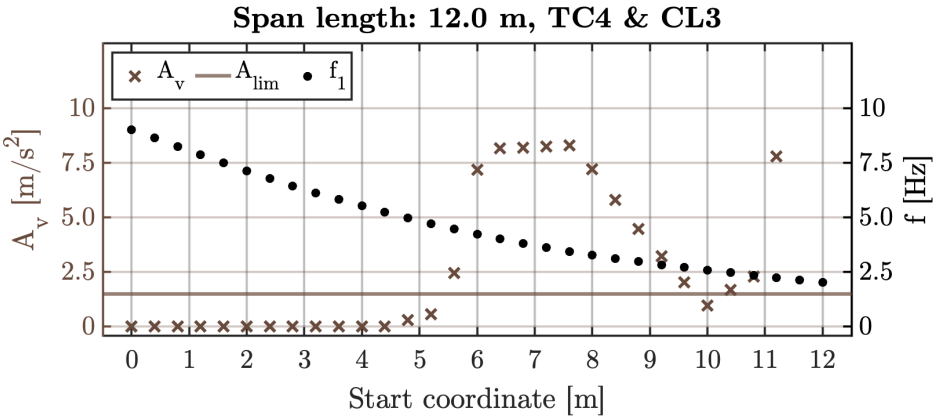

Figure 7.4 Resulting eigenfrequency and acceleration response for 12 meter span at different positions. Exceptional situation: TC4 & CL3

7.1.2 Results for 20 Meter Span

Figure 7.5 illustrates the maximum deflection, the maximum blade height and the minimum blade height for different sections of the blade, now considering a 20 meter long span. In contrast to the results of 12 meter long spans, the deflection is above the limit for all sections of the blade. Furthermore, the maximum and minimum height is almost constant regardless of start coordinate for this long span. This is due to the fact that the thicker root is included for all 20 meter sections.

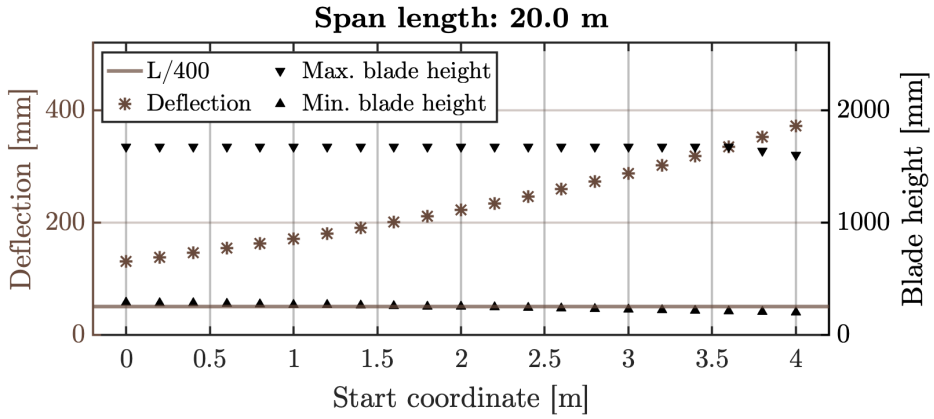

Figure 7.5 Resulting deflection together with minimum and maximum blade height for 20 meter span at different positions.

Hence, also the difference in mass of sections for different start coordinate is less considering 20 meter long sections. Consequently, the difference in eigenfrequency for different sections is less which can be seen in Figure 7.6. The acceleration is almost zero for frequencies up to 1.25 Hz and thereafter increase linearly with frequency up to a limiting maximum value for frequencies coinciding with the most likely frequencies of the first harmonic of the pedestrian load.

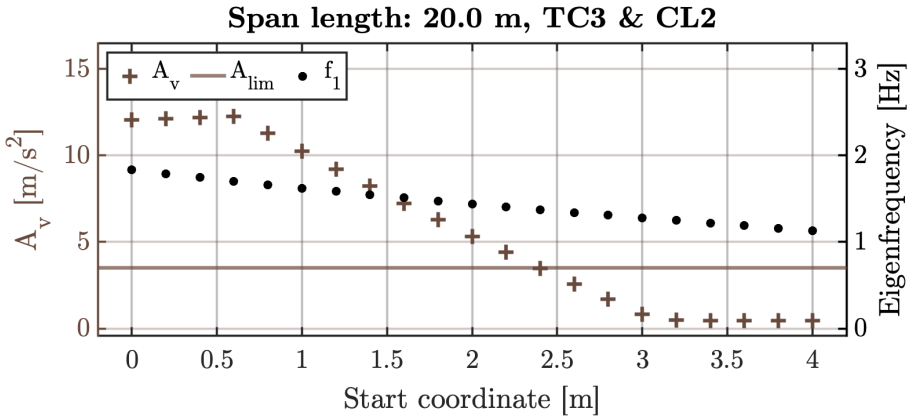

Figure 7.6 Resulting eigenfrequency and acceleration response for 20 meter span at different positions. Service state: TC3 & CL2

Considering the exceptional situation with TC4 and CL3, the eigenfrequency is lower, which is advantageous in this case for the acceleration response. But at the same time, the larger applied acceleration load for TC4 still resulted in an increase in maximum acceleration compared to the service state. The result for the exceptional situation is shown in Figure 7.7.

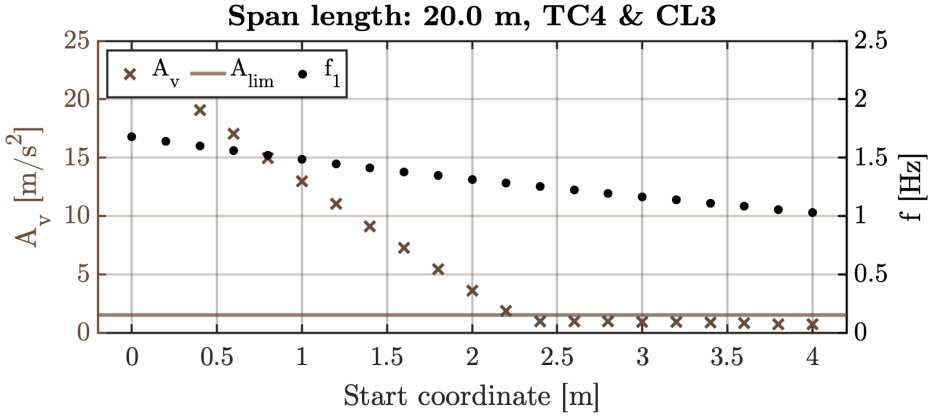

Figure 7.7 Resulting eigenfrequency and acceleration response for 20 meter span at different positions. Exceptional situation: TC4 & CL3

For the 20 meter span and TC4 there are also critical 1st horizontal and 2nd vertical modes for which accelerations had to be analysed. Figure 7.8 illustrates the eigenfrequency and acceleration response for the first horizontal mode for different sections. As seen in Figure 7.8 the horizontal frequencies are in the critical range only for the sections including the thinnest part of the blade. And the acceleration is not close to the critical acceleration for lateral lock-in in the range of 0.1 to 0.15 m/s^2.

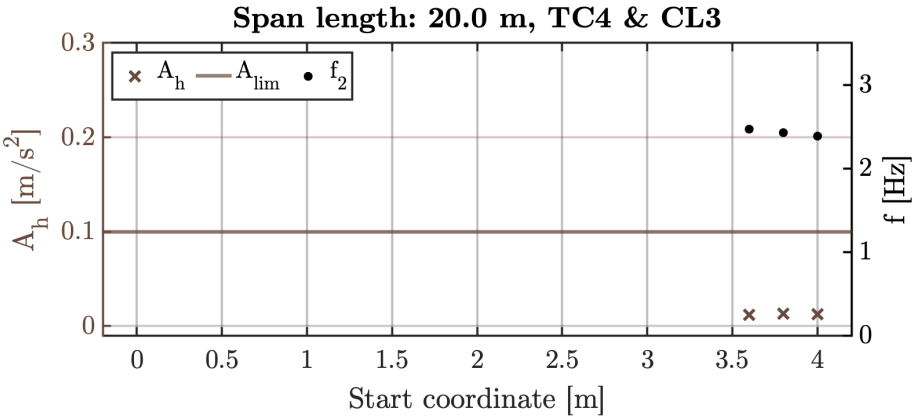

Figure 7.8 Resulting eigenfrequency and acceleration response for 1st horizontal mode for 20 meter span at different positions. Exceptional situation: TC4 & CL3

Figure 7.9 shows the resulting eigenfrequency and acceleration for the second vertical mode for different sections. For sections with start coordinates below 3.4 meters, the eigenfrequencies were above 5 Hz and therefore not included. For start coordinates above 3.4 meters, the eigenfrequency approaches the most critical interval considering the second harmonic. In the same manner, regarding maximum acceleration it Shows a tendency to approach the limit for acceleration for sections that includes the thinner sections.

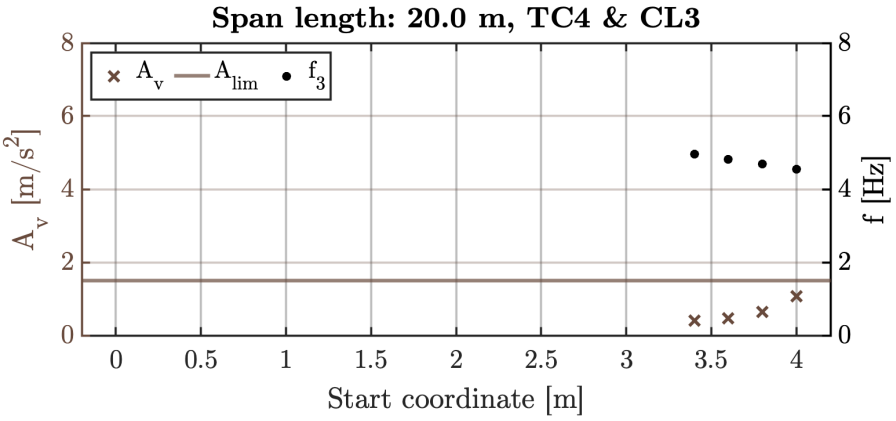

Figure 7.9 Resulting eigenfrequency and acceleration response for 2nd vertical mode for 20 meter span at different positions. Exceptional situation: TC4 & CL3

The optimal bridge sections for each studied length are visualised in Table 7.1. The best bridge section is characterised by the section that fulfils the deflection and acceleration criteria and has the lowest height. For the 16-meter span there are sections that fulfils the deflection but not the acceleration criteria and vice versa. For the 20-meter span there are no sections that fulfils the deflection criteria. Some sections satisfy the acceleration criteria but with large resulting deflections.

Table 7.1 The best sections for each span length characterised by the lowest constructional height.

Span length [m]	Start coord. [m]	Max. height [mm]	Deflection	Acceleration
6.0	18.0	333.7	✓	✓
8.0	14.5	452.0	✓	✓
10.0	9.0	993.8	✓	✓
12.0	5.2	1485.0	✓	✓
14.0	1.8	1675.0	✓	✓
16.0	1.6	1675.0	✓	✗
20.0	-	1675.0	✗	✗

Since the blade height varies for the sections, it is important to highlight the height along each span. The blade height for the best sections is plotted in Figure 7.10. For the 20-meter span the section with start coordinate of 0.0 meter is used since this section is the closest to fulfil the deflection criteria.

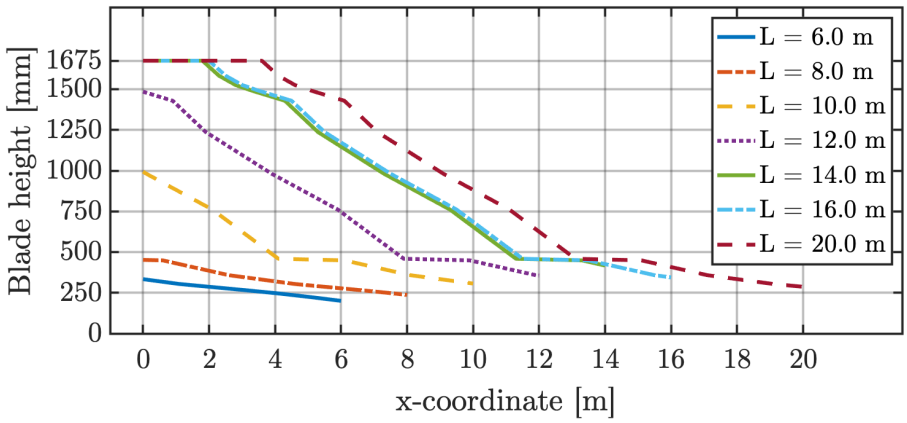

Figure 7.10 Blade height along each of the best blade sections for different span lengths

7.2 Sensitivity Study

The sensitivity analysis is limited to a study of some sections of the 12.0-meter blade section only. Deflections and accelerations for varying stiffness together with accelerations depending on damping and the five traffic classes were examined.

7.2.1 Stiffness

Figure 7.11 shows the maximum deflection with varying stiffness for the case of 12 meter long span with a start coordinate of 6.4 meters. What can be seen is that the

maximum deflection is rather sensitive to change of stiffness. Higher stiffness results in expected lower deflection. And on the contrary, if the stiffness is reduced to 75% of its original value, the resulting deflection is above the limit.

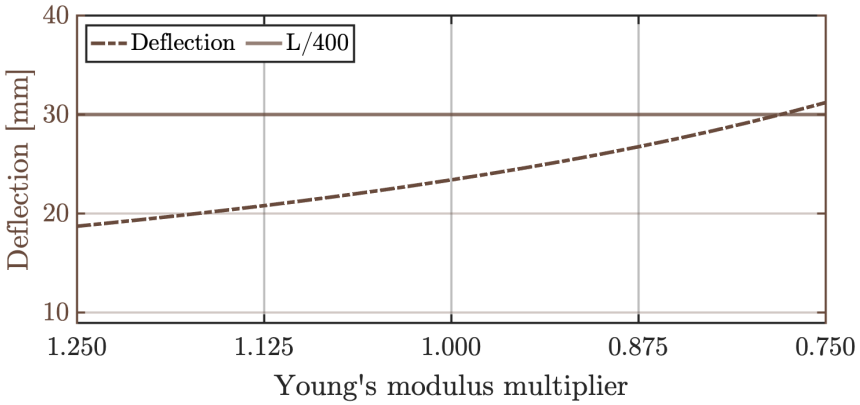

Figure 7.11 Deformations with varying stiffness (L = 12.0 m, start coord. = 6.4 m).

Figure 7.12 shows the acceleration response and eigenfrequency with varying stiffness. The resulting maximum acceleration is to a large extent dependent on the eigenfrequency of the structure. Since the stiffness affects the eigenfrequency, varying the stiffness will affect the acceleration. As seen in Figure 7.12, the frequency is decreasing with increasing stiffness and consequently, the acceleration is increasing when the eigenfrequency approaches the forcing frequency in accordance with the reduction factor.

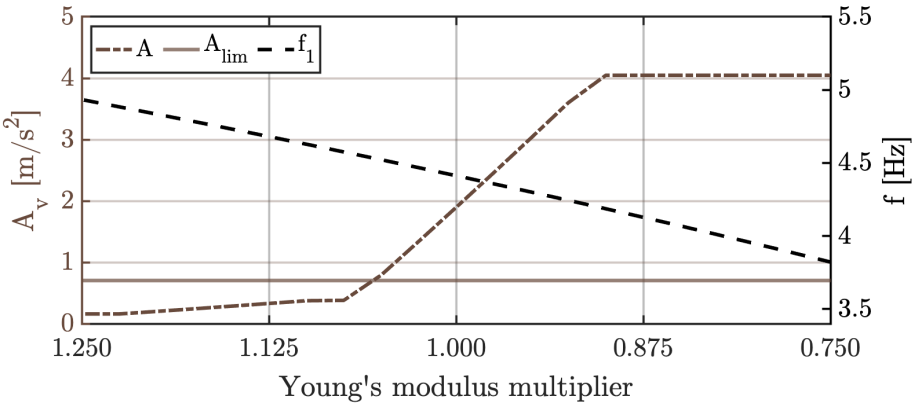

Figure 7.12 Acceleration response and eigenfrequency with varying stiffness, TC3 (L = 12.0 m, start coord. = 6.4 m).

Figure 7.13 shows the eigenfrequencies and corresponding peak accelerations with varying stiffness for TC3 for the same span length of 12 meters but with a start coordinate of 10.8 meters. For this specific case, the acceleration is below the limit for original stiffness since the eigenfrequency is in the interval between the critical frequencies for first and second harmonics. Therefore, both an increase and a de-

crease in stiffness can become critical depending on if the initial eigenfrequency is above or below a critical frequency interval.

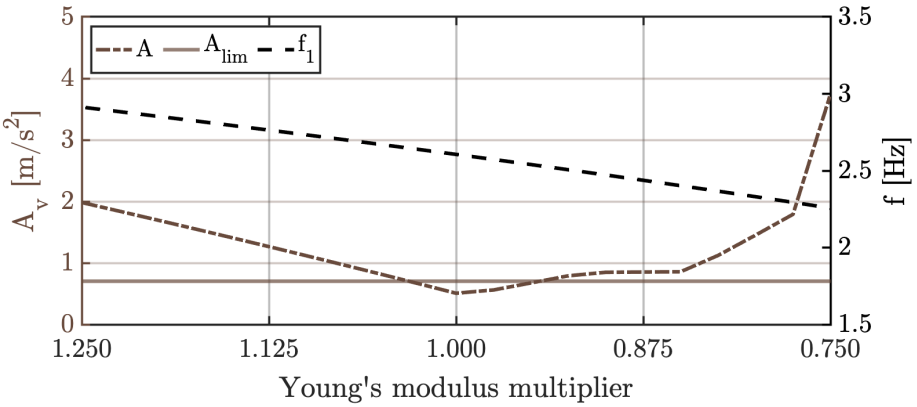

Figure 7.13 Acceleration response and eigenfrequency with varying stiffness, TC3 (L = 12.0 m, start coord. = 10.8 m).

7.2.2 Damping Ratio

Figure 7.14a shows the maximum acceleration with varying damping ratio for traffic classes 1-3. The equivalent pedestrians is plotted in 7.14b since this parameter varies for these traffic classes in accordance with Equation 3.2.

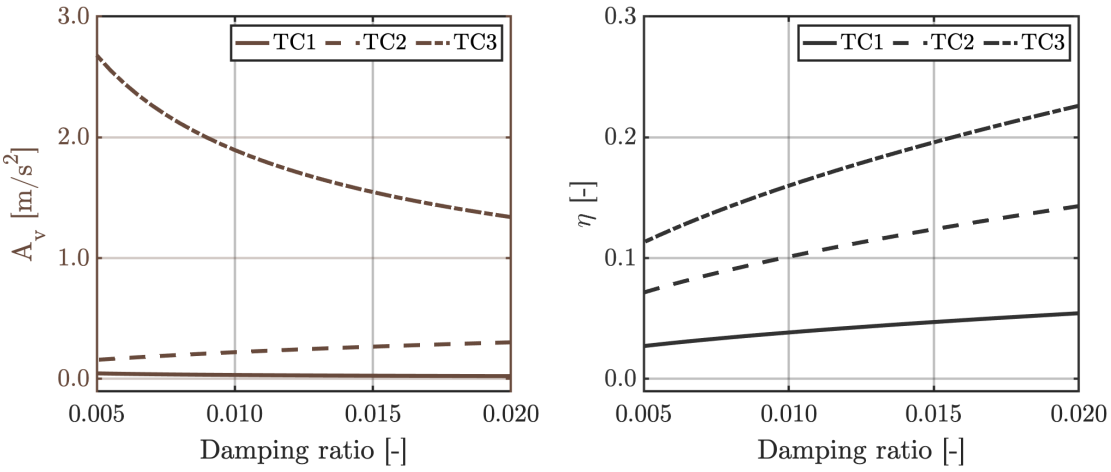

(a) Acceleration response **(b)** Equivalent pedestrians

Figure 7.14 Sensitivity analysis of one blade section (L = 12.0 m, start coord. = 6.4 m) with varying damping ratio and traffic classes 1-3

The acceleration is decreasing with increasing damping ratio for TC3, in agreement with equation 3.5 for maximum acceleration for the SDOF method. For TC2, a small increase of the maximum acceleration with increasing damping ratio can be observed. This may be since the acceleration load is influenced by the equivalent

pedestrians, hence also the damping ratio. Moreover, since the traffic classes have different contribution of pedestrian non-structural mass, the eigenfrequency varies for the different cases which could influence the acceleration response.

Figure 7.15 shows the resulting acceleration for TC4 & TC5. The results are expected since the equivalent pedestrians for these traffic classes are constant in accordance with Equation 3.3 together with the maximum acceleration for the SDOF method (Equation 3.5.)

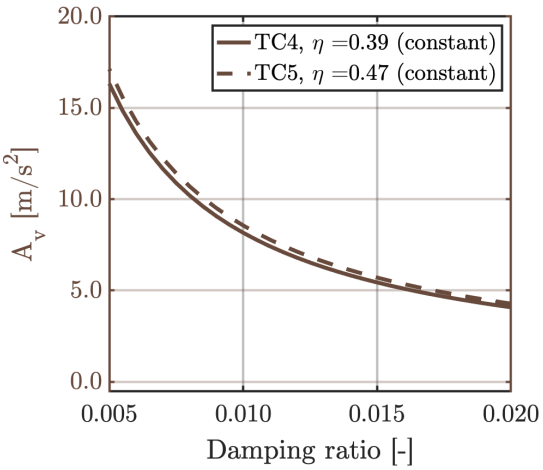

Figure 7.15 Sensitivity analysis of one blade section (L = 12.0 m, start coord. = 6.4 m) with varying damping ratio and traffic classes 4-5

7.2.3 Traffic Classes

The acceleration response for the whole frequency range is plotted in Figure 7.16 for the section of 12.0 meters with start coordinate 6.4 meter for all traffic classes. The peak acceleration occurs at different frequencies for the different traffic classes. This is since the structure has additional non-structural mass for increasing pedestrian density which results in lower eigenfrequencies. This could lead to cases where a less dense traffic class, for example TC3, has higher acceleration response than TC4 as the eigenfrequency for the lighter structure is within the most critical frequency.

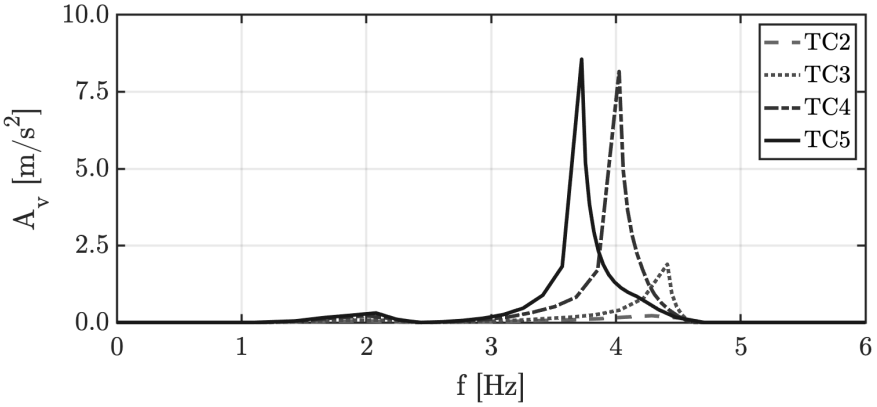

Figure 7.16 Sensitivity analysis of one blade section (L = 12.0 m, start coord. = 6.4 m) for traffic class 2-5 with the whole frequency range visualised. The acceleration for TC1 is zero for all frequencies

The significant difference observed in Figure 7.16 is not expected to be seen for a case with heavier non-FRP bridges where the non-structural mass of the pedestrians is a much smaller percentage of the total mass. In such a case, the peak acceleration is rather insensitive with regard to pedestrian density.

7.3 Alternative Solutions

In addition to the studied bridge configuration as described in Section 5.5 other configurations were studied in order to draw nuanced conclusions. If the surrounding environment allows for higher constructional height or an additional middle support these concepts could allow for longer wind turbine blade bridges.

7.3.1 Blade Orientation

As the longer blade spans has large deflections and the blade's bending stiffness is greater in horizontal direction the deflections should be lower if rotating the blades as illustrated in Figure 5.7.

An analysis was performed with the rotated blades for a span of 16.0 meters which has no viable sections fulfilling both the deflection and acceleration criteria. For the rotated blades it was noticed that the deflection criteria are fulfilled for all sections. However, for accelerations only spans with start coordinates up to 4.0 meters are viable for TC4. Also, it is noticed that the blade height is large, up to 2380 mm for most sections. See Appendix K for the resulting deflections and accelerations.

7.3.2 Additional Mid-support

An alternative solution, if the bridge for a specific configuration does not fulfil the criteria for maximum deflection or the criteria for maximum acceleration, can be to add an additional mid-support. Modification of the parametric script, including an

additional boundary condition for the centre node, constraining motion in vertical and lateral direction. Analyses was performed assuming a damping ratio of 1%. For the calculation of maximum deflection, the load was applied only in the weakest span. The resulting deflection and acceleration are presented in Table 7.2 for best sections fulfilling deflection and acceleration criteria for TC3.

Table 7.2 Results with an additional mid-support for TC3

Length	Start coord.	Max. height	Deflection	f_1	A_v
18.0 m	6.0 m	961 mm	22.4 mm	4.66 Hz	0.35 m/s^2
20.0 m	3.0 m	1675 mm	21.6 mm	4.75 Hz	0.26 m/s^2
22.0 m	0.0 m	1675 mm	20.8 mm	4.84 Hz	0.22 m/s^2

Table 7.3 shows the resulting deflection, eigenfrequency for the first vertical bending mode and maximum acceleration, for best sections fulfilling the deflection and acceleration criteria for TC4.

Table 7.3 Results with an additional mid-support for TC4

Length	Start coord.	Max. height	Deflection	f_1	A_v
18.0 m	5.0 m	961 mm	22.4 mm	4.87 Hz	0.46 m/s^2
20.0 m	2.0 m	1675 mm	16.7 mm	4.89 Hz	0.42 m/s^2
22.0 m	0.0 m	1675 mm	20.8 mm	4.39 Hz	3.75 m/s^2

8

Discussion

The aim has been to study and find viable blade sections appropriate for pedestrian bridge construction. From the beginning there were concerns that the whole blade would be capable of fulfilling neither the deflection nor the vibrational comfort criteria. This was confirmed early in the process, for confirmation, see the results of the longest studied section of 20.0 meter presented in Section 7.1.2. Another reasoning for studying specific sections extracted from a blade is that some sections has large constructional height which may have negative effects for the overall structure and surroundings. Moreover, this procedure can be utilised for other purposes as evaluation of a damaged blade for which a specific section should be excluded. During the visit of the decommissioned blade as described in Chapter 4 some minor damages on the blade were detected. See Appendix L for a collection of images from the visit.

8.1 Corporate Secrecy

It is troublesome that the large blade manufacturers decline any request of cooperation regarding the structural composition of the blade. However, it is understandable that the manufacturers do not want to supply this information based on secrecy and competitive purposes. It may be necessary for each country's governing body to enforce blade manufacturers to provide an end of life model together with an increased cost of landfill before any further progress can be made. Considering the extensive landfill of the wind turbine blades, it is alarming that wind power is deemed as environmentally friendly by the general public.

8.2 Studied Blade

It is important to assess the size of the members before construction. It was obvious that the size of the blade closest to the root would make sections with a start coordinate close to the root hard to justify. Although for this blade it would be possible to utilise sections with larger constructional height that has a starting point a few meters from the root. An example is the best section for the 12.0 meter span listed in Table 7.1. This section has a notably max height of 1500 mm. However, the height decreases along the blade length to approximately 350 mm as visualised in Figure 7.10. It is important to emphasise that newer and longer blades may have a

more optimised design enabling longer sections to be used for bridge construction.

8.3 Parametric Script

The parametric script developed for the analyses was written to be fully automated using a text file of sectional vertical and horizontal bending stiffness together with mass. Implying that any blade or other structure can be analysed if these parameters are known. For these analyses the height of each section was also included, it was not used for any calculations but to demonstrate its influence on the results. It is possible that the linear interpolation to 0.1 meter spacing using the supplied data as illustrated in Figure 5.3 is not fully accurate. However, after performing a verification of the beam model comparing its total mass, mass centre and eigenfrequencies to the given blade data and optimised shell model the beam model was deemed satisfactory. The verification is summarised in Table 5.2 and Table 5.3. On the contrary, the beam model is not able to accurately describe higher order mode shapes as described in Section 5.4.4. However, since the analyses shows that only the first, or second mode shape is within the critical frequency ranges and since the modal assurance criterion show good correlation for these modes together with similar eigenfrequencies as illustrated in Table 5.4, the beam model is usable.

8.4 Damping

In the performed analyses a constant damping ratio of 1% was assumed for all modes, this may not be a realistic assumption since measurements of FRP pedestrian bridges show that the damping increases for modes with higher eigenfrequency. An alternative could be to use the Rayleigh damping assumption for which the damping is frequency-dependent, but the factors α and β should represent experimentally seen damping behaviour to give accurate results. Assuming a constant damping ratio also enables better control of the input parameter during the parametric analysis Furthermore, studies have shown that even for low frequency modes the assumption of 1% might be too low since they do not take into account the effect of connections within the structure or the effect of human-structure interaction. But since this avoids the risk of having an overdamped system, this assumption is conservative. On the other hand, this means that in cases when the analyses show that the accelerations are a critical design parameter care must be taken when drawing conclusions whether a specific configuration is acceptable in terms of comfort.

8.5 Results

For this specific blade with sections longer than 10 meters it is not possible to achieve a bridge with acceptable accelerations, deflections and low height. A noticed tendency for the studied lengths up to 14.0 meters is that sections with some margin of acceptable deflections most often also fulfils the set acceleration criteria. This correlation is because stiffer sections have lower deflections and higher eigenfrequencies. However, longer lengths of 16.0 meters and above has eigenfrequencies within the critical range for reduction below 4.6 Hz leading to large accelerations for even the stiffest sections. As the results are case sensitive it is difficult to come up with a general suggestion of how to select the most suitable section, especially due to the uncertainty of exact stiffness and damping properties.

8.5.1 Comparison with Measured Dynamic Performance of FRP Bridges

To evaluate the feasibility of the concept, it is of interest to compare the results of the parametric study with measurements of the dynamic behaviour of FRP bridges with similar span lengths and eigenfrequencies. A comparison with the results for a 16 meter long span, presented in Figure J.17 with the measurements of the dynamic performance of a lively 16.8 meter long FRP pedestrian bridge, for a section with similar eigenfrequency of around 2.3 Hz. The bridge studied by Živanović et al. (2020) has a damping ratio of 1.7% compared to the assumed 1%. The peak acceleration for the studied bridge in Živanović et al. (2020) is around 10 m/s^2 and the resulting maximum acceleration in Figure J.17 is above 10 m/s^2. This shows that using the studied blades for longer spans may result in a bridge even more susceptible to dynamic excitation than an FRP bridge specifically designed to be sensitive to pedestrian loads. However, the eigenfrequency is to a large extent dependent on which section to use. If a section including the root is used for a 16 meter long span, the eigenfrequency is higher and closer to the frequency interval for the second harmonic. This can be compared to Parson's bridge (Wei et al., 2019), a 16.9 meter long box section FRP bridge with an eigenfrequency of 4.88 Hz and a peak acceleration of around 5 m/s^2. For a section with similar eigenfrequency in Figure J.17 the acceleration peak is around 2.5 m/s^2 assuming TC3 and around 6 m/s^2 for TC4, see Figure J.18.

8.5.2 Sensitivity Analysis

As there was uncertainty regarding remaining stiffness capacity together with damping ratio a sensitivity analysis was performed to study the influence of the parameters. The estimated stiffness of the blade is largely dependent on the reducing conversion factor. Since the reduction may be over or underestimated the case of both increased and decreased stiffness was studied. Moreover, the influence of the difficult to estimate damping ratio was studied, it was noticed that in general higher damping implies lower accelerations. However, as the equivalent pedestrian is influenced by the damping for some traffic classes as shown within the analysis there

may be cases where the acceleration gets slightly higher. This implies that extensive analyses have to be performed in the case of constructing a blade bridge. The damping ratio of 1% used for the analyses was deemed to be conservative since the damping for FRP is generally higher leading to lower accelerations. The study was limited to a small number of sections due to the extensive analyses required for the sensitivity analysis.

8.6 Other Configurations

Due to the large deflection of the blades, it would be possible to rotate the blades 90° utilising its larger bending stiffness in vertical direction. For this concept the drawback is the even larger constructional height but as seen in Appendix K the deflection criteria for the 16 meter blade is fulfilled for all sections. This implies that this concept can be utilised when there are no strict requirements of appearance or height below the bridge. However, not all sections can be used as the horizontal accelerations may be critical for start coordinates away from the root.

The results in Section 7.3.2 shows that it could be possible to use longer sections of the blades utilising a mid-support, if the site specific conditions allow for it. A lower construction height in one of the spans is possible due to the geometry of the blade which could act as a passageway if there are requirements on vertical clearance under the bridge. One disadvantage with the configuration is that it can be difficult to properly secure the bridge deck and other connections since the standing blades contributing to a lower contact area to the deck.

8.7 Improvements

If the serviceability requirement with regard to acceleration is not fulfilled, one alternative can be to post-install dampers on the bridge. For example, viscous dampers or tuned mass dampers. The optimal solution would be to take advantage of the hollow space inside of the wind turbine blades. Studies exist on implementing TMD's inside of wind turbine blades, when in service for their intended use. This shows that it might be possible to install dampers inside of the blades, also when used as structural members in pedestrian bridges. However, this needs more investigation concerning dynamic behaviour as well as cost efficiency to be considered a viable solution.

9

Conclusion and Recommendations on Further Studies

The aim of the project was to, through a parametric study, analyse the response of wind turbine blades when used as main structural elements in pedestrian bridges. The following objectives had to be accomplished, a literature study regarding pedestrian bridge dynamics and FRP, verification of the usage of a beam model for the parametric study and the development of a Python script compatible with the finite element analysis software BRIGADE/Plus.

Based on the verification presented in Chapter 5 the analyses can be conducted using equivalent beam sections for reproducing global response of deflection, frequency, and accelerations for the wind turbine blade. A parametric Python script compatible with the finite element software BRIGADE/Plus was developed to automate the process of analysing several sections along any wind turbine blade with known stiffness and mass properties.

The results of the parametric study presented in Chapter 7 together with the literature review in Chapter 2 has found that in order to have confidence about acceptable dynamic behaviour in a real case an eigenfrequency of at least around 5 Hz for the first vertical frequency is required. However, it is still needed to study the accelerations since they can be unacceptable even for these relatively high frequencies. On the other hand, an option is to accept that installation of TMD or other types of dampers are needed and just check that the deflection criteria is satisfied.

For the studied blade and bridge configuration, the parametric study indicates that sections up to 14.0 meters are possible to use with the assumed stiffness and damping properties. However, due to the uncertainty of the stiffness based on conversion factors and damping which is difficult to assess, in general when designing, a sensitivity analysis should be required for each possible concept. Furthermore, full scale testing may be necessary to validate both the material properties and the dynamic behaviour after construction.

A recommendation is that more specific guidelines for pedestrian induced vibrations for FRP footbridges should be developed, to encourage and ensure the integrity of possible upcoming wind turbine blade bridges as well as other fibre reinforced polymer bridges.

One limitation of the project is the overall difficulty to achieve data for decommissioned blades, such as material properties and mechanical properties due to the secrecy within the wind turbine blade manufacturing. Therefore, the possibility to draw general conclusions regarding possible span lengths applicable for other blades is limited. To make progress in this area, greater transparency within the field is necessary.

In the future it is possible that the blade manufacturer will be more cooperative about the structural properties of the most common blades. If so, further analyses could be performed with more confidence using models supplied by manufacturers. Further studies regarding damage assessment, durability and cost efficiency should be performed before construction to prove the adequacy of the blade bridge conceptualisation. A suggestion is to study these parameters within an upcoming thesis to conclude if blade bridges are feasible in the long term. Another suggestion for further research is to study the effect of dampers, for example develop a more standardised and cost effective damper that is tuned for a certain model of wind turbine blades.

Bibliography

Agarwal, B. D., Broutman, L. J., & Chandrashekhara, K. (2006). *Analysis and performance of fibre composites* (3rd edition). Wiley.

Alshannaq, A., Scott, D., Bank, L., Bermek, M., & Gentry, R. (2019). Structural reuse of de-commissioned wind turbine blades in civil engineering applications. https://doi.org/10.12783/asc34/31317

Andersen, N., Eriksson, O., Hillman, K., & Wallhagen, M. (2016). Wind turbines' end-of-life: Quantification and characterisation of future waste materials on a national level. *Energies*, *9*. https://doi.org/10.3390/en9120999

Baus, U., & Schlaich, M. (2008). Dynamics, vibrations. *Footbridges: Structure design history* (Pages 100–103). Birkhäuser Basel. https://doi.org/10.1007/978-3-7643-8222-3_9

BBC. (2002). 'wobbly' millennium bridge fixed. *BBC News*. http://news.bbc.co.uk/2/hi/uk_news/england/1829053.stm

Beauson, J., & Brøndsted, P. (2016). Wind turbine blades: An end of life perspective. https://doi.org/10.1007/978-3-319-39095-6_23

Bladena. (2019). *Wind turbine blades: Handbook*. KIRT x THOMSEN.

Campbell, F. (2010). *Structural composite materials* [eBook]. Materials Park : A S M International.

Clarke, J. L. (1996). *Structural design of polymer composites: Eurocomp design code*. Taylor Francis.

CROW. (2019). *CROW-CUR Recommendation 96:2019: Fibre-reinforced polymers in buildings and civil engeineering structures* (technical report). CROW.

Damberg, H. (2001). *Komposithandboken: Polymerbaserade fiberkompositer*. Industrilitteratur AB.

Danish Standards Foundation. (2007). *Conditions for the construction of wind turbines in denmark (DS 472:2007)* (technical report). Danish Standards Foundation.

European Commission - Joint Research Centre. (2009). *Design of lightweight footbridges for human induced vibrations* (technical report). JRC.

European Commission - Joint Research Centre. (2016). *Prospect for new guidance in the design of frp* (technical report). JRC.

Fairs, M. (2002). Arup: We have fixed the millennium bridge. *Building*. http://building.co.uk/news/arup-we-have-fixed-the-millennium-bridge/1015137.article

Feder, F., Feldmuller, M., Peeren, C., & Speksnijder, S. (2019). Blade bridge strandpark lindholm.

Fu, Z.-F., & He, J. (2001). *Modal analysis* [eBook]. Elsevier Science Technology.

Griffith, D. T., & Ashwill, T. D. (2011). *The sandia 100-meter all-glass baseline wind turbine blade: Snl100-00* (technical report). Sandia National Laboratories. Albuquerque, New Mexico.

Ingólfsson, E., Georgakis, C., & Jönsson, J. (2012). Pedestrian-induced lateral vibrations of footbridges: A literature review. *Engineering Structures*, *45*, 21–52. https://doi.org/10.1016/j.engstruct.2012.05.038

Ladson, C. L., & Brooks Jr, C. W. (1974). *Development of a computer program to obtain ordinates for naca 6- and 6a-series airfoils* (technical report). National Aeronautics and Space Administration (NASA). Washington, D.C.

Meng. (2020). Structure design and analysis of a novel forward-folding rotor used in a downwind horizontal-axis turbine [conference paper]. *IOP Conference Series Materials Science and Engineering*, *825*. https://doi.org/10.1088/1757-899X/825/1/012002

Mishnaevsky, L., Branner, K., Petersen, H. N., Beauson, J., McGugan, M., & Sørensen, B. F. (2017). Materials for wind turbine blades: An overview. *Materials*, *10*(11). https://doi.org/10.3390/ma10111285

Nygren, D., & Kullberg, J. (2020). *Reuse of decommissioned wind turbine blades in pedestrian bridges* (Master's thesis). Chalmers University of Technology.

Pastor, M., Binda, M., & T.Harcarik. (2012). Modal assurance criterion. *Procedia Engineerig*, *48*, 543–548. https://doi.org/10.1016/j.proeng.2012.09.551

Pedersen, D. S. (2021). Personal communication.

Re-Wind. (2021). *Driving innovation in the re-use of decommissioned wind turbine blades*. https://www.re-wind.info

Russell, J., Wei, X., Živanović, S., & Kruger, C. (2020). Vibration serviceability of a gfrp railway crossing due to pedestrians and train excitation. *Engineering Structures*, *219*, 110756. https://doi.org/10.1016/j.engstruct.2020.110756

SIMULIA. (2014). *Abaqus 6.14 analysis user's guide*. Dassault Systèmes Simulia Corp.

Suhail, R., Chen, J.-F., Gentry, R., Taristro-Hart, B., Xue, Y., & Bank, L. (2019). Analysis and design of a pedestrian bridge with decommissioned frp windblades and concrete.

Swedish Standards Institute. (2002). *Basis of structural design (SS-EN 1990)* (technical report). Svenska institutet för standarder.

Swedish Standards Institute. (2005). *Basis of structural design (SS-EN 1990/A1:2005)* (technical report). Svenska institutet för standarder.

The Swedish Transport Administration. (2019). *Krav brobyggande: Tdok 2016:* (technical report).

The technical department for transport, roads and bridges engineering and road safety of France. (2006). *Footbridges, assessment of vibrational behaviour of footbridges under pedestrian loading* (technical report). (Service d'études techniques des routes et autoroutes - Sétra).

Uyttersprot, J., & De Corte, W. (2021). Measured dynamic properties of web-core sandwich panel frp composite footbridges and their relation to pedestrian comfort analysis. *Composite Structures*, *259*, 113236. https://doi.org/10.1016/j.compstruct.2020.113236

Uyttersprot, J., De Corte, W., & Ingelbinck, B. (2021). Influence of sls design requirements on the material consumption and self-weight of web-core sandwich panel frp composite footbridges. *Composite Structures*, *262*, 113334. https://doi.org/10.1016/j.compstruct.2020.113334

Wang, B., Bachtiar, E. V., Yan, L., Kasal, B., & Fiore, V. (2019). Flax, basalt, e-glass frp and their hybrid frp strengthened wood beams: An experimental study. *Polymers*, *11*(8). https://doi.org/10.3390/polym11081255

Wei, X., Russell, J., Živanović, S., & Toby Mottram, J. (2019). Measured dynamic properties for frp footbridges and their critical comparison against structures made of conventional construction materials. *Composite Structures*. https://doi.org/10.1016/j.compstruct.2019.110956

Yan, L., Chouw, N., & Jayaraman, K. (2014). Flax fibre and its composites – a review. *Composites Part B: Engineering*, *56*, 296–317. https://doi.org/10.1016/j.compositesb.2013.08.014

Živanović, S., Feltrin, G., Mottram, J. T., & Brownjohn, J. M. W. (2014). Vibration performance of bridges made of fibre reinforced polymer. In F. N. Catbas (Editor), *Dynamics of civil structures, volume 4* (Pages 155–162). Springer International Publishing.

Živanović, S., Russell, J. M., & Racic, V. (2020). Vibration performance of a lightweight frp footbridge under human dynamic excitation. In S. Pakzad (Editor), *Dynamics of civil structures, volume 2* (Pages 111–114). Springer International Publishing.

Zoghi, M. (2013). *The international handbook of frp composites in civil engineering*. Taylor Francis.

A

Blade Bridge in Aalborg, Denmark

A footbridge made of decommissioned wind turbine blades is planned to be constructed during 2021 in Aalborg, Denmark. The project was initiated by locals in the area and is now lead by Aalborg municipality. Several companies are involved in the project where wind blade manufacture Siemens Gamesa is one of them. An interview was conducted with David Stien Pedersen on the 3rd of February 2021. Pedersen has worked at Siemens Gamesa for 13 years as Senior Project Manager and is involved in the blade bridge project in Aalborg.

The bridge will consist of two 49-meter long blades used for testing purposes. The blades will be oriented in opposite longitudinal direction to each other where the roots on each side will be utilised as dressing rooms for the nearby beach, see Figure A.1 for illustration of the bridge (Feder et al., 2019).

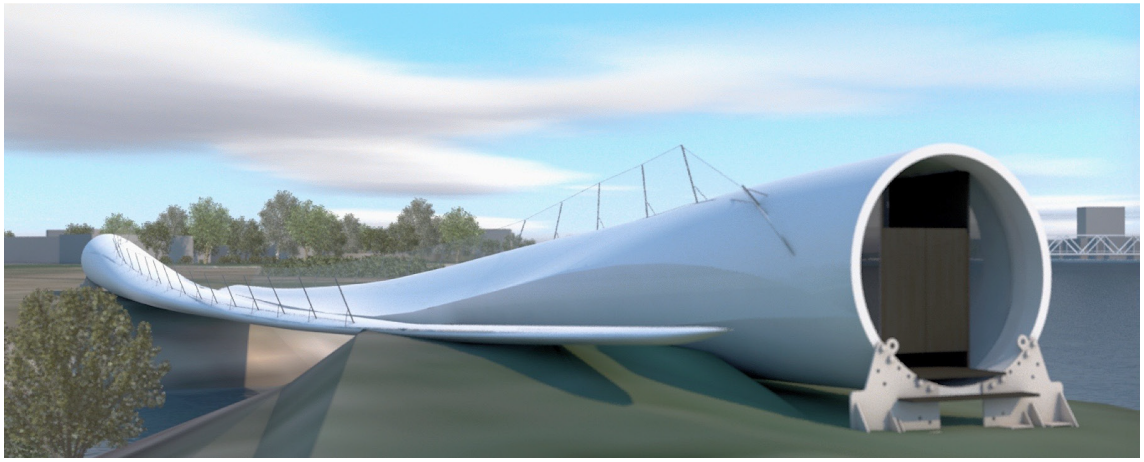

Figure A.1 Illustration of the bridge by Superuse Studios (Feder et al., 2019)

Advantageous in this project according to Pedersen (2021) is the collaboration between Siemens Gamesa and technical consultant company Cowi which can evaluate the result of the modelling from Siemens Gamesa for bridge applications. There is secrecy of the exact composition of the blades since blade manufactures do not want the composition and blade design to be available to other companies. Even though the blades are relatively old, smaller blade manufacturers still can benefit from this information.

Another advantage is that a lot of work can be done in factory before the blades are transported to the site, for example surface treatment to ensure a proper bond with the applied laminate which will act as the walking path. Pedersen suggests that the transportation of the blades to the site should follow standard guidelines for transportation of wind turbine blades. This minimises the risk of damage of the blades during transportation and also the cost.

Regarding damage assessment the leading edge of the blade, when used as a rotor blade, could be eroded from hitting raindrops in the air. However, this is stated to be an easy repair, the structural integrity of the member is not affected. Also, according to Pedersen there is no need to repaint the blades. Inspection of the blades may be necessary after installation to ensure no damages has occurred during this phase.

In other cases not involving the blade manufacturer directly, there can be difficulties to obtain exact models of the blades and it may be necessary to perform full scale testing in order to determine the capacity. A suggestion for the future is that blade manufactures provide an extensive end-of-life model.

Neither blade manufactures nor the owners of the wind turbines do want to take any responsibility for the decommissioned blades when later used for other purposes. Therefore, in this project, an insurance company take all the responsibility. For this case there is most likely an advantage that Siemens Gamesa supplies their own results as a basis for the structural analysis.

According to Pedersen the fatigue life of a non damaged blade should not be of concern since blades is seen to complete fatigue testing for three times its fatigue lifetime. For a 50 meter long blade the fatigue test consists of subjecting the blade to a load deflecting the tip up to 14 meters. This loading is repeated with 2 million cycles. Regarding dynamic behaviour, the eigenfrequency of the planned bridge is below 5 Hz, Pedersen indicates that it is difficult to decide the damping coefficient for the structure. Furthermore, that there are various thoughts about if the dynamic behaviour of the bridge will be a problem or not.

Reusing the wind turbine blades as bridge members is a good option to reduce the environmental impact from the industry. As of today, even though there are viable recycling methods, such as burning the epoxy for energy production and reusing the glass fibre as replacement of part of the silica in cement, almost all wind turbine blades are sent to landfill. Pedersen states that landfill today is the cheapest option due to political decisions and implies that the cost must increase in order for the blade owners to consider sustainable methods. Although Pedersen estimates that the total mass of decommissioned wind turbine blades compared to the total land fill mass is low, and could be around 1-2 % of total land fill in the future.

B

Shell Model Modes

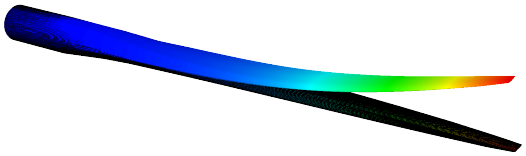

Figure B.1 1st vertical mode

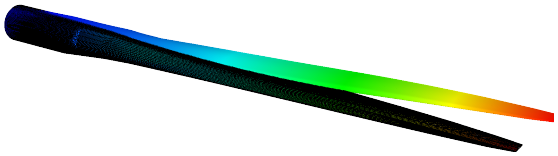

Figure B.2 1st horizontal mode

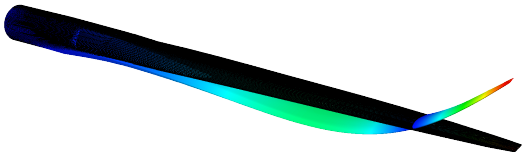

Figure B.3 2nd vertical mode

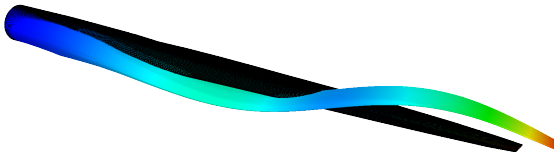

Figure B.4 2nd horizontal mode

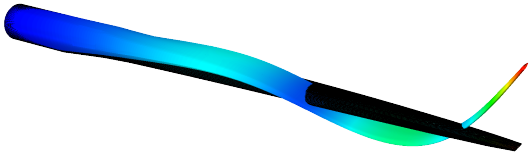

Figure B.5 3rd vertical mode

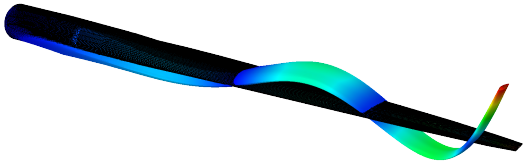

Figure B.6 4th vertical mode

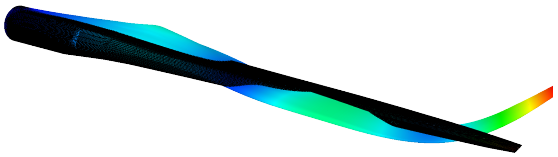

Figure B.7 3rd horizontal mode

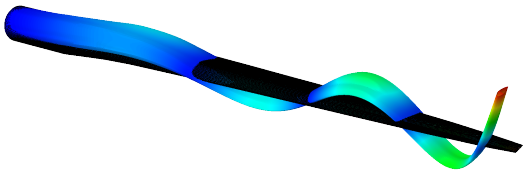

Figure B.8 5th vertical mode

C
Beam Model Modes

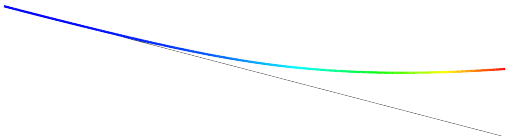

Figure C.1 1st vertical mode

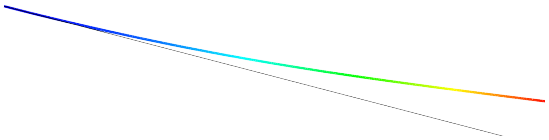

Figure C.2 1st horizontal mode

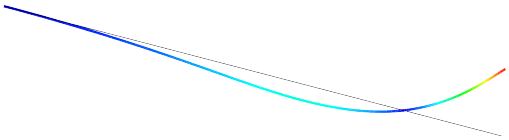

Figure C.3 2nd vertical mode

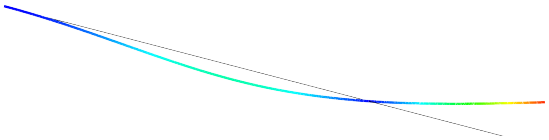

Figure C.4 2nd horizontal mode

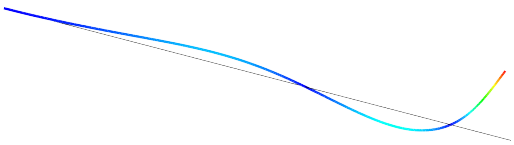

Figure C.5 3rd vertical mode

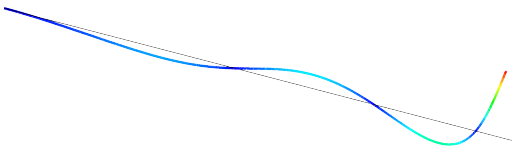

Figure C.6 4th vertical mode

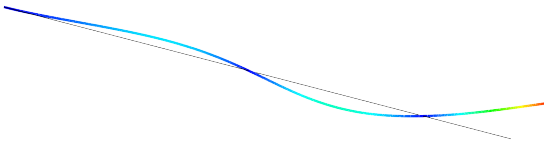

Figure C.7 3rd horizontal mode

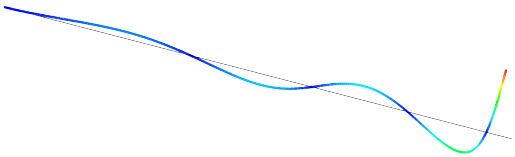

Figure C.8 5th vertical mode

D

Comparison of Mode Shapes

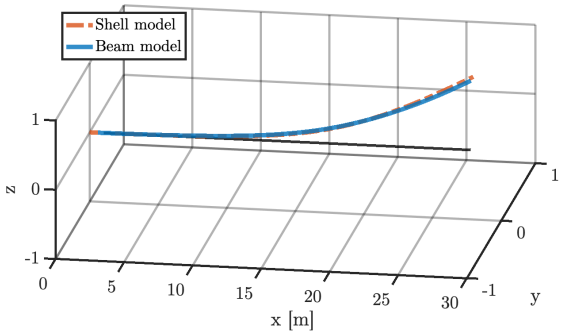

Figure D.1 1st vertical mode

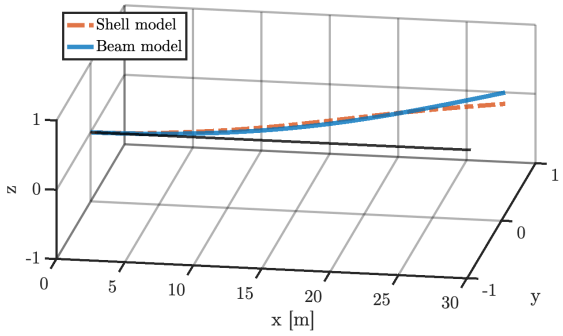

Figure D.2 1st horizontal mode

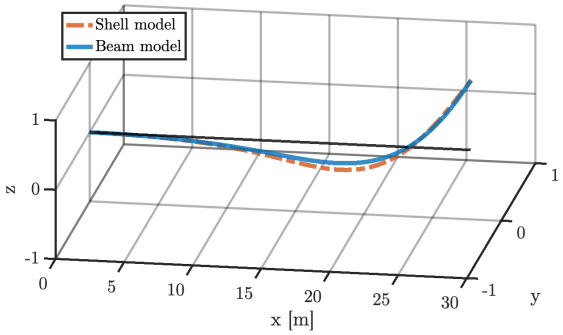

Figure D.3 2nd vertical mode

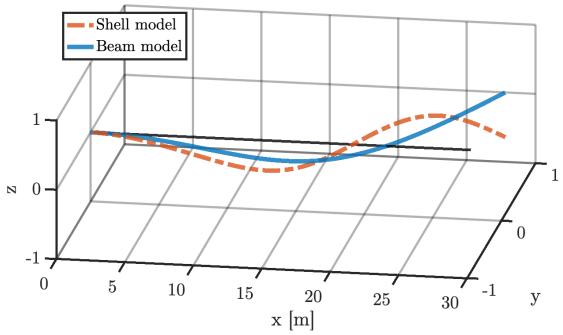

Figure D.4 2nd horizontal mode

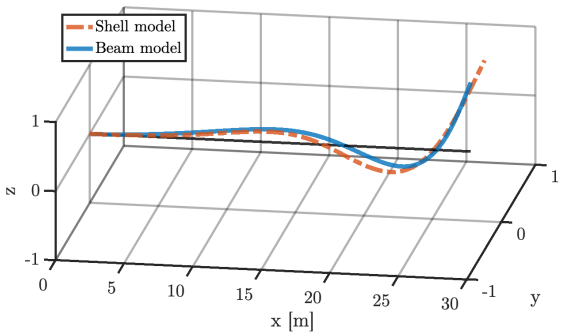

Figure D.5 3rd vertical mode

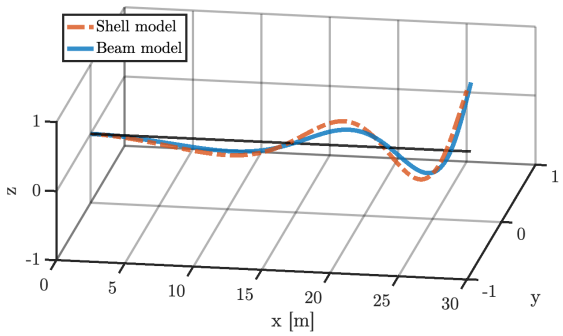

Figure D.6 4th vertical mode

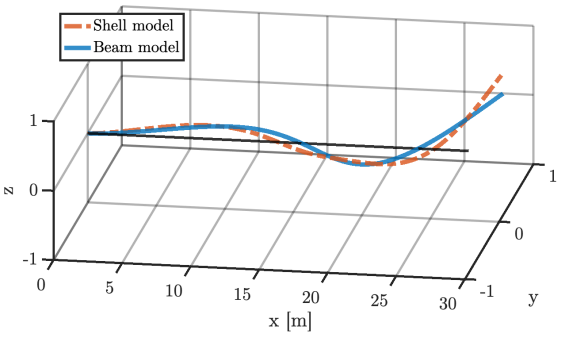

Figure D.7 3rd horizontal mode

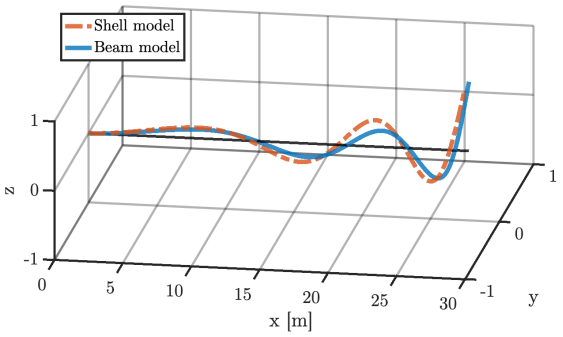

Figure D.8 5th vertical mode

E

Analytical Calculations

Analytical calculations for a simplified case, assuming constant cross-section, constant stiffness and uniform mass distribution. The eigenfrequencies and accelerations is computed using the SDOF method described in JRC *Design of Lightweight Footbridges for Human Induced Vibrations* (EUR 23984 EN) and *Footbridges, assessment of vibrational behaviour of footbridges under pedestrian loading* by Sétra.

(1)

Johan Dahlén
Christoffer Härnborg

1. Deflection

References

[1] SS-EN 1991-2-EN (2003) Eurocode 1: Actions on structures - Part 2: Traffic loads on bridges

[2] SS-EN 1990/A1:2005 (2005) Eurocode: Basis of structural design

1.1 Indata

Length of span

$l := 18\ \boldsymbol{m}$

Width of bridge deck

$b := 1.9\ \boldsymbol{m}$

Stiffness

$EI_y := 300\ \boldsymbol{MN \cdot m^2}$

Conversion factor accounting for reduced material properties,
see Section 5.5.4 Conversion factors

$\eta := 0.58$

1.2 Calculation of maximum deflection in SLS

Load, SS-EN 1991-2-EN 4.3.5 Load Model 4 crowd loading [1]

$q := 5 \cdot 1.9\ \frac{\boldsymbol{kN}}{\boldsymbol{m}} = 9.5\ \frac{\boldsymbol{kN}}{\boldsymbol{m}}$

Partial factor SLS, Table A2.2 SS-EN 1990/A1:2005 [2]

$\psi_1 := 0.4$

Maximum deflection

$$\delta_{max} := \frac{5 \cdot \psi_1 \cdot q \cdot l^4}{384 \cdot \eta \cdot EI_y} = 29.9\ \boldsymbol{mm}$$

(1)

Johan Dahlén
Christoffer Härnborg

2. Eigenfrequencies and acceleration

References

[1] CROW. (2019) CROW-CUR *Recommendation 96:2019: Fibre reinforced polymers in buildings and civil engineering structures* (technical report)

[2] European Commission - Joint Research Centre. (2009). *Design of lightweight footbridges for human induced vibrations* (technical report). JRC

[3] The technical department for transport, roads and bridges engineering and road safety of France. (2006). *Footbridges, assesment of vibrational behaviour of footbridges under pedestrian loading* (technical report). (Service d'étudestechniques des routes et autoroutes - Sétra)

2.1 Indata

Dimensions

$l := 18\ \boldsymbol{m}$ $b := 1.9\ \boldsymbol{m}$

Loaded surface

$S := l \cdot b = 34.2\ \boldsymbol{m}^2$

Blade mass per length

$m_1 := 200\ \frac{\boldsymbol{kg}}{\boldsymbol{m}}$

Weight of pedestrian, EN 23984 9.1 [2]

$P := 700\ \boldsymbol{N}$

Density of pedestrians, TC3, EN 23984 Table 4.3 [2]

$d_{TC3} := 0.5 \cdot \frac{1}{\boldsymbol{m}^2}$

Number of pedestrians

$n_{TC3} := d_{TC3} \cdot S = 17.1$

(2)

Johan Dahlén
Christoffer Härnborg

Total weight of pedestrians

$G_{TC} := n_{TC3} \cdot P = 11.97\ \boldsymbol{kN}$

Weight of deck

$G_{deck} := \frac{1540\ \frac{\boldsymbol{N}}{\boldsymbol{m}}}{\boldsymbol{g}} = 157\ \frac{\boldsymbol{kg}}{\boldsymbol{m}}$

Weight of bridge including mass of pedestrians and deck

$\rho S_{TC} := m_1 + \frac{\frac{G_{TC}}{\boldsymbol{g}}}{l} + G_{deck} = 424.8\ \frac{\boldsymbol{kg}}{\boldsymbol{m}}$

2.2 Calculation of eigenfrequencies

Stiffness in vertical- and horizontal direction

$EI_v := 300\ \boldsymbol{MN \cdot m^2}$

$EI_h := 600\ \boldsymbol{MN \cdot m^2}$

Conversion factor, CROW-CUR [1]

$\eta := 0.9^3 = 0.729$ See Section 5.5.4 Conversion factors

$EI_v := EI_v \cdot \eta = 218.7\ \boldsymbol{MN \cdot m^2}$

$EI_h := EI_h \cdot \eta = 437.4\ \boldsymbol{MN \cdot m^2}$

Vertical frequencies, SETRA 5.2.1.2 & Table 3.2 [3]

$f_{1.v} := \frac{9.87}{2 \cdot \boldsymbol{\pi} \cdot l^2} \cdot \sqrt{\frac{EI_v}{\rho S_{TC}}} = 3.5\ \boldsymbol{Hz}$

$f_{2.v} := \frac{39.5}{2 \cdot \boldsymbol{\pi} \cdot l^2} \cdot \sqrt{\frac{EI_v}{\rho S_{TC}}} = 13.9\ \boldsymbol{Hz}$

(3)

Johan Dahlén
Christoffer Härnborg

Horizontal frequencies, SETRA 5.2.1.2 & Table 3.2 [3]

$$f_{1.h} := \frac{9.869}{2 \cdot \pi \cdot l^2} \cdot \sqrt{\frac{EI_h}{\rho S_{TC}}} = 4.9 \ \boldsymbol{Hz}$$

$$f_{2.h} := \frac{39.478}{2 \cdot \pi \cdot l^2} \cdot \sqrt{\frac{EI_h}{\rho S_{TC}}} = 19.7 \ \boldsymbol{Hz}$$

2.3 Dynamic analysis

Damping

$\xi := 0.01$

Pedestrian load, EN 23984 4.5.1.2 Table 4.8 [2]

$P_v := 280 \ \boldsymbol{N}$ Vertical

$P_l := 140 \ \boldsymbol{N}$ Longitudinal

$P_h := 35 \ \boldsymbol{N}$ Lateral

Number of equivalent pedestrians, for TC1 to TC3, EN 23984 4.5.1.2 Table 4.8 [2]

$$n'_{TC} := \frac{10.8 \cdot \sqrt{\xi \cdot n_{TC3}}}{S} = 0.13 \ \frac{1}{\boldsymbol{m}^2}$$

Reduction coefficient, Vertical

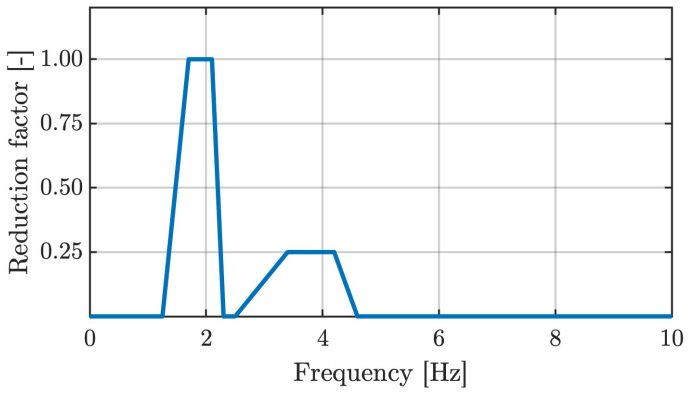

(4)

Johan Dahlén
Christoffer Härnborg

Reduction coefficient - vertical

$$\psi_{1.v} := \begin{cases} 0 & \text{if } f_{1.v} \le 1.25 \cdot Hz \\ \dfrac{f_{1.v} - 1.25 \cdot Hz}{0.45 \cdot Hz} & \text{else if } 1.25 \cdot Hz < f_{1.v} \le 1.75 \cdot Hz \\ 1 & \text{else if } 1.75 \cdot Hz < f_{1.v} \le 2.1 \cdot Hz \\ 1 - \dfrac{f_{1.v} - 2.1 \cdot Hz}{0.2 \cdot Hz} & \text{else if } 2.1 \cdot Hz < f_{1.v} \le 2.3 \cdot Hz \\ 0 & \text{else if } 2.3 \cdot Hz < f_{1.v} \le 2.5 \cdot Hz \\ \dfrac{f_{1.v} - 2.5 \cdot Hz}{4 \cdot 0.9 \cdot Hz} & \text{else if } 2.5 \cdot Hz < f_{1.v} \le 3.4 \cdot Hz \\ 0.25 & \text{else if } 3.4 \cdot Hz < f_{1.v} \le 4.2 \cdot Hz \\ 0.25 - \dfrac{f_{1.v} - 4.2 \cdot Hz}{4 \cdot 0.4 \cdot Hz} & \text{else if } 4.2 \cdot Hz < f_{1.v} \le 4.6 \cdot Hz \\ 0 & \text{else if } f_{1.v} > 4.6 \cdot Hz \end{cases} = 0.25$$

Amplitudes for TC3

$$q_{1.v} := P_v \cdot n'_{TC} \cdot \psi_{1.v} = 9.1 \ \frac{N}{m^2}$$

Lineload amplitude TC3

$$F_{1.v} := b \cdot q_{1.v} = 0.02 \ \frac{kN}{m}$$

Maximum vertical acceleration TC3

$$a_{max} := \frac{1}{2 \cdot \xi} \cdot \frac{4 \cdot F_{1.v}}{\pi \cdot \rho S_{TC}} = 2.6 \ \frac{m}{s^2}$$

F

Parametric Script

The parametric script was written using the integrated development environment PyCharm Community Edition 2020.3.3. The script can be easily modified for sensitivity analyses with varying damping ratio and/or elastic modulus for a set number of iterations. When studying some other concepts as the standing blades and an additional support some minor modifications were done. For the standing blade (rotated 90°) the vertical and horizontal stiffness were switched. For the additional support an end boundary condition was copied, and its position was set to half the length of the nodal list (in the middle of the span). For deflections the variable load was applied only in the weakest span. This were done by looping only the second half (weakest span) of the nodal list in the load application. These analyses were verified in the same way as the original script.

```python
# Written by Christoffer Härnborg & Johan Dahlén
# Date of completion 2021-04-21

# Python script compatible with BRIGADE/Plus for performing frequency, acceleration, and
# deflection analyses for a bridge/beam. A txt-file containing sectional coordinates,
# bending stiffness in both directions, mass, and height (optional) is required.

# Several analyses for different sections of the beam can be performed which has to be specified.
# Results is automatically saved in txt-file named after the specific analysis performed.

# [1] European Commission - Joint Research Centre. (2009). Design of lightweight
# footbridges for human induced vibrations (technical report). JRC

# [2] Swedish Standards Institute. (2005). Basis of structural design (SS-EN 1990/A1:2005).
# Svenska institutet för standarder.

from part import *
from material import *
from section import *
from assembly import *
from step import *
from interaction import *
from load import *
from mesh import *
from optimization import *
from job import *
from sketch import *
from visualization import *
from connectorBehavior import *
from math import *
import numpy as np

# Delete previous instances
Mdb()
mdb.saveAs(pathName='C:/Users/SEAHHC/Desktop/parametric/para.cae')

# Parametric scripting
# Step distance, minimum 0.1 stepping
iter_step = 0.5

lseg = 12

# Define limiting coordinates [m]
a1_1 = 0
a2_2 = 24

# Define start and end damping (linear variation)
damping_1 = 0.01
damping_2 = 0.01

# Choose traffic class 1-5
TC = 4

# Choose comfort class 1-4
CL = 3

a2_1 = a1_1 + lseg
a1_2 = a2_2 - lseg

nr_iter = (a1_2 - a1_1) / iter_step

a1_list = np.linspace(a1_1, a1_2, int(nr_iter + 1))
a2_list = np.linspace(a2_1, a2_2, int(nr_iter + 1))
damping_list = np.linspace(damping_1, damping_2, int(nr_iter + 1))

print(damping_list)
print(a1_list)
print(a2_list)

# --- Constant values --- #
# [1] - Load per pedestrian [N] - Acceleration analysis
H = 700

# SLS load in N/m2, Pa
sls_load = 5000

# Width of deck [m]
wdeck = 1.9

# Non structural mass [kg/m] from Nygren. D, Kullberg. J (2020)
```

```
nonstruct = 1540 / 9.81

# Number of eigenvalues requested
eignum = 10

# Conversion factors
ct = 0.9
cm = 0.9
cv = 0.8
cf = 0.9

# Set max value for critical f (longitudinal, vertical & horizontal)
l_crit = 5.0
v_crit = 5.0
h_crit = 2.5

# Number of modalpoints
modalpoints = 150

# --- Formulas --- #
# Conversion factors frequency analysis (is multiplied with Young's modulus)
n_freq = ct * cm * cf

# Conversion factors SLS analysis (is multiplied with Young's modulus)
n_sls = ct * cm * cv * cf

# Define lists to append results for each iteration
para_iter = []
para_xstart = []
para_xend = []
para_TC = []
para_CL = []
para_Ares = []
para_Amax = []
para_mode = []
para_slsres = []
para_slsmax = []
para_damp = []
para_height1 = []
para_height2 = []
para_freq = []
para2_xstart = []
para2_xend = []

# Initiate parametric looping
for p_nr in range(len(a1_list)):
    print('-----------------------------------------------')
    print('------- Iteration ' + str(p_nr + 1) + ' of ' + str(len(a1_list)) + ' initiated ---------')
    print('-----------------------------------------------')

    Mdb()
    para_A = []
    a1 = a1_list[p_nr]
    dampingratio = damping_list[p_nr]

    # End coordinate
    a2 = a1 + lseg

    # Create empty lists to append sectional data from text file
    Mass = []
    dist = []
    EI_flap = []
    EI_edge = []
    height = []

    with open('data6.txt') as infile:
        for line in infile:
            dist.append(float(line.split()[0]))
            Mass.append(float(line.split()[1]))
            EI_flap.append(float(line.split()[2]))
            EI_edge.append(float(line.split()[3]))
            height.append(float(line.split()[4]))

    # If end coordinate is outside valid range set end coordinate to blade length
    if a2 > dist[-1]:
        print('Warning! End coordinate: ' + str(a2) + ' m is out of range: ' + str(dist[-1]) + ' m')
        a2 = dist[-1]
        print('New end coordinate: ' + str(a2) + ' m')

    # If segment length is equal to zero
```

```
    if lseg < 0.1:
        print('Warning! span length cant be zero')
        lseg = 1.0
        print('New span length: ' + str(lseg) + ' m')

    # Extract the data only in the specified span between a1 and a2
    l = len(dist)
    a1 = int(round(a1 * 10))
    a2 = int(round(a2 * 10) + 1)
    dist = dist[a1:a2]
    ldeck = dist[-1] - dist[0]
    Mass = Mass[a1:a2]
    EI_flap = EI_flap[a1:a2]
    EI_edge = EI_edge[a1:a2]
    height = height[a1:a2]

    # Calculate pedestrian load based on traffic class [N/m]
    if TC == 1:
        varload = 15 * H / (dist[-1] - dist[0])
    elif TC == 2:
        varload = 0.2 * H * wdeck
    elif TC == 3:
        varload = 0.5 * H * wdeck
    elif TC == 4:
        varload = 1.0 * H * wdeck
    elif TC == 5:
        varload = 1.5 * H * wdeck
    else:
        print('Traffic class ' + str(TC) + ' does not exist, choose between 1-5')
        exit()

    # [1] - Max allowed acceleration based on Comfort Class.
    # A_max = [(Vertical + longitudinal),(Horizontal)]
    if CL == 1:
        A_max = [0.50, 0.1]
    elif CL == 2:
        A_max = [0.70, 0.1]
    elif CL == 3:
        A_max = [1.50, 0.1]
    elif CL == 4:
        A_max = [100, 0.1]
        print('CL4 = Unacceptable accelerations')
    else:
        print('Comfort class: ' + str(CL) + 'does not exist')
        exit()

    # Calculate total bridge mass
    totMass = 0
    for i in range(len(Mass) - 1):
        totMass += (dist[i + 1] - dist[i]) * Mass[i]

    # Disregard pedestrian mass if it is below 10% of total mass
    totvarload = varload / 9.81 * ldeck
    if totvarload / (totvarload + totMass) < 0.1:
        print('Pedestrian mass below 10 % of total mass')
        varload = 0

    # Total non structural mass [kg/m]
    nonload = nonstruct + varload / 9.81

    # SLS load for deformation acc. to SS-EN 1990/A1:2005 [N/m]
    slsload = 0.4 * sls_load * wdeck

    # Display the current classes in the message area
    print('Traffic Class: TC' + str(TC))
    print('Comfort Class: CL' + str(CL))

    # Display the masses in the message area
    print('SLS total mass:   ' + str(round((slsload / 9.81) * ldeck, 1)) + ' kg')
    print('Blade total mass: ' + str(round(totMass, 1)) + ' kg')

    # Display total length and for which intervals the bridge spans
    print("Length:   " + str(ldeck) + ' m')
    print("Interval: " + str(dist[0]) + ' - ' + str(dist[-1]) + ' m')


    # Define function to calculate inertia in y and z direction for hollow rectangular sections
    def inertia(b, h, t):
        b2 = b - 2 * t
        h2 = h - 2 * t
```

```
241         return (b * h ** 3) / 12 - (b2 * h2 ** 3) / 12, (h * b ** 3) / 12 - (h2 * b2 ** 3) / 12
242
243
244     # Young's modulus in MPA
245     E = 20 * 10 ** 3
246
247     # Density in kg/m3
248     d = 1600
249
250     # Set limit for max iterations
251     max_iter = 3000
252
253     # Allowed deviation for EI and mass
254     tol = 0.001
255
256     # Increment if criteria fails
257     inc = tol
258
259     # Define EI1 and EI2 to start the iteration
260     EI1 = 0
261     EI2 = 0
262
263     # Start guesses
264     b = 1
265     h = 1
266     t = 0.05
267     myMass = 700
268
269     # Set iteration counter to start value = 0
270     nr = 0
271
272     # Sectional property list
273     masslist = []
274     blist = []
275     hlist = []
276     tlist = []
277     EI1list = []
278     EI2list = []
279
280     # Beam iteration for each section
281     for i in range(len(Mass)):
282         nr = 0
283         while not (1 - tol) * EI_flap[i] < EI1 < (1 + tol) * EI_flap[i] \
284                 or not (1 - tol) * EI_edge[i] < EI2 < (1 + tol) * EI_edge[i] \
285                 or not (1 - tol) * Mass[i] < myMass < (1 + tol) * Mass[i]:
286             I1, I2 = inertia(b, h, t)
287             EI1 = I1 * E
288             EI2 = I2 * E
289
290             # STIFFNESS FLAP
291             if not (1 - tol) * EI_flap[i] < EI1 < (1 + tol) * EI_flap[i]:
292                 if (1 + tol) * EI_flap[i] > EI1:
293                     h = (1 + inc) * h
294
295                 else:
296                     h = (1 - inc) * h
297
298             # STIFFNESS EDGE
299             if not (1 - tol) * EI_edge[i] < EI2 < (1 + tol) * EI_edge[i]:
300                 if (1 + tol) * EI_edge[i] > EI2:
301                     b = (1 + inc) * b
302
303                 else:
304                     b = (1 - inc) * b
305
306             # MASS
307             if not (1 - tol) * Mass[i] < myMass < (1 + tol) * Mass[i]:
308                 if (1 + tol) * Mass[i] > myMass:
309                     t = (1 + inc) * t
310
311                 else:
312                     t = (1 - inc) * t
313
314             myMass = (h * b - ((h - 2 * t) * (b - 2 * t))) * d
315
316             nr += 1
317
318             if nr == max_iter:
319                 print("Maximum nr. of iterations reached for section " + str(i))
320                 if not (1 - tol) * EI_flap[i] < EI1 < (1 + tol) * EI_flap[i]:
```

```
                    print("EI flap:  " + str(round((1 - tol) * EI_flap[i], 3))
                          + " < " + str(round(EI1, 3)) + " < "
                          + str(round((1 + tol) * EI_flap[i], 3)))
                if not (1 - tol) * EI_edge[i] < EI2 < (1 + tol) * EI_edge[i]:
                    print("EI edge:  " + str(round((1 - tol) * EI_edge[i], 2))
                          + " < " + str(round(EI2, 2)) + " < "
                          + str(round((1 + tol) * EI_edge[i], 2)))
                if not (1 - tol) * Mass[i] < myMass < (1 + tol) * Mass[i]:
                    print("Mass:  " + str(round((1 - tol) * Mass[i], 2))
                          + " < " + str(round(myMass, 2)) + " < "
                          + str(round((1 + tol) * Mass[i], 2)))
                print('\n')
                break

        # Append results from iteration
        tlist.append(round(t, 3))
        masslist.append(round(myMass, 3))
        blist.append(round(b, 3))
        hlist.append(round(h, 3))
        EI1list.append(round(EI1, 2))
        EI2list.append(round(EI2, 2))

    h = hlist
    b = blist
    t = tlist

    # Convert to SI-units (loaded as MNm2 in file) and apply the conversion factor
    Efreq = n_freq * E * 10 ** 6

    # ----- BRIGADE scripting ----- #
    # Create material
    mdb.models['Model-1'].Material(name='GFRP')
    mdb.models['Model-1'].materials['GFRP'].Density(table=((d,),))
    mdb.models['Model-1'].materials['GFRP'].Elastic(table=((Efreq, 0.3),))

    # Draw the geometry line between start and end point
    mdb.models['Model-1'].ConstrainedSketch(name='__profile__', sheetSize=200.0)
    mdb.models['Model-1'].sketches['__profile__'].Line(point1=(dist[0], 0.0), point2=(
        dist[-1], 0.0))
    mdb.models['Model-1'].sketches['__profile__'].geometry.findAt((dist[-1] - 0.01, 0.0))
    mdb.models['Model-1'].sketches['__profile__'].HorizontalConstraint(
        addUndoState=False, entity=
        mdb.models['Model-1'].sketches['__profile__'].geometry.findAt((dist[-1] - 0.01, 0.0),
                                                                      ))
    mdb.models['Model-1'].Part(dimensionality=THREE_D, name='Part-1', type=
    DEFORMABLE_BODY)
    mdb.models['Model-1'].parts['Part-1'].BaseWire(sketch=
                                                   mdb.models['Model-1'].sketches['__profile__'])

    # Create datums
    for x in dist:
        mdb.models['Model-1'].parts['Part-1'].DatumPlaneByPrincipalPlane(offset=x,
                                                                         principalPlane=YZPLANE)

    # Partitioning
    for i in range((len(mdb.models['Model-1'].parts['Part-1'].datums) - 2)):
        mdb.models['Model-1'].parts['Part-1'].PartitionEdgeByDatumPlane(datumPlane=
                               mdb.models['Model-1'].parts['Part-1'].datums[i + 3],
                               edges=mdb.models['Model-1'].parts['Part-1']
                              .edges.findAt(((dist[i], 0.0, 0.0),)))

    # Create beam profiles for all sections
    for i in range(len(dist)):
        mdb.models['Model-1'].BoxProfile(a=h[i], b=b[i], name='Profile-' + str(i + 1), t1=t[i],
                                         uniformThickness=ON)

    # Create beam sections for all profiles
    for i in range(len(dist)):
        mdb.models['Model-1'].BeamSection(consistentMassMatrix=False, integration=
        DURING_ANALYSIS, material='GFRP', name='Section-' + str(i + 1), poissonRatio=0.3,
                                          profile='Profile-' + str(i + 1), temperatureVar=LINEAR)

    # Assign sections
    for i in range(len(dist) - 1):
        mdb.models['Model-1'].parts['Part-1'].Set(edges=
        mdb.models['Model-1'].parts['Part-1'].edges.findAt(
            ((dist[i] + 0.01, 0.0, 0.0),)),
            name='Set-' + str(i + 1))

        mdb.models['Model-1'].parts['Part-1'].SectionAssignment(offset=0.0, offsetField='',
```

```
                                offsetType=MIDDLE_SURFACE, region= mdb.models['Model-1'].parts
                                ['Part-1'].sets['Set-' + str(i + 1)], sectionName=
                                'Section-' + str(i + 1),thicknessAssignment=FROM_SECTION)

        mdb.models['Model-1'].parts['Part-1'].assignBeamSectionOrientation(method=
                                    N1_COSINES, n1=(0.0, 0.0, -1.0),
                                    region=mdb.models['Model-1'].
                                    parts['Part-1'].sets['Set-' + str(i + 1)])

    # Divide non structural mass for application on each node:
    length = []
    influence = []
    nodemass = []

    # Iterate the length for each segment (distance between nodes)
    for i in range(len(dist) - 1):
        length.append(round(dist[i + 1] - dist[i], 3))

    # Iterate the influence load area for each node
    for i in range(len(dist) - 2):
        influence.append(length[i] / 2 + length[i + 1] / 2)

    # Apply on half the load at the ends (half the influence area)
    influence.insert(0, length[0] / 2)
    influence.append(length[-1] / 2)

    # Append all node loads in a list
    for i in influence:
        nodemass.append(i * nonload)

    # Apply all node loads in BRIGADE/Plus
    for i in range(len(dist)):
        mdb.models['Model-1'].parts['Part-1'].engineeringFeatures.PointMassInertia(
            alpha=0.0, composite=0.0, mass=nodemass[i], name='Inertia-' + str(i), region=Region(
                vertices=mdb.models['Model-1'].parts['Part-1'].vertices.findAt(((dist[i], 0.0,
                                                                                 0.0),), )))

    # Assembly
    mdb.models['Model-1'].rootAssembly.DatumCsysByDefault(CARTESIAN)
    mdb.models['Model-1'].rootAssembly.Instance(dependent=OFF, name='Part-1-1',
                                            part=mdb.models['Model-1'].parts['Part-1'])

    # BC
    sup1 = dist[1]  # Relative position for start BC
    sup2 = dist[-2]  # Relative position for end BC

    # Apply start BC
    mdb.models['Model-1'].rootAssembly.Set(name='Set-1', vertices=
    mdb.models['Model-1'].rootAssembly.instances['Part-1-1'].vertices.findAt(((sup1, 0.0, 0.0),)))
    mdb.models['Model-1'].DisplacementBC(amplitude=UNSET, createStepName='Initial',
                                         distributionType=UNIFORM, fieldName='', localCsys=None,
                                         name='BC-1', region=mdb.models['Model-1'].rootAssembly.sets
                                         ['Set-1'],u1=SET, u2=SET, u3=SET)

    # Apply end BC
    mdb.models['Model-1'].rootAssembly.Set(name='Set-2', vertices=
    mdb.models['Model-1'].rootAssembly.instances['Part-1-1'].vertices.findAt(((sup2, 0.0, 0.0),)))
    mdb.models['Model-1'].DisplacementBC(amplitude=UNSET, createStepName='Initial',
                                         distributionType=UNIFORM, fieldName='', localCsys=None,
                                         name='BC-2', region=mdb.models['Model-1'].rootAssembly.sets
                                         ['Set-2'],u2=SET, u3=SET)

    # Seed Edges
    for i in range(len(dist) - 1):
        mdb.models['Model-1'].rootAssembly.seedEdgeBySize(constraint=FINER,
                                        deviationFactor=0.1, edges=mdb.models['Model-1'].
                                        rootAssembly.instances['Part-1-1'].
                                        edges.findAt(((dist[i] + 0.01, 0.0, 0.0),)), size=0.11)

    # Generate mesh
    mdb.models['Model-1'].rootAssembly.generateMesh(regions=(
        mdb.models['Model-1'].rootAssembly.instances['Part-1-1'],))

    # Frequency step
    mdb.models['Model-1'].FrequencyStep(name='Frequency', numEigen=eignum
                                        , previous='Initial')

    # Create job
    mdb.Job(model='Model-1', name='Freq-Job')
    mdb.jobs['Freq-Job'].setValues(description='', memory=50, memoryUnits=PERCENTAGE,
```

```
                                    numCpus=1, numDomains=1)
    mdb.Job(name='Freq-Job', model='Model-1')
    mdb.jobs['Freq-Job'].setValues(description='', memoryUnits=PERCENTAGE, memory=50,
                                    numCpus=1, numDomains=1)

    # Submit job
    mdb.jobs['Freq-Job'].setValues(queue='BrigadePlusQueue')
    mdb.jobs['Freq-Job'].submit(datacheckJob=False)

    # Wait for completion in order to wait for frequency results
    mdb.jobs['Freq-Job'].waitForCompletion()

    res = session.openOdb(name='C:/Users/SEAHHC/Desktop/parametric/Freq-Job.odb')
    session.viewports['Viewport: 1'].setValues(displayedObject=res)

    # Display the BC positions
    print('BC1 :' + str(sup1) + ' m')
    print('BC1 :' + str(sup2) + ' m')

    # Set the result window in order to extract results
    step1 = res.steps['Frequency']
    region = step1.historyRegions['Assembly ASSEMBLY']
    freqData = region.historyOutputs['EIGFREQ'].data

    # Save all eigenvalues in a list
    eiglist = []
    for i in range(eignum):
        eiglist.append(round(freqData[i][1], 4))

    # Mode shape check
    # Create empty lists to append mode nr in corresponding mode shape
    v_mode = []
    h_mode = []
    l_mode = []
    lcount = 0
    div_node = []

    for frame in range(eignum):
        U1list = []
        U2list = []
        U3list = []
        count = 0
        load_div = []
        for i in range(len(dist)):
            # Extract all deflections (x = U1, y = U2, z = U3) and append in corresponding list
            U3 = res.steps['Frequency'].frames[frame + 1].fieldOutputs['U'].values[i].data[2]
            U2 = res.steps['Frequency'].frames[frame + 1].fieldOutputs['U'].values[i].data[1]
            U1 = res.steps['Frequency'].frames[frame + 1].fieldOutputs['U'].values[i].data[0]
            U3list.append(round(U3, 8))
            U2list.append(round(U2, 8))
            U1list.append(round(U1, 8))

        # Check in which direction deflection is highest and use that list for finding mode shape.
        if max(U3list) > (max(U1list) + max(U2list)):
            list = U3list
        elif max(U1list) > (max(U2list) + max(U3list)):
            list = U1list
        else:
            list = U2list

        # Iteration to find mode number and the node of the load divider(s).
        for j in range(1, len(list) - 1):
            a1 = list[j - 1]
            a2 = list[j]
            a3 = list[j + 1]

            # Get the mode nr. For each "peak" in the deflection add 1 to the counter.
            if abs(a2) > abs(a1):
                if abs(a2) > abs(a3):
                    count = count + 1

            # For each load divider (when the deflection goes past 0)
            # append the position of that node(s). Only do this if we are between the supports
            if 5 < j < (len(dist) - 5):
                if abs(a2) < abs(a1):
                    if abs(a2) < abs(a3):
                        load_div.append(j)

        # Check mode type (vertical, longitudinal, horizontal or rigid body mode)
        # If little to none deflection in all directions assume rigid body mode
```

```
561         if max(U1list) + max(U2list) + max(U3list) < 0.001:
562             # print('Rigid body mode')
563             v_mode.append(0)
564             h_mode.append(0)
565             l_mode.append(0)
566             div_node.append(0)
567 
568         # Vertical body mode, append mode number and eventual load dividers
569         elif max(U3list) > max(U2list):
570             v_mode.append(count)
571             h_mode.append(0)
572             l_mode.append(0)
573             div_node.append(load_div)
574 
575         # Horizontal body mode, append mode number and eventual load dividers
576         elif max(U1list) > (max(U2list) + max(U3list)):
577             lcount = lcount + 1
578             v_mode.append(0)
579             h_mode.append(0)
580             l_mode.append(lcount)
581             div_node.append(load_div)
582 
583         # Longitudinal body mode, append mode number and eventual load dividers
584         else:
585             v_mode.append(0)
586             h_mode.append(count)
587             l_mode.append(0)
588             div_node.append(load_div)
589 
590     # Display critical eigenfrequencies
591     crit_mode = []
592     # Check if the modes is critical and if so display which mode it is together
593     # with mode nr and frequency. Example: Critical mode(s): Vertical mode Nr: 1, 4.03 Hz
594     print('Critical mode(s):')
595     for i in range(eignum):
596         if v_mode[i] != 0:
597             if eiglist[i] <= v_crit:
598                 crit_mode.append((eiglist[i], v_mode[i], 0, div_node[i]))
599                 para_freq.append(eiglist[i])
600                 print('Vertical mode ' + 'Nr: ' + str(v_mode[i]) + ', f = '
601                       + str(round(eiglist[i], 2)) + ' Hz')
602 
603         if h_mode[i] != 0:
604             if eiglist[i] <= h_crit:
605                 crit_mode.append((eiglist[i], h_mode[i], 1, div_node[i]))
606                 para_freq.append(eiglist[i])
607                 print('Horizontal mode ' + 'Nr: ' + str(h_mode[i]) + ', f = '
608                       + str(round(eiglist[i], 2)) + ' Hz')
609 
610         if l_mode[i] != 0:
611             if eiglist[i] <= l_crit:
612                 crit_mode.append((eiglist[i], l_mode[i], 2, div_node[i]))
613                 para_freq.append(eiglist[i])
614                 print('Longitudinal mode ' + 'Nr: ' + str(l_mode[i]) + ', f = '
615                       + str(round(eiglist[i], 2)) + ' Hz')
616 
617     if not crit_mode:
618         print('--------------------------')
619         print('--- No critical modes ---')
620         print('--------------------------')
621         para_freq.append(min([x for x in eiglist if x != 0]))
622         para2_xstart.append(dist[0])
623         para2_xend.append(dist[-1])
624         para_Amax.append(0)
625         para_Ares.append(0)
626         para_mode.append(0)
627 
628     # --- Acceleration analysis ---#
629 
630     # Vertical (and longitudinal) load reduction
631     mdb.models['Model-1'].TabularAmplitude(
632         data=((0.0, 0.0), (1.25, 0.0), (1.7, 1.0), (2.1, 1.0),
633               (2.3, 0.0), (2.5, 0.0),(3.4, 0.25), (4.2, 0.25),
634               (4.6, 0.0), (10.0, 0.0)), name='Amp-v',
635         smooth=SOLVER_DEFAULT, timeSpan=STEP)
636 
637     # Horizontal load reduction
638     mdb.models['Model-1'].TabularAmplitude(
639         data=((0.0, 0.0), (0.5, 0.0), (0.7, 1.0), (1.0, 1.0),
640               (1.2, 0.0), (10.0, 0.0)), name='Amp-h',
```

```
641         smooth=SOLVER_DEFAULT, timeSpan=STEP)
642 
643     # Steady state modal step
644     mdb.models['Model-1'].SteadyStateModalStep(directDamping=((2, 20, dampingratio),),
645                                frequencyRange=((0.1, 10.0, modalpoints, 3),),
646                                name='Modal',previous='Frequency')
647 
648     # Acceleration load application
649     Ares_list = []
650     Amax_list = []
651     # For each critical frequency get the acceleration load and
652     # maximum allowed acceleration depending on mode shape.
653     for c in range(len(crit_mode)):
654         # divs = load dividers
655         divs = crit_mode[c][3]
656 
657         # Get the max acceleration load per pedestrian (P) based on mode shape according to [1]
658         # Vertical modes
659         if crit_mode[c][2] == 0:
660             P = 280
661             Max_acc = A_max[0]
662 
663         # Horizontal modes
664         elif crit_mode[c][2] == 1:
665             P = 35
666             Max_acc = A_max[1]
667 
668         # Longitudinal modes
669         else:
670             P = 140
671             Max_acc = A_max[0]
672 
673         S = wdeck * ldeck  # Deck area for equivalent pedestrians calculation
674 
675         # Check traffic class and decide equivalent pedestrians (n_prim)
676         # based on pedestrians per area and damping ratio
677         # Get the final acceleration load (accload) to by applied in acceleration analysis
678         if TC == 1:
679             n_prim = 10.8 * sqrt(dampingratio * 15 / S) / S
680             accload = n_prim * P / (dist[-1] - dist[0])
681         elif TC == 2:
682             n_prim = 10.8 * sqrt(dampingratio * 0.2 * S) / S
683             accload = n_prim * P * wdeck
684         elif TC == 3:
685             n_prim = 10.8 * sqrt(dampingratio * 0.5 * S) / S
686             accload = n_prim * P * wdeck
687         elif TC == 4:
688             n_prim = 1.85 * sqrt(1.0 * S) / S
689             accload = n_prim * P * wdeck
690         else:
691             n_prim = 1.85 * sqrt(1.5 * S) / S
692             accload = n_prim * P * wdeck
693         length = []
694         influence = []
695         nodeload = []
696 
697         # If no load dividers, calculate the load as for non structural mass
698         # -> One direction whole span
699         for i in range(len(dist) - 1):
700             length.append(round(dist[i + 1] - dist[i], 3))
701 
702         for i in range(len(dist) - 2):
703             influence.append(length[i] / 2 + length[i + 1] / 2)
704 
705         influence.insert(0, length[0] / 2)
706         influence.append(length[-1] / 2)
707 
708         for i in influence:
709             nodeload.append(i * accload)
710 
711         # [1] - If load dividers, change the application direction for each load divider as
712         # visulised in thesis chapter: Acceleration
713         if divs:
714             dividers = []
715             for i in range(len(divs)):
716                 dividers.append(divs[i])
717             dividers.insert(0, 0)
718             dividers.insert(len(dividers), ldeck * 10)
719             for i in range(len(dividers) - 1):
720                 if (i % 2) == 0:
```

```
                    d1 = int(dividers[i])
                    d2 = int(dividers[i + 1])
                    nodeload[d1:d2] = [element * -1 for element in nodeload[d1:d2]]

        # Check if vertical, horizontal or longitudinal mode and assign loads in
        # the correct direction
        if crit_mode[c][2] == 0:
            para_mode.append(0)
            for i in range(len(dist)):
                mdb.models['Model-1'].ConcentratedForce(amplitude='Amp-v',
                                                cf3=(nodeload[i] + 0j),createStepName='Modal',
                                                distributionType=UNIFORM, field='', localCsys=None,
                                                name='Acc-load-' + str(i + 1), region=
                                                Region(vertices=mdb.models['Model-1'].
                                                rootAssembly.instances['Part-1-1']
                                                .vertices.findAt(((dist[i], 0.0, 0.0),), )))
        if crit_mode[c][2] == 1:
            para_mode.append(1)
            for i in range(len(dist)):
                mdb.models['Model-1'].ConcentratedForce(amplitude='Amp-h', cf2=(nodeload[i] + 0j),
                                            createStepName='Modal',distributionType=UNIFORM,
                                            field='', localCsys=None,
                                            name='Acc-load-' + str(i + 1), region=Region(
                                            vertices=mdb.models['Model-1'].rootAssembly.instances[
                                            'Part-1-1'].vertices.findAt(
                                            ((dist[i], 0.0, 0.0),), )))

        if crit_mode[c][2] == 2:
            para_mode.append(2)
            for i in range(len(dist)):
                mdb.models['Model-1'].ConcentratedForce(amplitude='Amp-v', cf1=(nodeload[i] + 0j),
                                            createStepName='Modal',
                                            distributionType=UNIFORM, field='', localCsys=None,
                                            name='Acc-load-' + str(i + 1), region=
                                            Region(vertices=mdb.models['Model-1'].
                                            rootAssembly.instances['Part-1-1'].vertices.findAt(
                                            ((dist[i], 0.0, 0.0),), )))

        # Job
        mdb.Job(model='Model-1', name='Acc-Job-' + str(c + 1))
        mdb.jobs['Acc-Job-' + str(c + 1)].setValues(description='', memory=50,
                                                    memoryUnits=PERCENTAGE,
                                                    numCpus=1, numDomains=1)
        mdb.Job(name='Acc-Job-' + str(c + 1), model='Model-1')
        mdb.jobs['Acc-Job-' + str(c + 1)].setValues(description='', memoryUnits=PERCENTAGE,
                                                    memory=50, numCpus=1, numDomains=1)

        # Submit job
        mdb.jobs['Acc-Job-' + str(c + 1)].setValues(queue='BrigadePlusQueue')
        mdb.jobs['Acc-Job-' + str(c + 1)].submit(datacheckJob=False)

        mdb.jobs['Acc-Job-' + str(c + 1)].waitForCompletion()

        res = session.openOdb(name='C:/Users/SEAHHC/Desktop/parametric/Acc-Job-'+str(c+1)+'.odb')
        session.viewports['Viewport: 1'].setValues(displayedObject=res)

        # Retrive accelerations
        session.viewports['Viewport: 1'].odbDisplay.basicOptions.setValues(
            numericForm=COMPLEX_MAGNITUDE)

        print(' ------------------------------------')
        print(' --- Retrieving max acceleration ---')
        print(' ------------------------------------')
        nodemax = []
        flist = []
        nrframes = res.steps['Modal'].frames[-1].incrementNumber
        # Analyse the whole defined frequency range (nrframes)
        for i in range(nrframes):
            maxnode = 0
            A = res.steps['Modal'].frames[i].fieldOutputs['A']
            for j in range(len(dist)):
                # Find and save the max acceleration for each node
                A1 = abs(max(A.values[j].magnitude, A.values[j].conjugateData[0],
                             A.values[j].conjugateData[1],
                             A.values[j].conjugateData[2]))
                if abs(A1) > maxnode:
                    maxnode = A1

            # Append the max acceleration (nodemax) for each node and
            # its corresponding frequency (flist)
```

```
            nodemax.append(maxnode)
            A_analysis = max(nodemax)
            flist.append(res.steps['Modal'].frames[i].frequency)

        # Display the maximum acceleration together with allowable acceleration
        print('Maximum acceleration: ' + str(round(A_analysis, 2)) + ' m/s^2')
        print('Allowable acceleration: ' + str(Max_acc) + ' m/s^2')
        Ares_list.append(A_analysis)
        Amax_list.append(Max_acc)
        para_Ares.append(A_analysis)
        para_Amax.append(Max_acc)
        para2_xstart.append(dist[0])
        para2_xend.append(dist[-1])
        if Max_acc < A_analysis:
            print('Acceleration NOT ok!')
        else:
            print('Acceleration ok!')

    # --- SLS deflection calculation ---#
    # ------ BRIGADE scripting ------- #

    # Reduce Young's modulus with defined conversion factor (n_sls)
    Esls = n_sls * E * 10 ** 6

    # Create second model (with Esls instead of Efreq, otherwise the models are identical)
    mdb.Model(modelType=STANDARD_EXPLICIT, name='Model-2')

    # Create material
    mdb.models['Model-2'].Material(name='GFRP')
    mdb.models['Model-2'].materials['GFRP'].Density(table=((d,),))
    mdb.models['Model-2'].materials['GFRP'].Elastic(table=((Esls, 0.3),))

    # Draw the geometry line between start and end point
    mdb.models['Model-2'].ConstrainedSketch(name='__profile__', sheetSize=200.0)
    mdb.models['Model-2'].sketches['__profile__'].Line(point1=(dist[0], 0.0), point2=(
        dist[-1], 0.0))
    mdb.models['Model-2'].sketches['__profile__'].geometry.findAt((dist[-1] - 0.01, 0.0))
    mdb.models['Model-2'].sketches['__profile__'].HorizontalConstraint(
        addUndoState=False, entity=
        mdb.models['Model-2'].sketches['__profile__'].geometry.findAt((dist[-1] - 0.01, 0.0),
                                                                      ))
    mdb.models['Model-2'].Part(dimensionality=THREE_D, name='Part-1', type=
    DEFORMABLE_BODY)
    mdb.models['Model-2'].parts['Part-1'].BaseWire(sketch=
                                                   mdb.models['Model-2'].sketches['__profile__'])

    # Create datums
    for x in dist:
        mdb.models['Model-2'].parts['Part-1'].DatumPlaneByPrincipalPlane(offset=x,
                                                                         principalPlane=YZPLANE)

    # Partitioning with datums
    for i in range((len(mdb.models['Model-2'].parts['Part-1'].datums) - 2)):
        mdb.models['Model-2'].parts['Part-1'].PartitionEdgeByDatumPlane(datumPlane=
                                            mdb.models['Model-2'].parts['Part-1'].datums[i + 3],
                                            edges=mdb.models['Model-2'].parts['Part-1']
                                            .edges.findAt(((dist[i], 0.0, 0.0),)))

    # Create beam profiles for all sections
    for i in range(len(dist)):
        mdb.models['Model-2'].BoxProfile(a=h[i], b=b[i], name='Profile-' + str(i + 1),
                                         t1=t[i], uniformThickness=ON)

    # Create beam sections for all profiles
    for i in range(len(dist)):
        mdb.models['Model-2'].BeamSection(consistentMassMatrix=False, integration=
        DURING_ANALYSIS, material='GFRP', name='Section-' + str(i + 1), poissonRatio=0.3,
                                          profile='Profile-' + str(i + 1), temperatureVar=LINEAR)

    # Assign sections
    for i in range(len(dist) - 1):
        mdb.models['Model-2'].parts['Part-1'].Set(edges=
        mdb.models['Model-2'].parts['Part-1'].edges.findAt(
            ((dist[i] + 0.01, 0.0, 0.0),)),
            name='Set-' + str(i + 1))

        mdb.models['Model-2'].parts['Part-1'].SectionAssignment(offset=0.0,
                                                 offsetField='', offsetType=MIDDLE_SURFACE, region=
                                                 mdb.models['Model-2'].parts['Part-1'].sets[
                                                'Set-' + str(i + 1)], sectionName=
```

```
                                            'Section-' + str(i + 1),
                                            thicknessAssignment=FROM_SECTION)

        mdb.models['Model-2'].parts['Part-1'].assignBeamSectionOrientation(method=
                                                N1_COSINES, n1=(0.0, 0.0, -1.0), region=
                                                mdb.models['Model-2'].parts['Part-1'].sets[
                                                'Set-' + str(i + 1)])

    # Assembly
    mdb.models['Model-2'].rootAssembly.DatumCsysByDefault(CARTESIAN)
    mdb.models['Model-2'].rootAssembly.Instance(dependent=OFF, name='Part-1-1',
                                            part=mdb.models['Model-2'].parts['Part-1'])

    # SLS step
    mdb.models['Model-2'].StaticStep(name='SLS', previous='Initial')

    # SLS load variable
    length = []
    influence = []
    nodeload = []

    for i in range(len(dist) - 1):
        length.append(round(dist[i + 1] - dist[i], 3))

    for i in range(len(dist) - 2):
        influence.append(length[i] / 2 + length[i + 1] / 2)

    influence.insert(0, length[0] / 2)
    influence.append(length[-1] / 2)

    for i in influence:
        nodeload.append(i * (slsload))

    # Apply variable SLS load and non structural load
    for i in range(len(dist)):
        mdb.models['Model-2'].ConcentratedForce(cf3=-nodeload[i], createStepName='SLS',
                                            distributionType=UNIFORM, field='', localCsys=None,
                                            name='SLSvar-' + str(i), region=
                                            Region(
                                            vertices=mdb.models['Model-2'].rootAssembly.
                                            instances['Part-1-1'].vertices.findAt(
                                            ((dist[i], 0.0, 0.0),), )))

    # Apply start BC
    sup1 = dist[1]
    sup2 = dist[-2]
    mdb.models['Model-2'].rootAssembly.Set(name='Set-1', vertices=
    mdb.models['Model-2'].rootAssembly.instances['Part-1-1'].vertices.findAt(((sup1, 0.0, 0.0),)))
    mdb.models['Model-2'].DisplacementBC(amplitude=UNSET, createStepName='Initial',
                                        distributionType=UNIFORM, fieldName='',
                                        localCsys=None, name='BC-1',
                                        region=mdb.models['Model-2'].rootAssembly.sets['Set-1'],
                                        u1=SET, u2=SET, u3=SET)

    # Apply end BC
    mdb.models['Model-2'].rootAssembly.Set(name='Set-2', vertices=
    mdb.models['Model-2'].rootAssembly.instances['Part-1-1'].vertices.findAt(((sup2, 0.0, 0.0),)))
    mdb.models['Model-2'].DisplacementBC(amplitude=UNSET, createStepName='Initial',
                                        distributionType=UNIFORM, fieldName='',
                                        localCsys=None, name='BC-2',
                                        region=mdb.models['Model-2'].rootAssembly.sets['Set-2'],
                                        u2=SET, u3=SET)

    # Seed Edges
    for i in range(len(dist) - 1):
        mdb.models['Model-2'].rootAssembly.seedEdgeBySize(constraint=FINER,
                                                deviationFactor=0.1, edges=
                                                mdb.models['Model-2'].rootAssembly.
                                                instances['Part-1-1'].edges.
                                                findAt(((dist[i] + 0.01,
                                                0.0, 0.0),)),size=0.11)
    # Generate mesh
    mdb.models['Model-2'].rootAssembly.generateMesh(regions=(
        mdb.models['Model-2'].rootAssembly.instances['Part-1-1'],))

    # Create Job
    mdb.Job(model='Model-2', name='SLS-job')
    mdb.jobs['SLS-job'].setValues(description='', memory=50, memoryUnits=PERCENTAGE,
                                numCpus=1, numDomains=1)
    mdb.Job(name='SLS-job', model='Model-2')
```

```
    mdb.jobs['SLS-job'].setValues(description='', memoryUnits=PERCENTAGE,
                                  memory=50, numCpus=1, numDomains=1)

    # Submit job
    mdb.jobs['SLS-job'].setValues(queue='BrigadePlusQueue')
    mdb.jobs['SLS-job'].submit(datacheckJob=False)

    mdb.jobs['SLS-job'].waitForCompletion()

    # Results
    res = session.openOdb(name='C:/Users/SEAHHC/Desktop/parametric/SLS-job.odb')
    session.viewports['Viewport: 1'].setValues(displayedObject=res)

    # Find the max delfection
    u = res.steps['SLS'].frames[-1].fieldOutputs['U']
    maxU = 0
    for i in range(len(dist)):
        u3 = u.values[i].data[2]
        if abs(u3) > abs(maxU):
            maxU = u3
            pos = u.values[i].nodeLabel

    # [2] - Allowed deflection = L/400
    # Display the max. height of blade together with max deflection and allowed deflection (L/400)
    print('Max height of blade: ' + str(int(max(height * 1000))) + ' mm')
    print(
        "Max deflection: " + str(abs(round((maxU) * 1000, 2))) + ' mm' + ' at: x = '
        + str(dist[pos] - dist[0]) + ' m')

    print("L/400: " + str(2.5 * ldeck) + ' mm')
    if abs(maxU) > ldeck / 400:
        print('-> Deflection NOT ok!')
    else:
        print('-> Deflection ok!')

    print('-------------------------------------------------')
    print('------ Iteration ' + str(p_nr + 1) + ' of ' + str(len(a1_list)) + ' completed -------')
    print('-------------------------------------------------')

    # Summarise and display the results.
    print(' ')
    print('------------- SUMMARY --------------')
    print(' ')
    print('Traffic Class:   TC' + str(TC))
    print('Comfort Class:   CL' + str(CL))
    print('Blade height:    ' + str(int(max(height * 1000))) + ' mm')
    print('Bridge span:     ' + str(ldeck) + ' m')
    print("Interval:        " + str(dist[0]) + ' - ' + str(dist[-1]) + ' m')
    print('Damping ratio:   ' + str(dampingratio))
    print(' ')
    if not crit_mode:
        print('There are no critical frequencies')

    if len(crit_mode) == 1:
        print('There is one critical eigenfrequency:')

    if len(crit_mode) > 1:
        print('There are ' + str(len(crit_mode)) + ' critical frequencies:')

    print(' ')
    counter = 0
    for i in range(eignum):
        if v_mode[i] != 0:
            if eiglist[i] <= v_crit:
                print('f' + str(i) + ' = ' + str(round(eiglist[i], 2)) + ' Hz, '
                      + 'Vertical mode ' + 'Nr: ' + str(v_mode[i]))
                print('Resulting acceleration: ' + str(round(Ares_list[counter], 2)) + ' m/s2')
                print('Allowed acceleration:   ' + str(round(Amax_list[counter], 2)) + ' m/s2')
                print(' ')
                counter = counter + 1
        if h_mode[i] != 0:
            if eiglist[i] <= h_crit:
                print('f' + str(i) + ' = ' + str(round(eiglist[i], 2)) + ' Hz, '
                      + 'Horizontal mode ' + 'Nr: ' + str(h_mode[i]))
                print('Resulting acceleration: ' + str(round(Ares_list[counter], 4)) + ' m/s2')
                print('Allowed acceleration:   ' + str(round(Amax_list[counter], 4)) + ' m/s2')
                print(' ')
                counter = counter + 1
        if l_mode[i] != 0:
            if eiglist[i] <= l_crit:
```

```
1041                print('f' + str(i) + ' = ' + str(round(eiglist[i], 2)) + ' Hz, '
1042                      + 'Longitudinal mode ' + 'Nr: ' + str(l_mode[i]))
1043                print('Resulting acceleration: ' + str(round(Ares_list[counter], 2)) + ' m/s2')
1044                print('Allowed acceleration:   ' + str(round(Amax_list[counter], 2)) + ' m/s2')
1045                print(' ')
1046                counter = counter + 1
1047
1048    print(' ')
1049
1050    print('SLS analysis: ')
1051    print("Max deflection: " + str(abs(round((maxU) * 1000, 1))) + ' mm')
1052    print("L/400:          " + str(round(2.5 * ldeck, 1)) + ' mm')
1053
1054    # Append results for each iteration
1055    para_iter.append(p_nr + 1)
1056    para_xstart.append(dist[0])
1057    para_xend.append(dist[-1])
1058    para_TC.append(TC)
1059    para_CL.append(CL)
1060    para_slsres.append(maxU)
1061    para_slsmax.append(ldeck / 400)
1062    para_damp.append(dampingratio)
1063    para_height1.append(min(height))
1064    para_height2.append(max(height))
1065
1066 # Append the results to txt file for post processing
1067 a = np.array([para_xstart, para_xend, para_TC,
1068               para_CL, para_slsres, para_slsmax, para_damp, para_height1, para_height2])
1069 mat = np.matrix(a)
1070 with open('1_results-L' + str(lseg) + str(TC) + str(CL) + '.txt', 'wb') as f:
1071     for line in mat:
1072         np.savetxt(f, line, fmt='%.8f')
1073
1074 b = np.array([para2_xstart, para2_xend, para_freq, para_Ares, para_Amax, para_mode])
1075 mat = np.matrix(b)
1076 with open('2_results-L' + str(lseg) + str(TC) + str(CL) + '.txt', 'wb') as f:
1077     for line in mat:
1078         np.savetxt(f, line, fmt='%.8f'
```

G

Parametric Script Verification

Verification of the parametric script and its utilisation in BRIGADE/Plus. Verification is done with the thinnest 20 meter section (start coordinate = 4.0 m) to capture more than one critical eigenfrequency to verify the acceleration analysis for different modes. The summary of the iteration displayed in BRIGADE/Plus is shown in Figure G.1. Flapwise = Vertical and Edgewise = Horizontal.

```
------------ SUMMARY -------------

Traffic Class:   TC4
Comfort Class:   CL3
Blade height:    1601 mm
Bridge span:     20.0 m
Interval:        4.0 - 24.0 m
Damping ratio:   0.01

There are 3 critical frequencies:

f1 = 1.03 Hz, Flapwise mode Nr: 1
Resulting acceleration: 0.8 m/s2
Allowed acceleration:   1.5 m/s2

f2 = 2.39 Hz, Edgewise mode Nr: 1
Resulting acceleration: 0.0136 m/s2
Allowed acceleration:   0.1 m/s2

f3 = 4.55 Hz, Flapwise mode Nr: 2
Resulting acceleration: 1.15 m/s2
Allowed acceleration:   1.5 m/s2


SLS analysis:
Max deflection: 371.5 mm
L/400:          50.0 mm
```

Figure G.1 Summary extracted by the script for the studied iteration

G.1 Geometry

As seen in Figure G.2 the start interval used in BRIGADE/Plus corresponds to the coordinates 4.0 and 24.0 meters given by the script.

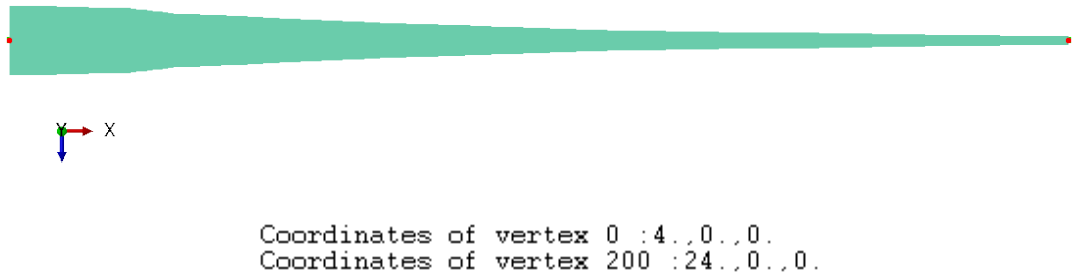

Figure G.2 Start (vertex 0) and end (vertex 200) coordinate. Blade visualised with beam profiles rendered

The maximum height corresponds to the height at 4.0 meters in the input text-file as illustrated in Figure G.3

x [m]	Mass [kg/m]	EI_flap [MN/m2]	EI_edge [MN/m2]	Height [mm]
4	240	863	1050	1601.4

Figure G.3 Sectional properties at radius 4.0 meters

Which is in line with the maximum height of 1601 mm shown in the iteration summary.

G.2 Mass

The mass for the blade is extracted as 2428.4 kg for the interval multiplying the sectional mass with the sectional length of 0.1 m for each section. The non structural mass from the bridge deck which is 1540 kN/m is multiplied with the length (20.0 m) resulting in a deck mass of 3139.7 kg. For this iteration TC4 is used implying a pedestrian density of 1.0/m^2. Each pedestrian weight is 700 N leading to a total pedestrian mass of 2711.5 kg (deck width = 1.9 m). All masses summed is equal to 8279.6 kg. This is verified by querying the mass properties of the assembly in BRIGADE/Plus resulting in 8278.2 kg as visualised in Figure G.4

```
Mass properties:
  Volume: 1.52
  Volume centroid: 11.96,6.67e-016,-2.41e-016
  Mass: 8278.18
```

Figure G.4 Mass properties for the studied blade

The margin of error between the masses is deemed to be insignificant (0.017 %) and should not influence the overall results. This small difference is due to the tolerance set for the beam iteration.

G.3 Frequency analysis

For the studied section there are three critical eigenfrequencies for which the acceleration need to be verified. The 1st vertical mode has a frequency of 1.03 Hz the BRIGADE/Plus result is shown in Figure G.5. The program indicates that the mode is mode number 2 since the first mode is a rigid body mode.

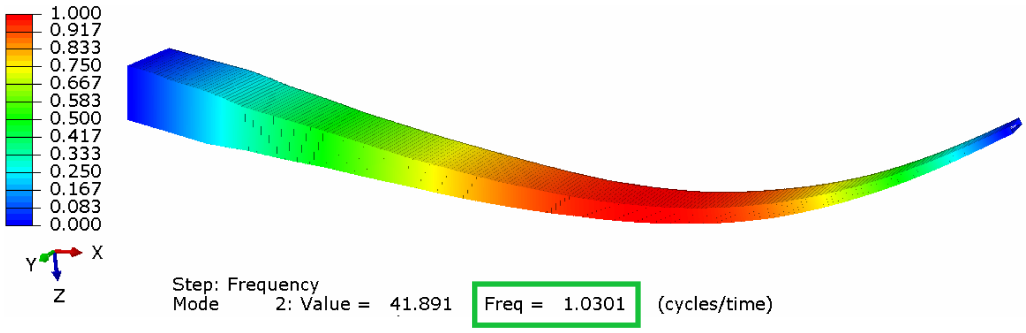

Figure G.5 1st vertical mode with beam profiles rendered

The 1st horizontal mode has a frequency of 2.39 Hz the BRIGADE/Plus result is shown in Figure G.6.

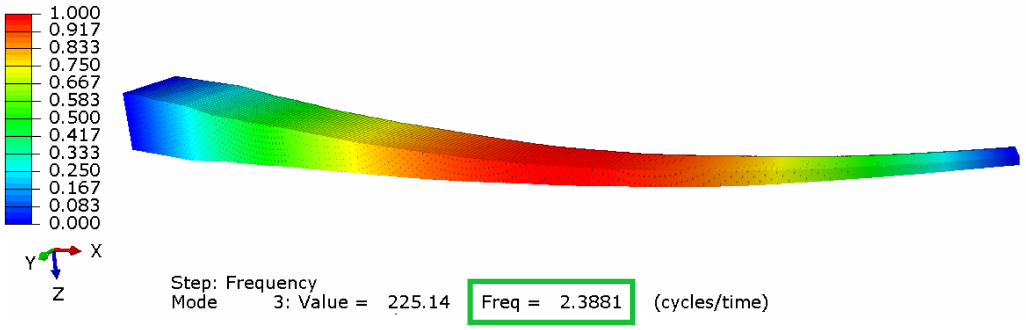

Figure G.6 1st horizontal mode with beam profiles rendered

The 2nd vertical mode has a frequency of 4.55 Hz the BRIGADE/Plus result is shown in Figure G.7.

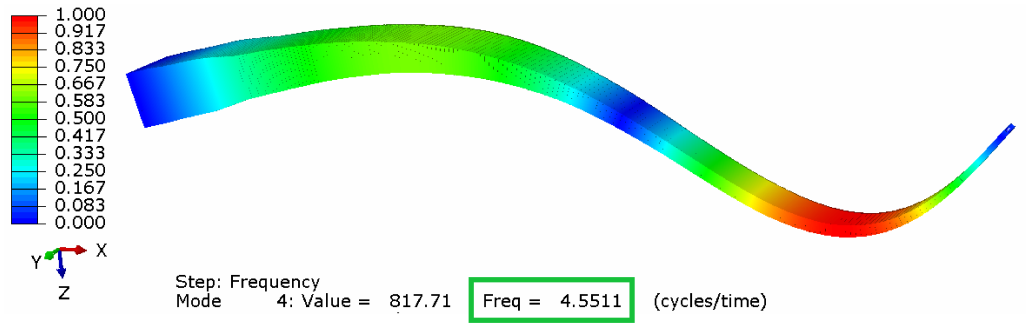

Figure G.7 2nd vertical mode with beam profiles rendered

All critical eigenfrequencies corresponds well to the frequencies extracted by the script (Figure G.1) based on the analyses.

G.4 Acceleration analysis

An analysis of the critical modes and its shapes is performed within the script to apply the acceleration forces with the correct direction and magnitude.

G.4.1 1 st vertical mode

The first critical mode and the by the script applied acceleration is illustrated in G.8.

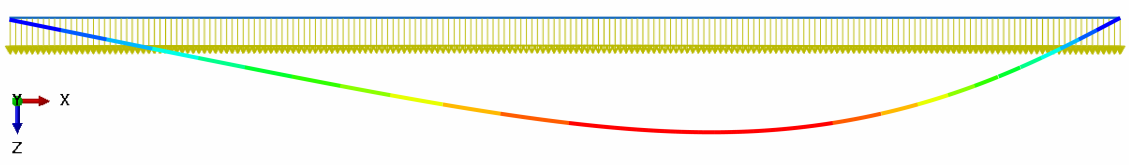

Figure G.8 Acceleration load application 1st vertical mode

Moreover a verification has to be done regarding load magnitude. The load manager window can be studied to verify that the correct magnitude and reduction factor is utilised. First the equivalent pedestrians can be calculated as 0.30 using Equation 3.3 (S = 38 m^2 & n = 38. The vertical acceleration load is 280 N. Since the load is applied on each node with 0.1 meter intervals the load of 280 N has to be multiplied with the influence area for each node which is 0.1 m multiplied the width of 1.9 m. This results in a load of 15.960 N for each load which match the value applied by the script as seen in the load editor in Figure G.9

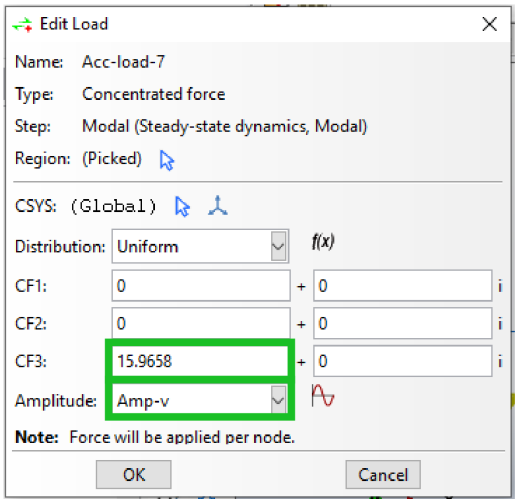

Figure G.9 Nodal acceleration load. 1st vertical mode

Also, it can be seen in Figure G.9 that the vertical reduction coefficient as illustrated in Figure 3.1a is included.

The resulting acceleration for all nodes and frequencies can be plotted using BRIGADE/-Plus to verify the maximum acceleration extracted by the script. For this mode the maximum acceleration is according to the given summary in Figure G.1 equal to

0.80 m/s^2 which match well with the maximum acceleration plot visualised Figure G.10.

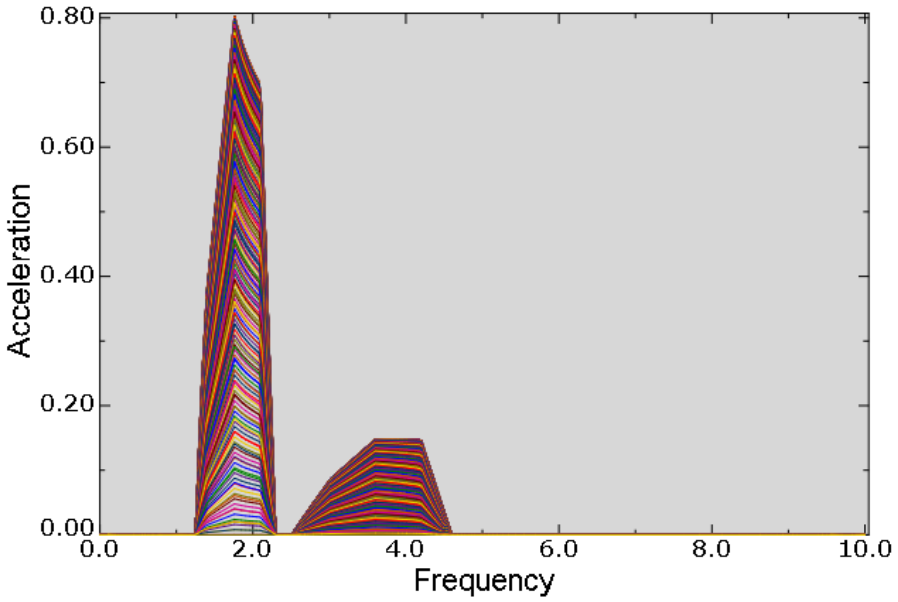

Figure G.10 Resulting acceleration for all nodes. 1st vertical mode

G.4.2 1 st horizontal mode

The first critical mode and its acceleration application is illustrated in G.11.

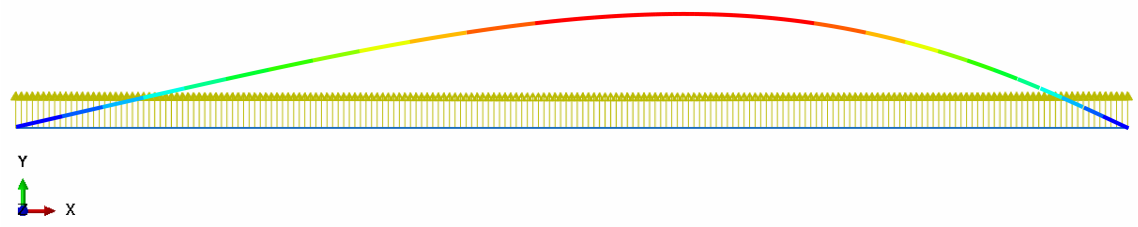

Figure G.11 Acceleration load application 1st horizontal mode

For the 1st horizontal mode the acceleration load is as for the case above constant. However as the mode is horizontal the load per pedestrian is 35 N and the horizontal reduction coefficient should be utilised. Using the same equivalent pedestrians of 0.30 and influence area per node as above the resulting force is 1.995 N per node which match the value applied by the script as seen in the load editor in Figure G.12.

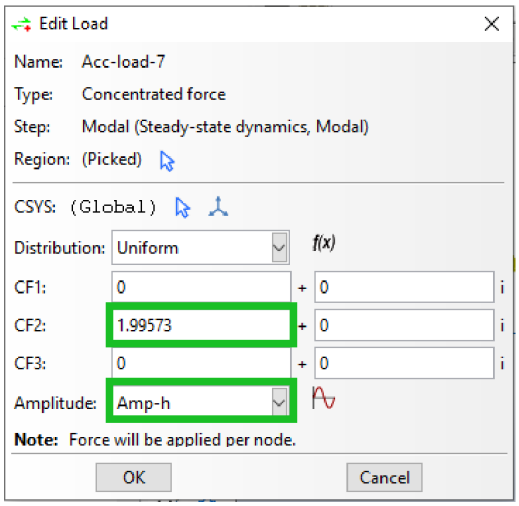

Figure G.12 Nodal acceleration load. 1st horizontal mode

For this mode the maximum acceleration is according to the given summary in Figure G.1 equal to 0.0136 m/s^2 which match well with the maximum acceleration plot visualised Figure G.13.

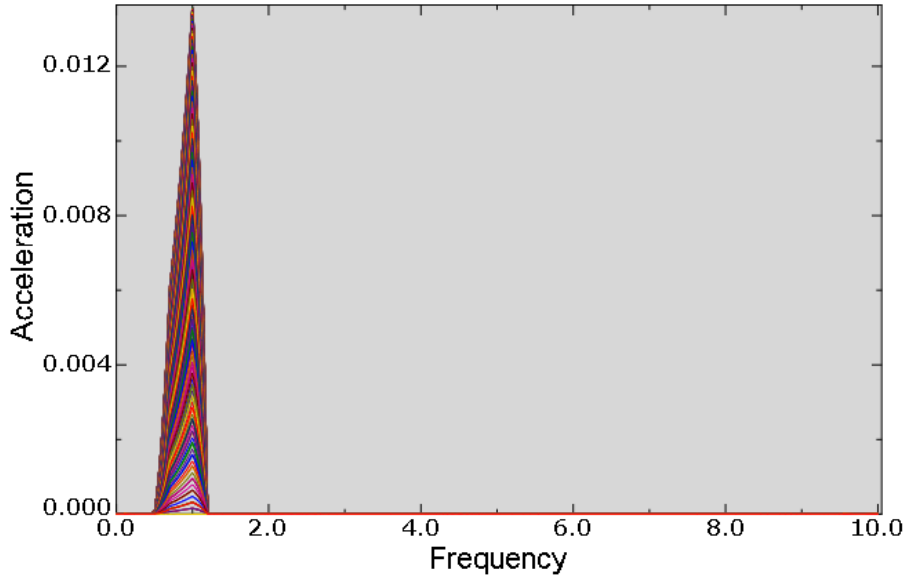

Figure G.13 Resulting acceleration for all nodes. 1st horizontal mode

G.4.3 2 nd vertical mode

For the 2nd vertical mode the load magnitude and reduction coefficient is the same as for the 1st vertical mode. However, the acceleration load should be applied as described in Section 5.6.2 which the script takes into consideration for all mode shapes.

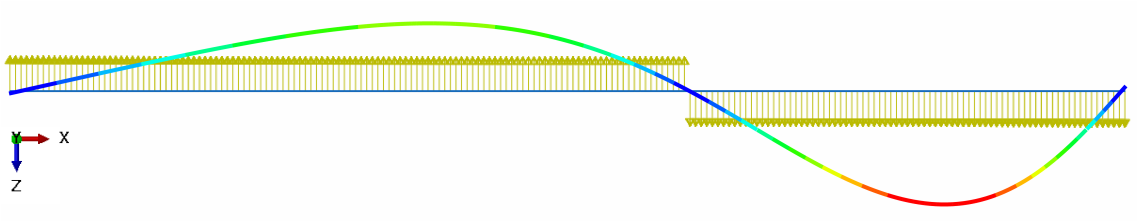

Figure G.14 Acceleration load application 2nd vertical mode

For this mode the maximum acceleration is according to the given summary in Figure G.1 equal to 1.15 m/s^2 which match well with the maximum acceleration plot visualised Figure G.15.

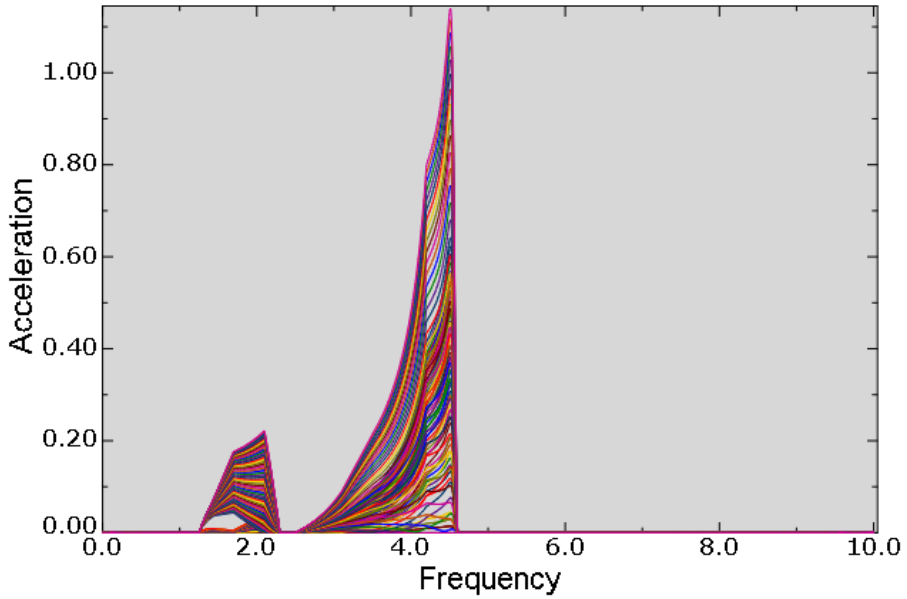

Figure G.15 Resulting acceleration for all nodes. 2nd vertical mode

G.5 Deflection analysis

For the deflection analysis the perceived deflection by the variable load of 2 kPa is calculated. This implies that the load on each node with influence area of 0.19 m^2 is equal to 380 N. For the two end nodes the influence area is half of the other nodes producing a load of 190 N at both ends. This is verified by inspecting the load manager for the deflection model which is illustrated in Figure G.16a & G.16b

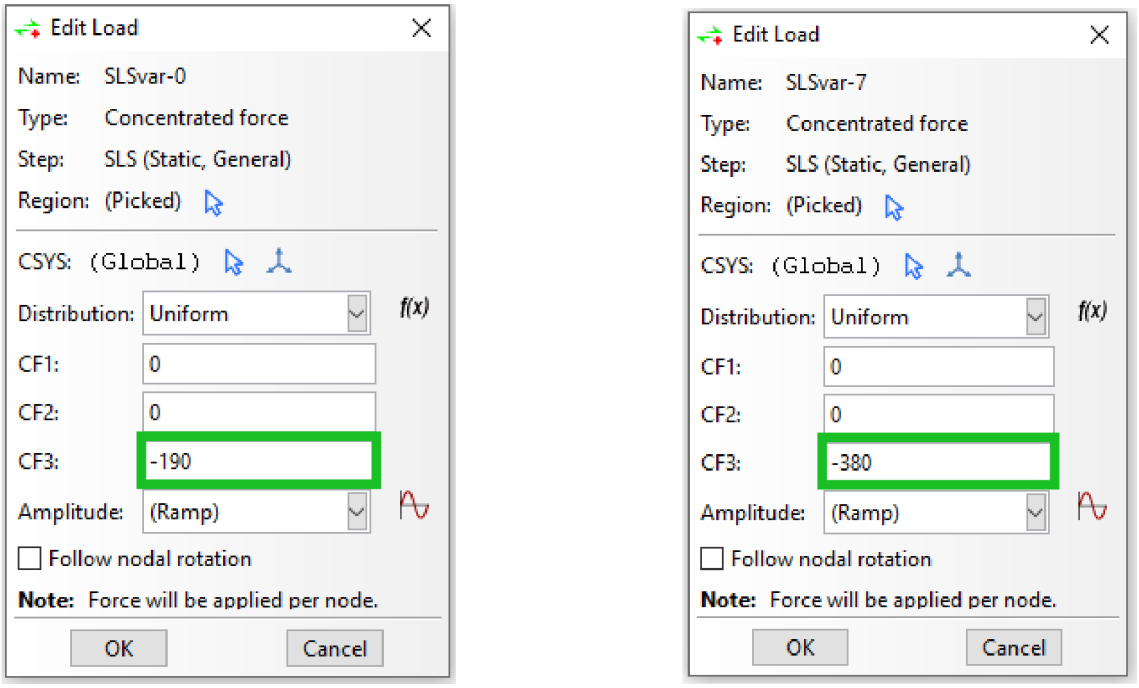

(a) End nodes **(b)** Other nodes

Figure G.16 Applied deflection load for deflection analysis in BRIGADE/Plus

To verify that no other forces or masses was included in the deflection analysis the the reaction force was extracted resulting in a total reaction force of 76 kN which is equal to the total applied deflection load of 2 kPa $\cdot$ 38 m^2 = 76 kN

The total deflection can be verified by visualising the deflected blade in BRIGADE/-Plus as shown in Figure G.17 which is 371.5 mm . The maximum deflection retrieved by the script is according to G.1 equal to 371.5 mm which implies that the deflection retrieval is done in a correct manner.

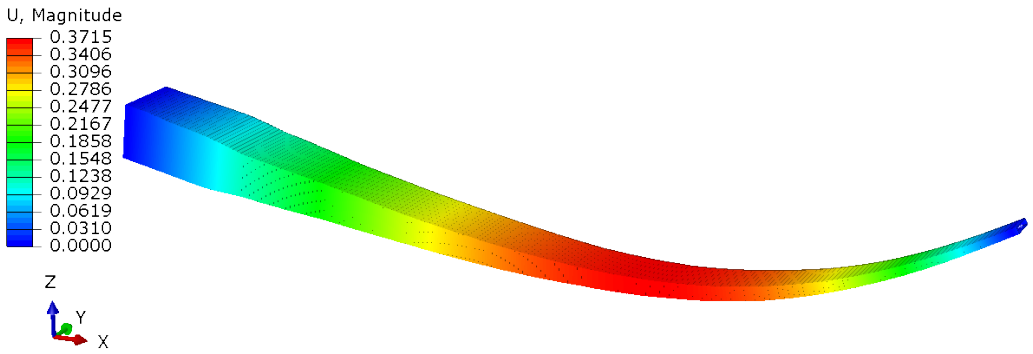

Figure G.17 Resulting deflection with beam profiles rendered

H

Parametric Analysis Output

Presentation of result output in BRIGADE/Plus command window when performing the parametric script. Written to enable the user to verify and follow the calculations made. Flapwise = Vertical and Edgewise = Horizontal

H.1 Example 1: L = 12.0 no critical frequencies

Start iteration

```
-----------------------------------------------
------- Iteration 6 of 25 initiated ---------
-----------------------------------------------
A new model database has been created.
The model "Model-1" has been created.
Traffic Class: TC4
Comfort Class: CL3
SLS total mass:   4648.3 kg
Blade total mass: 1973.6 kg
Length:   12.0 m
Interval: 2.5 - 14.5 m
```

Frequency analysis

```
Critical mode(s):
-------------------------
--- No critical modes ---
-------------------------
```

Deflection and summary

```
Max height of blade: 1675 mm
Max deflection: 7.71 mm at: x = 7.2 m
L/400: 30.0 mm
-> Deflection ok!
-----------------------------------------------
-------- Iteration 6 of 25 completed ----------
-----------------------------------------------

------------ SUMMARY --------------

Traffic Class:   TC4
Comfort Class:   CL3
Blade height:    1675 mm
Bridge span:     12.0 m
Interval:        2.5 - 14.5 m
Damping ratio:   0.01

There are no critical frequencies


SLS analysis:
Max deflection: 7.7 mm
L/400:          30.0 mm
```

H.2 Example 2: L = 12.0 one critical frequency

Start iteration

```
-----------------------------------------------
------- Iteration 25 of 25 initiated ---------
-----------------------------------------------
A new model database has been created.
The model "Model-1" has been created.
Traffic Class: TC4
Comfort Class: CL3
SLS total mass:   4648.3 kg
Blade total mass: 1079.1 kg
Length:   12.0 m
Interval: 12.0 - 24.0 m
```

Frequency analysis

```
Critical mode(s):
Flapwise mode Nr: 1, f = 2.04 Hz
```

Acceleration analysis

```
 ----------------------------------
 --- Retrieving max acceleration ---
 ----------------------------------
Maximum acceleration: 34.52 m/s^2
Allowable acceleration: 1.5 m/s^2
Acceleration NOT ok!
```

Deflection and summary

```
Max height of blade: 625 mm
Max deflection: 96.35 mm at: x = 7.0 m
L/400: 30.0 mm
-> Deflection NOT ok!
-----------------------------------------------
-------- Iteration 25 of 25 completed ---------
-----------------------------------------------

------------- SUMMARY --------------

Traffic Class:   TC4
Comfort Class:   CL3
Blade height:    625 mm
Bridge span:     12.0 m
Interval:        12.0 - 24.0 m
Damping ratio:   0.01

There is one critical eigenfrequency:

f1 = 2.04 Hz, Flapwise mode Nr: 1
Resulting acceleration: 34.52 m/s2
Allowed acceleration:   1.5 m/s2


SLS analysis:
Max deflection: 96.3 mm
L/400:          30.0 mm
```

H.3 Example 3: L = 20.0 several critical frequencies

Start iteration

```
-----------------------------------------------
------- Iteration 21 of 21 initiated ---------
-----------------------------------------------
A new model database has been created.
The model "Model-1" has been created.
Traffic Class: TC4
Comfort Class: CL3
SLS total mass:   7747.2 kg
Blade total mass: 2428.4 kg
Length:   20.0 m
Interval: 4.0 - 24.0 m
```

Frequency analysis

```
Critical mode(s):
Flapwise mode Nr: 1, f = 1.03 Hz
Edgewise mode Nr: 1, f = 2.39 Hz
Flapwise mode Nr: 2, f = 4.55 Hz
```

1st vertical acceleration analysis

```
 ----------------------------------
 --- Retrieving max acceleration ---
 ----------------------------------
Maximum acceleration: 0.73 m/s^2
Allowable acceleration: 1.5 m/s^2
Acceleration ok!
```

1st horizontal analysis

```
 ----------------------------------
 --- Retrieving max acceleration ---
 ----------------------------------
Maximum acceleration: 0.01 m/s^2
Allowable acceleration: 0.1 m/s^2
Acceleration ok!
```

2nd vertical acceleration analysis

```
 ----------------------------------
 --- Retrieving max acceleration ---
 ----------------------------------
Maximum acceleration: 1.08 m/s^2
Allowable acceleration: 1.5 m/s^2
Acceleration ok!
```

Deflection and summary

```
Max height of blade: 1601 mm
Max deflection: 371.53 mm at: x = 12.7 m
L/400: 50.0 mm
-> Deflection NOT ok!
------------------------------------------------
-------- Iteration 21 of 21 completed ---------
------------------------------------------------

------------- SUMMARY --------------

Traffic Class:   TC4
Comfort Class:   CL3
Blade height:    1601 mm
Bridge span:     20.0 m
Interval:        4.0 - 24.0 m
Damping ratio:   0.01

There are 3 critical frequencies:

f1 = 1.03 Hz, Flapwise mode Nr: 1
Resulting acceleration: 0.83 m/s2
Allowed acceleration:   1.5 m/s2

f2 = 2.39 Hz, Edgewise mode Nr: 1
Resulting acceleration: 0.0136 m/s2
Allowed acceleration:   0.1 m/s2

f3 = 4.55 Hz, Flapwise mode Nr: 2
Resulting acceleration: 1.15 m/s2
Allowed acceleration:   1.5 m/s2


SLS analysis:
Max deflection: 371.5 mm
L/400:          50.0 mm
```

I

Clarification of Result Presentation

Example of result presentation and further explanation using a blade length of 12.0 meter. As seen in Figure I.1 The x-axis of the plot is indicated by the start coordinate (leftmost coordinate from the blade root) for each section.

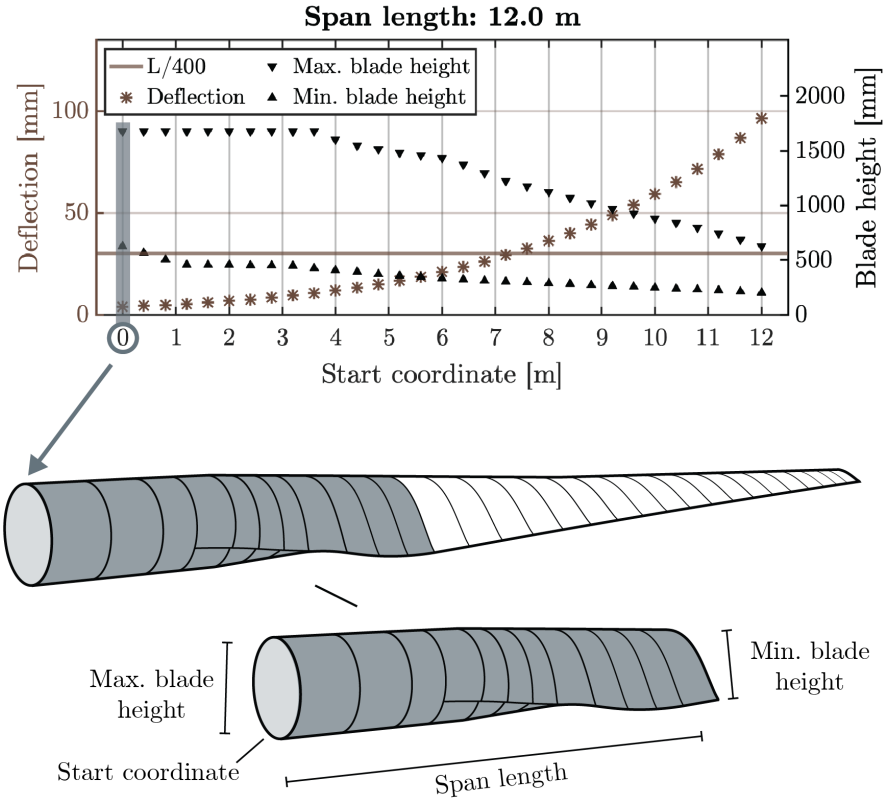

Figure I.1 Deflection - 12.0 m blade section with start coordinate 0.0 m visualised

Figure I.2 illustrates another section with start coordinate equal to 4.0 meter for the same 12 meter section as the example above.

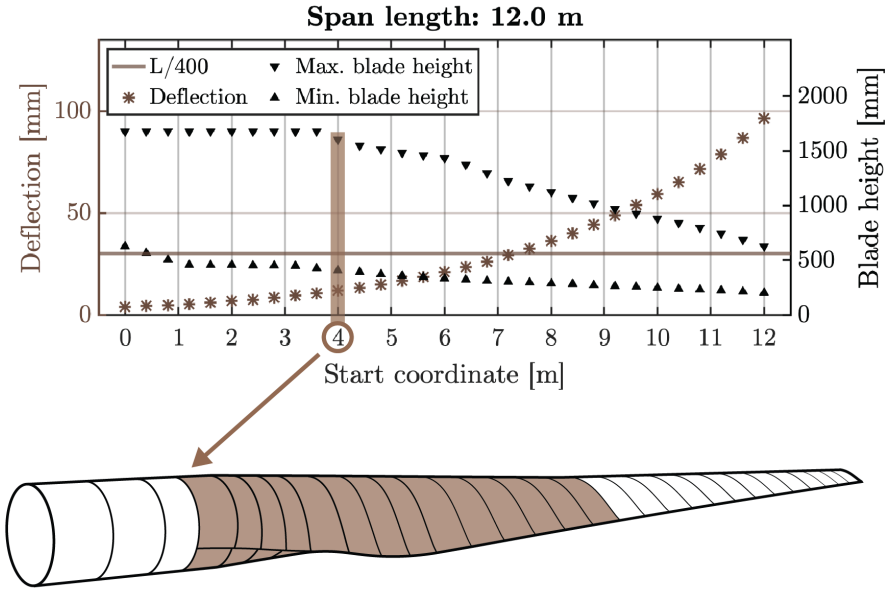

Figure I.2 Deflection - 12.0 m blade section with start coordinate 4.0 m visualised

The same method is used for plotting the acceleration results as seen in Figure I.3 visualising a start coordinate of 10.0 meter

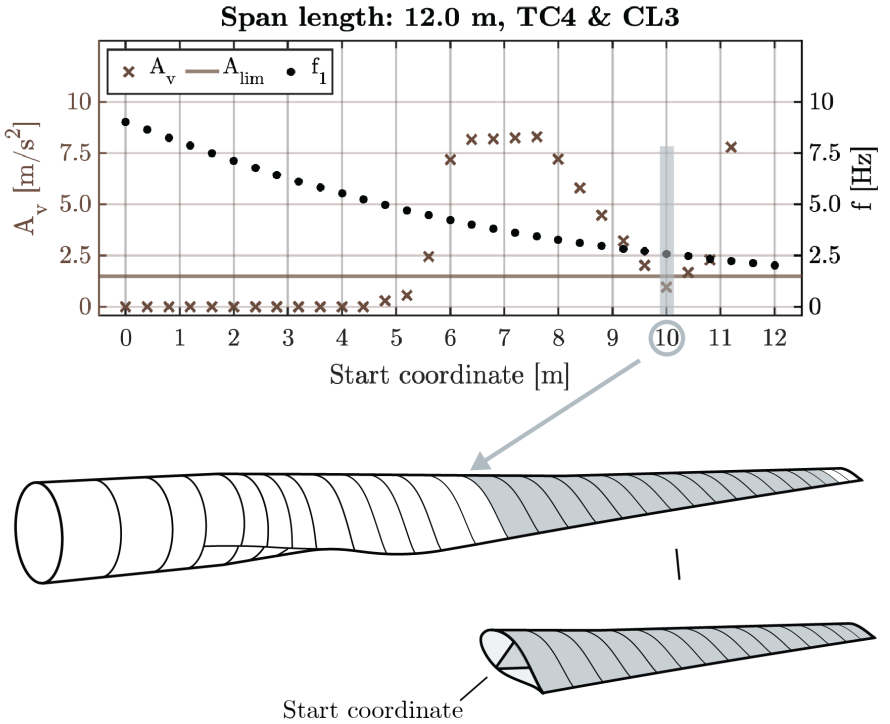

Figure I.3 Acceleration - 12.0 m blade section with start coordinate 10.0 m visualised

J

Results Parametric Analysis

J.1 L = 6.0 m

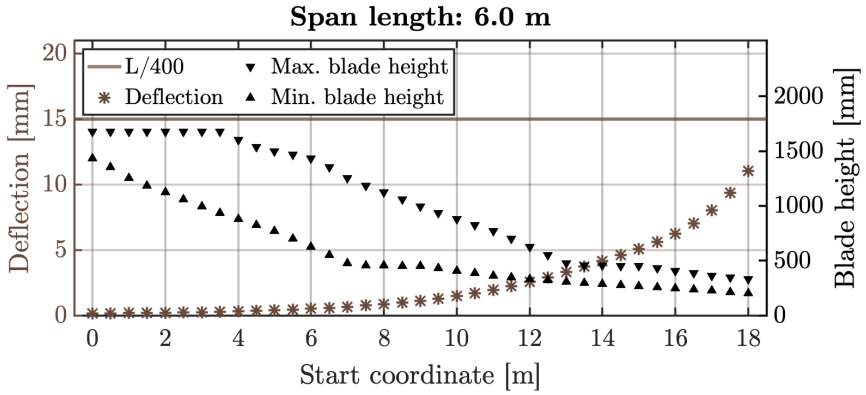

Figure J.1 Resulting deflection together with minimum and maximum blade height for 6 meter span at different positions.

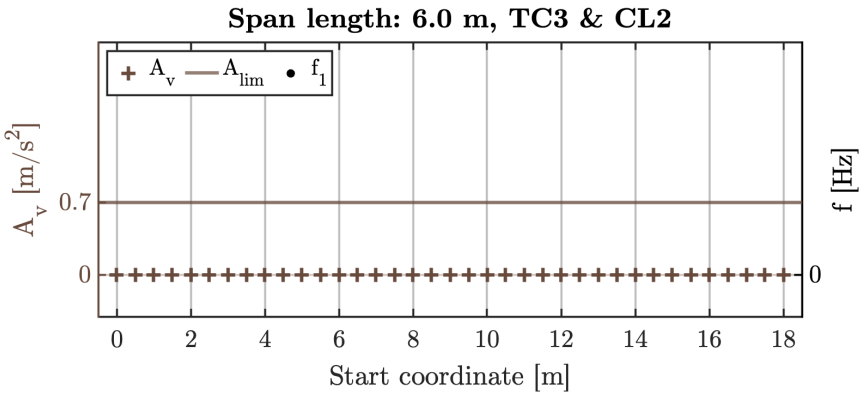

Figure J.2 Resulting eigenfrequency and acceleration response for 6 meter span at different positions. Service state: TC3 & CL2

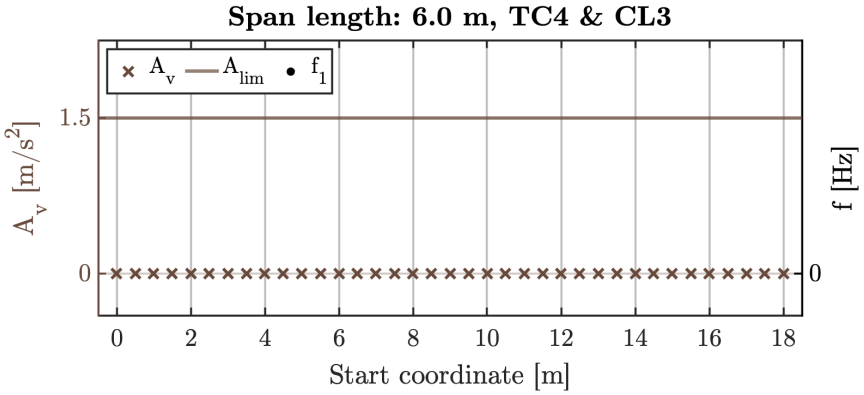

Figure J.3 Resulting eigenfrequency and acceleration response for 6 meter span at different positions. Exceptional situation: TC3 & CL4

J.2 L = 8.0 m

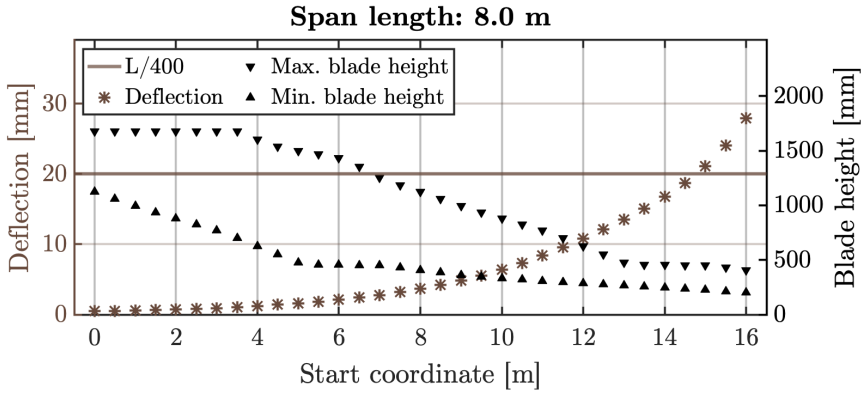

Figure J.4 Resulting deflection together with minimum and maximum blade height for 8 meter span at different positions.

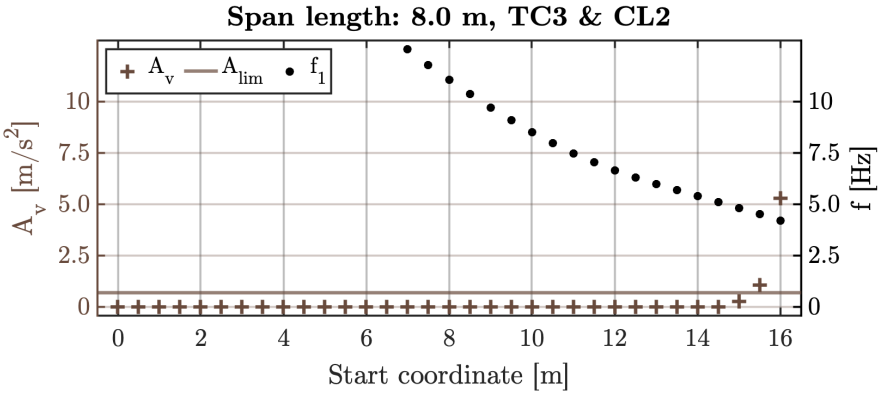

Figure J.5 Resulting eigenfrequency and acceleration response for 8 meter span at different positions. Service state: TC3 & CL2

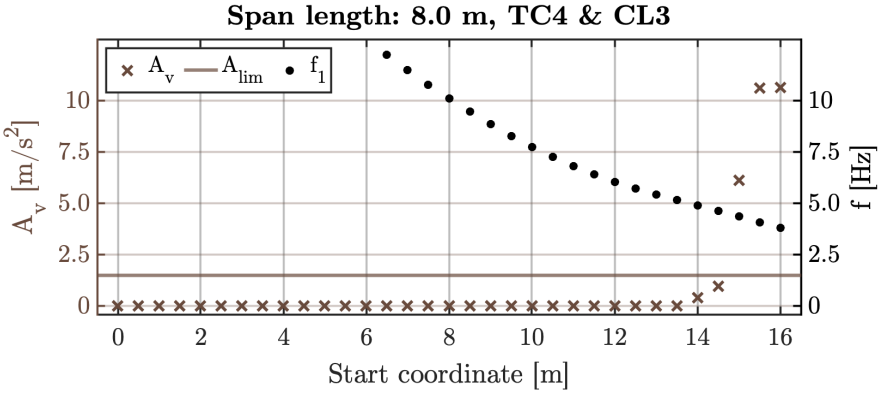

Figure J.6 Resulting eigenfrequency and acceleration response for 8 meter span at different positions. Exceptional situation: TC4 & CL3

J.3 L = 10.0 m

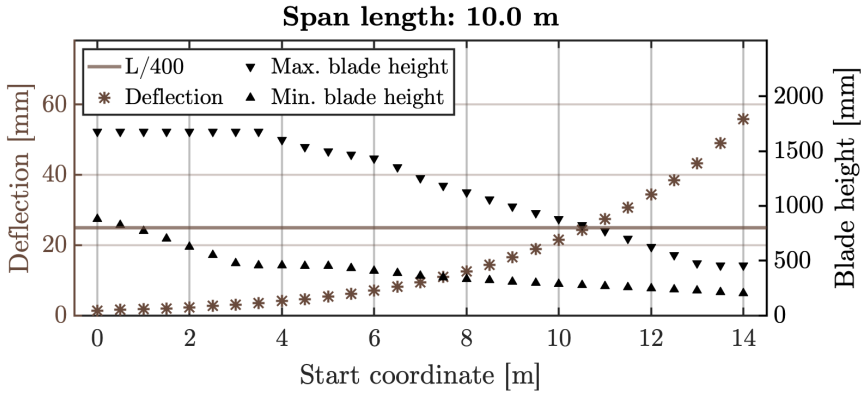

Figure J.7 Resulting deflection together with minimum and maximum blade height for 10 meter span at different positions.

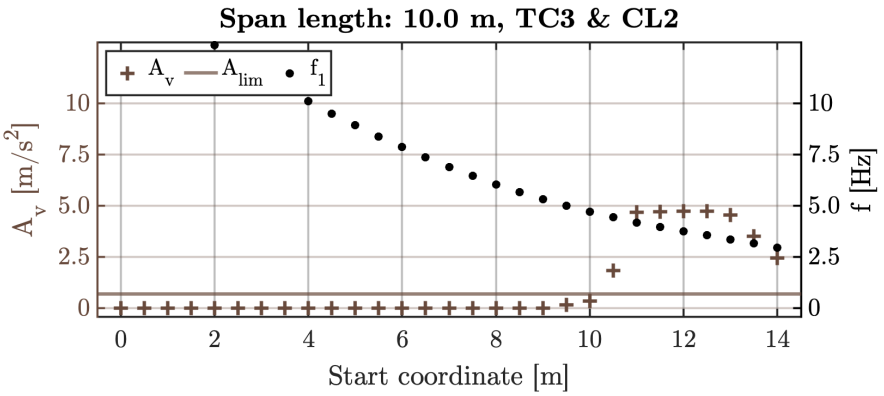

Figure J.8 Resulting eigenfrequency and acceleration response for 10 meter span at different positions. Service state: TC3 & CL2

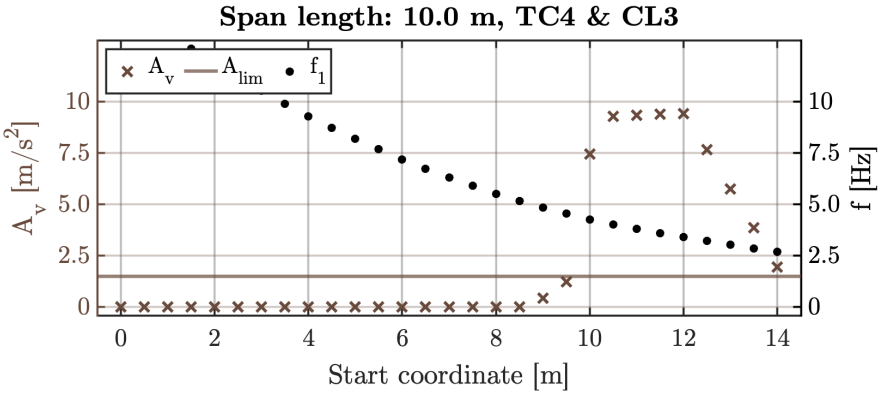

Figure J.9 Resulting eigenfrequency and acceleration response for 10 meter span at different positions. Exceptional situation: TC4 & CL3

J.4 L = 12.0 m

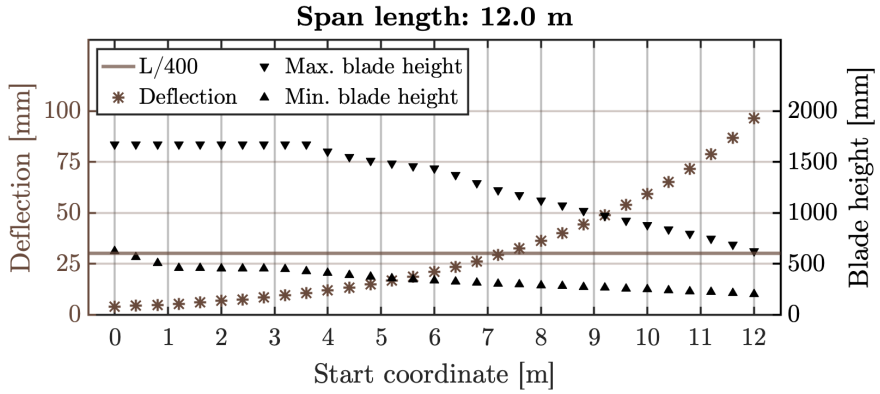

Figure J.10 Resulting deflection together with minimum and maximum blade height for 12 meter span at different positions.

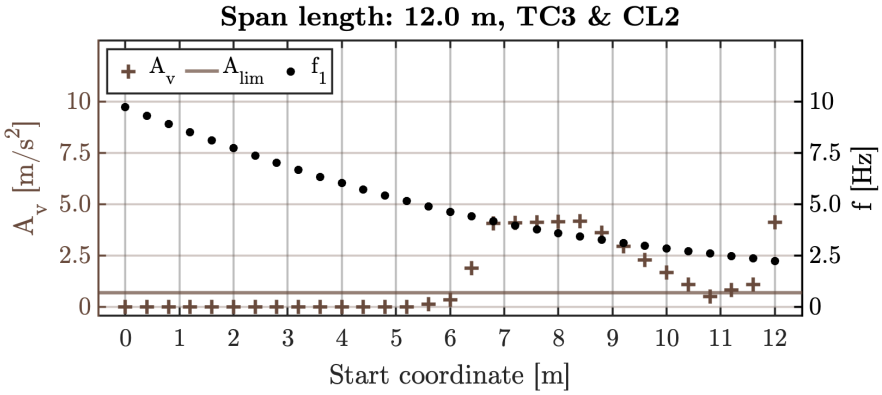

Figure J.11 Resulting eigenfrequency and acceleration response for 12 meter span at different positions. Service state: TC3 & CL2

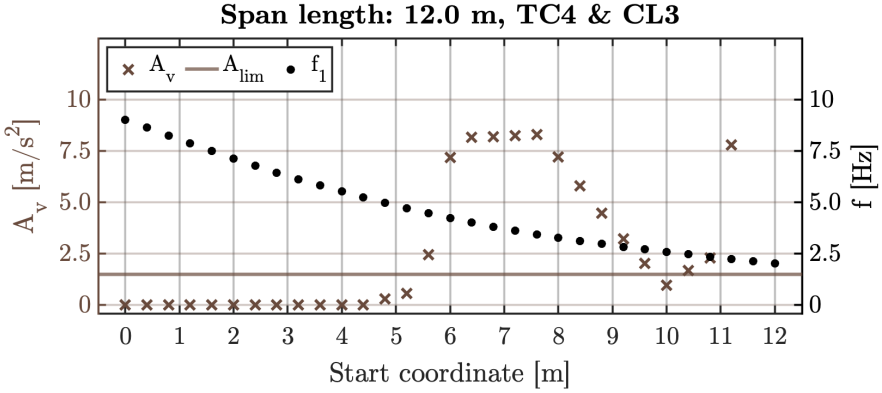

Figure J.12 Resulting eigenfrequency and acceleration response for 12 meter span at different positions. Exceptional situation: TC4 & CL3

J.5 L = 14.0 m

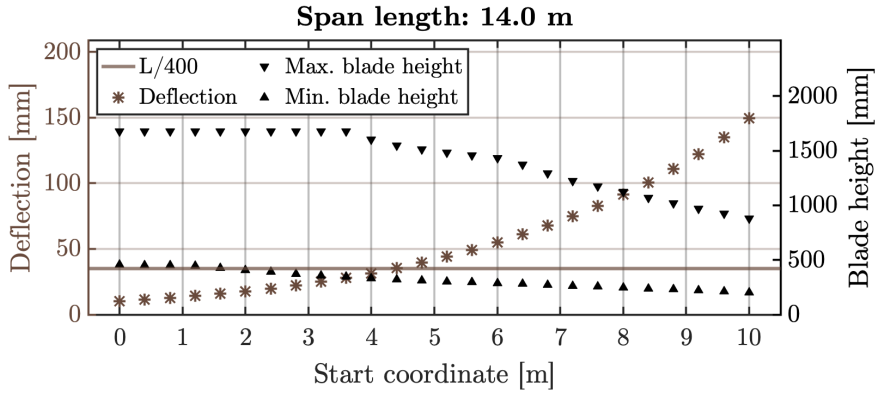

Figure J.13 Resulting deflection together with minimum and maximum blade height for 14 meter span at different positions.

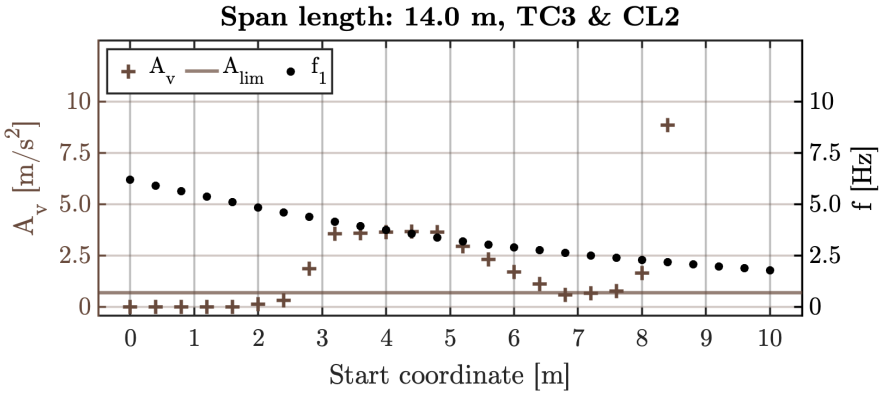

Figure J.14 Resulting eigenfrequency and acceleration response for 14 meter span at different positions. Service state: TC3 & CL2

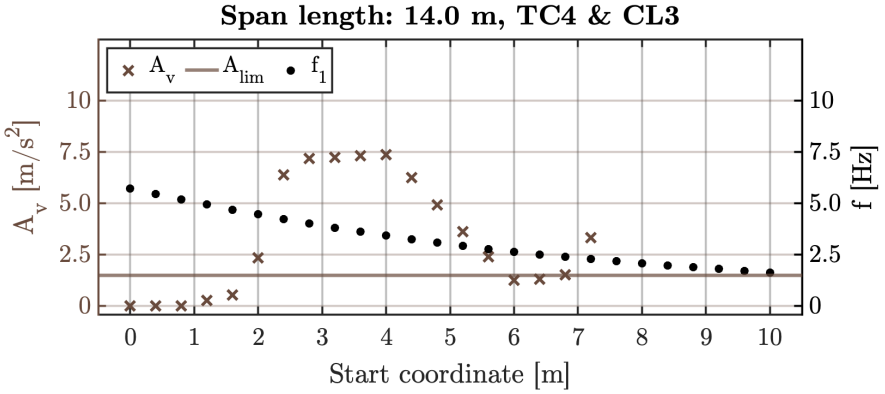

Figure J.15 Resulting eigenfrequency and acceleration response for 14 meter span at different positions. Exceptional situation: TC4 & CL3

J.6 L = 16.0 m

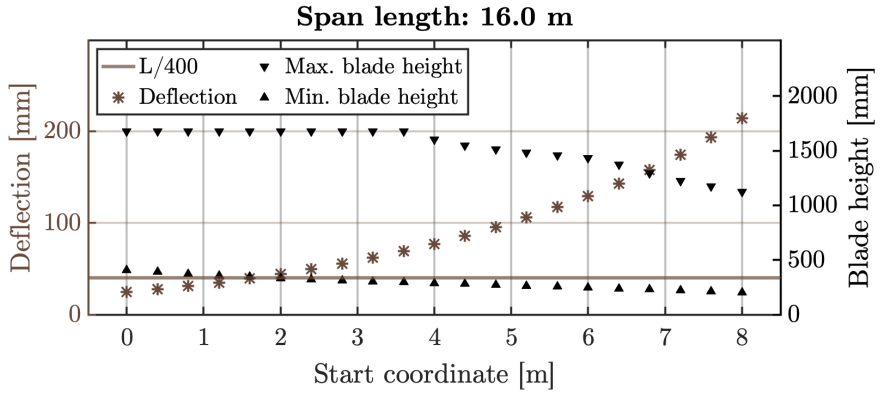

Figure J.16 Resulting deflection together with minimum and maximum blade height for 16 meter span at different positions.

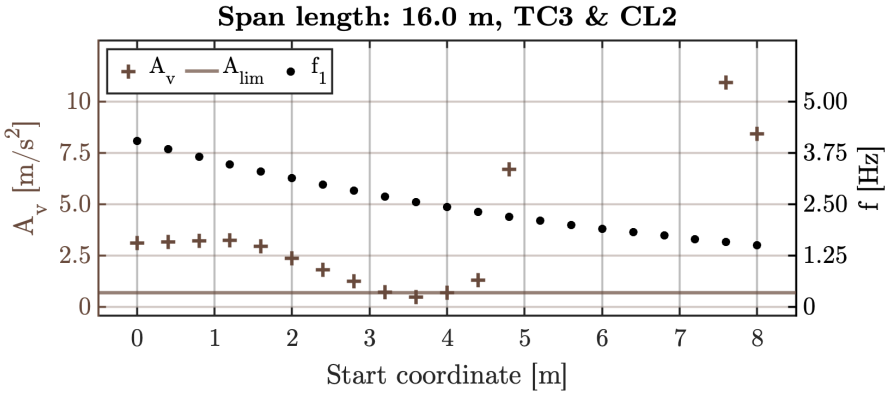

Figure J.17 Resulting eigenfrequency and acceleration response for 16 meter span at different positions. Service state: TC3 & CL2

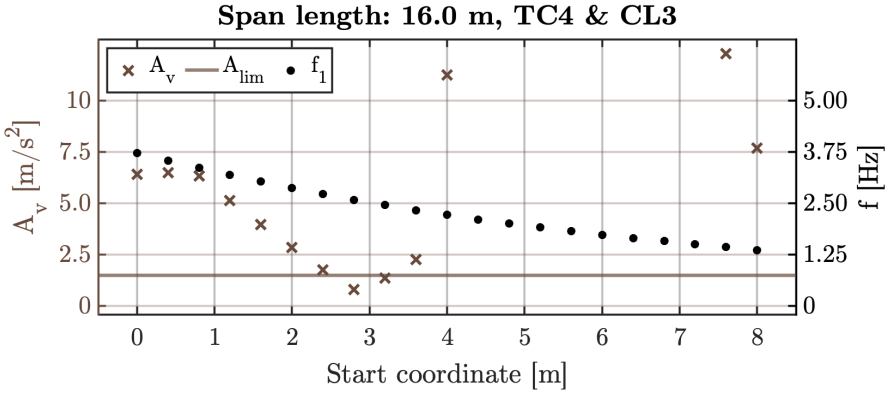

Figure J.18 Resulting eigenfrequency and acceleration response for 16 meter span at different positions. Exceptional situation: TC4 & CL3

J.7 L = 20.0 m

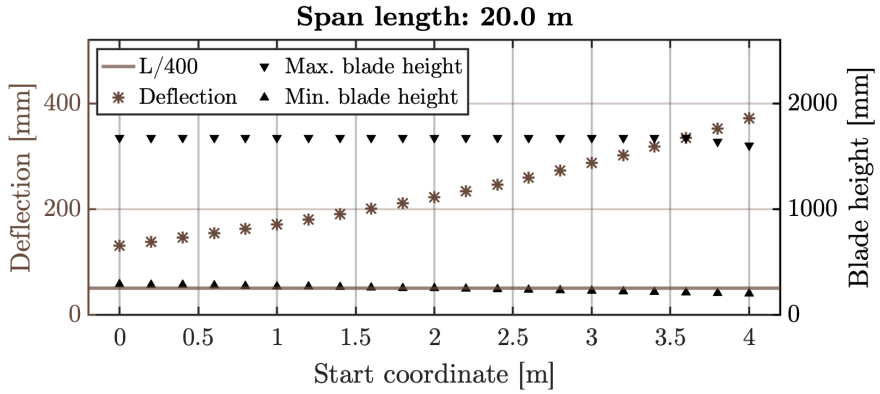

Figure J.19 Resulting deflection together with minimum and maximum blade height for 20 meter span at different positions.

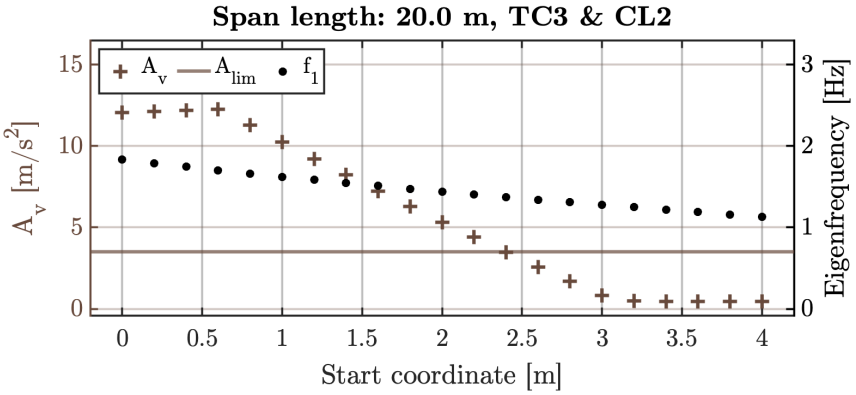

Figure J.20 Resulting eigenfrequency and acceleration response for 20 meter span at different positions. Service state: TC3 & CL2

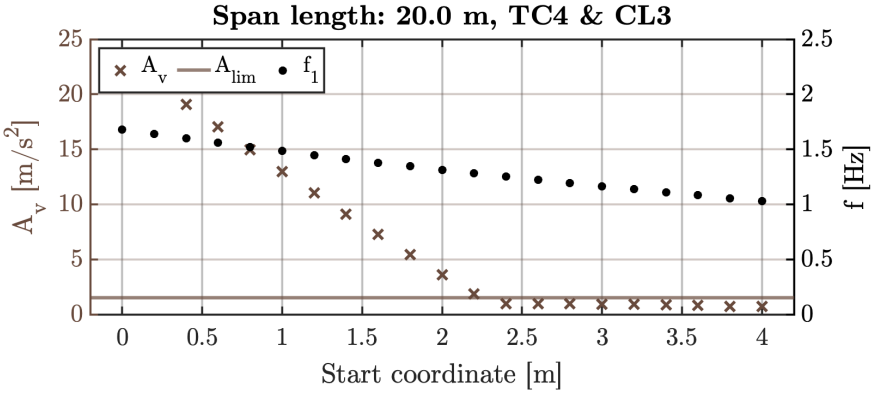

Figure J.21 Resulting eigenfrequency and acceleration response for 20 meter span at different positions. Exceptional situation: TC4 & CL3

For the 20 meter span and TC4 there are also critical 1st horizontal and 2nd vertical modes for which accelerations had to be calculated.

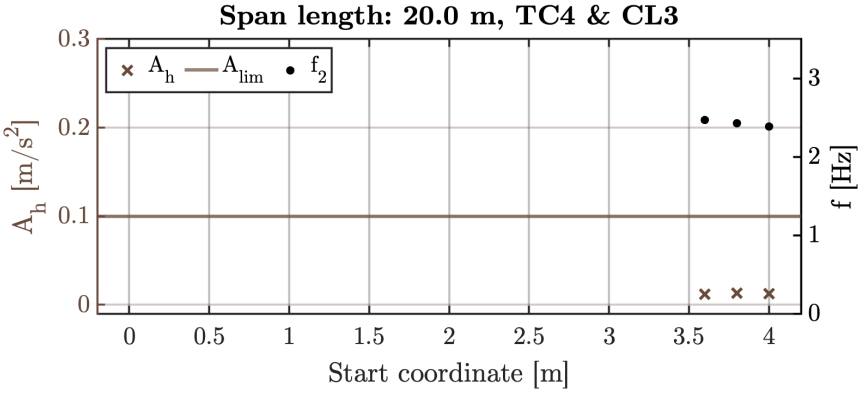

Figure J.22 Resulting eigenfrequency and acceleration response for 1st horizontal mode for 20 meter span at different positions. Exceptional situation: TC4 & CL3

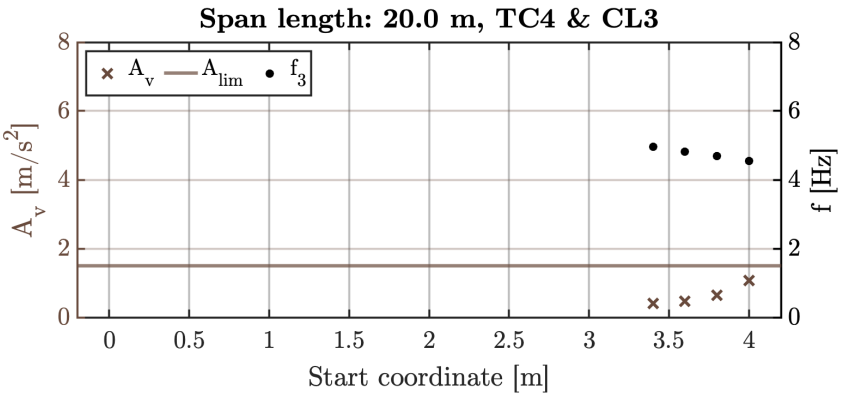

Figure J.23 Resulting eigenfrequency and acceleration response for 2nd vertical mode for 20 meter span at different positions. Exceptional situation: TC4 & CL3

K

Comparison Blade Orientation

Results for original and rotated section as illustrated in Figure K.1. Conducted to compare constructional height vs. deflection and acceleration response.

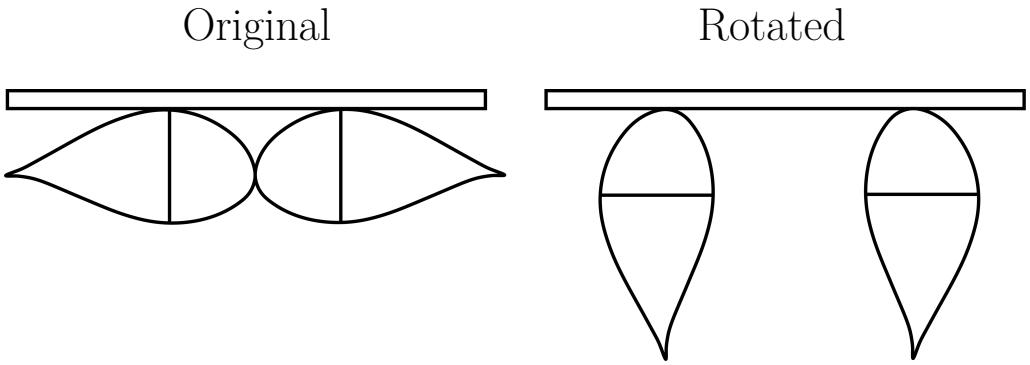

Figure K.1 Illustration of the original and flipped blade composition

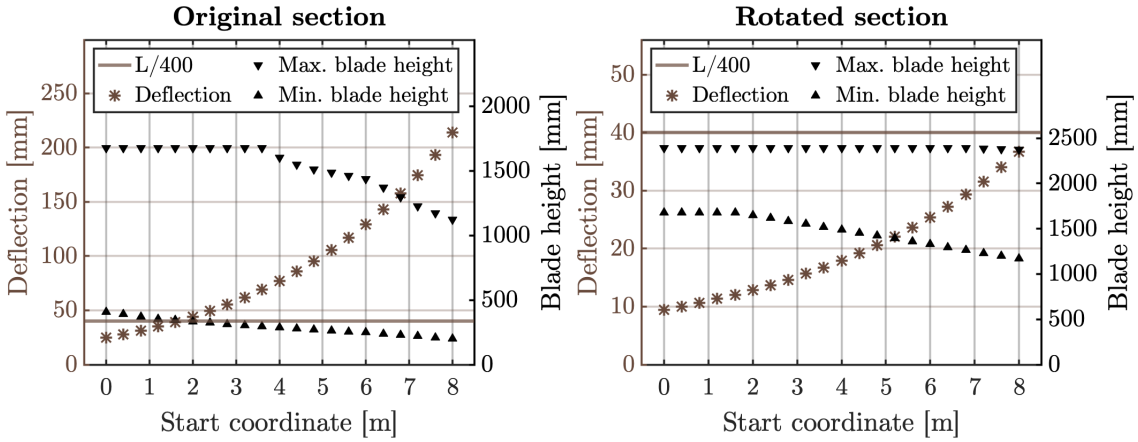

(a) Original section **(b)** Rotated section

Figure K.2 Deflection together with minimum and maximum blade height for 16 meter span at different positions.

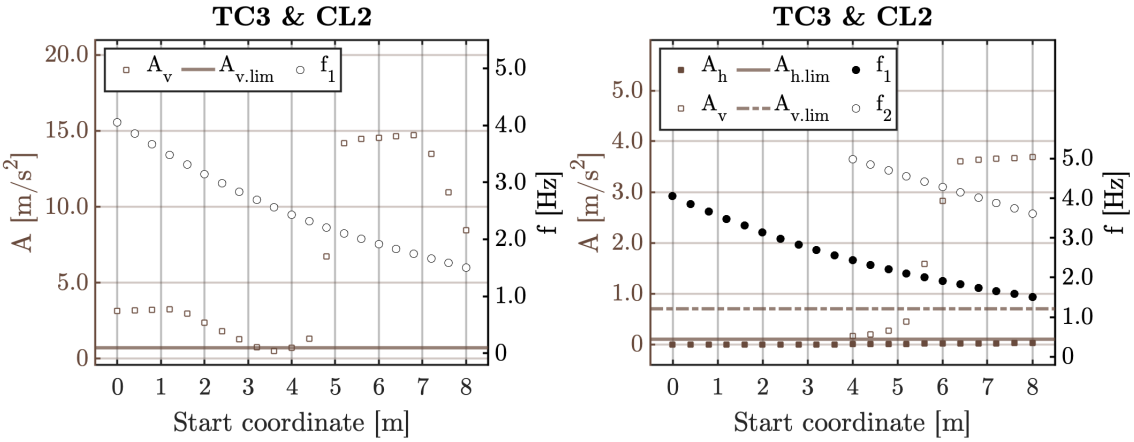

(a) Original section **(b)** Rotated section

Figure K.3 Acceleration response for 16 meter span at different positions (TC3 & CL2).

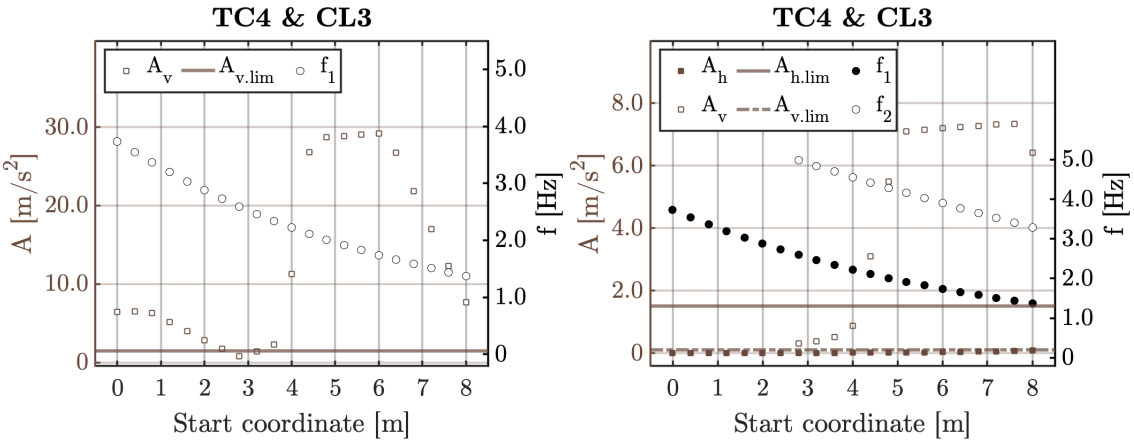

(a) Original section **(b)** Rotated section

Figure K.4 Acceleration response for 16 meter span at different positions (TC4 & CL3).

L

Pictures NWP28.3 ATV Blade

Figure L.1 Overview of the two decommissioned blades. Photograph: David Nygren

Figure L.2 Trailing edge (own photo).

Figure L.3 Leading edge (own photo).

Figure L.4 Interior of the blade, web and leading edge (own photo).

Figure L.5 Damage of leading edge with visible glass fibre weave (own photo).

DEPARTMENT OF ARCHITECTURE AND CIVIL ENGINEERING
CHALMERS UNIVERSITY OF TECHNOLOGY
Gothenburg, Sweden
www.chalmers.se

CHALMERS
UNIVERSITY OF TECHNOLOGY